The Geometric Minimum Action Method: A Least Action Principle on the Space of Curves

MATTHIAS HEYMANN
Courant Institute

AND

ERIC VANDEN-EIJNDEN
Courant Institute

Abstract

Freidlin-Wentzell theory of large deviations for the description of the effect of small random perturbations on dynamical systems is exploited as a numerical tool. Specifically, a numerical algorithm is proposed to compute the quasi-potential in the theory, which is the key object to quantify the dynamics on long time scales when the effect of the noise becomes ubiquitous: the equilibrium distribution of the system, the pathways of transition between metastable states and their rate, etc., can all be expressed in terms of the quasi-potential. We propose an algorithm to compute these quantities called the geometric minimum action method (gMAM), which is a blend of the original minimum action method (MAM) and the string method. It is based on a reformulation of the large deviations action functional on the space of curves that allows one to easily perform the double minimization of the original action required to compute the quasi-potential. The theoretical background of the gMAM in the context of large deviations theory is discussed in detail, as well as the algorithmic aspects of the method. The gMAM is then illustrated on several examples: a finite-dimensional system displaying bistability and modeled by a nongradient stochastic ordinary differential equation, an infinite-dimensional analogue of this system modeled by a stochastic partial differential equation, and an example of a bistable genetic switch modeled by a Markov jump process.

Contents

Communications on Pure and Applied Mathematics, Vol. LXI, 1052–1117 (2008)

1 Introduction and Main Results

Dynamical systems are often subject to random perturbations. Even when these perturbations have small amplitude, they have a profound impact on the dynamics on the appropriate time scale. For instance, perturbations result in transitions between regions around the stable equilibrium points of the deterministic dynamical system that would otherwise be impossible. Such transitions are responsible for metastable phenomena observed in many systems: regime changes in climate, nucleation events during phase transitions, conformation changes of biomolecules, and bistable behavior in genetic switches are just a few examples among many others.

When the amplitude of the random perturbations is small, the Freidlin-Wentzell theory of large deviations provides the right framework to understand their effects on the dynamics [6, 17, 19]. In a nutshell, the theory builds on the property that events with very little likelihood, when they occur, do so with high probability by following the pathway that is least unlikely. This makes rare events predictable, in a way that Freidlin-Wentzell theory of large deviations quantifies. The central object in the theory is an action functional whose minimum (subject to appropriate constraints) gives an estimate of the probability and the rate of occurrence of the rare event and whose minimizer gives the pathway of maximum likelihood by which this event occurs. A key practical question then becomes how to compute the minimum and minimizer of the Freidlin-Wentzell action functional. This question is the main topic of this paper. As we will see, it will lead us to reformulate the action minimization problem in a form that is convenient for numerical purposes but will also shed light on some interesting analytical properties of the minimizer.

Before going there, however, we begin with a brief summary of the main results of the Freidlin-Wentzell theory of large deviations that we will use. For simplicity of exposition, we focus here on the finite-dimensional case, but the theory can be extended to infinite dimensions (e.g., to situations where (1.3) below is replaced by a stochastic partial differential equation defining a stochastic process X^ε with values in some suitable Hilbert space [2]; situations of this type are considered in Section 4.2).

1.1 Freidlin-Wentzell Theory of Large Deviations

As mentioned above, the central object in the theory is an action functional: if the state space of the dynamical system is embedded in $\mathbb{R}^n$ and if $C(0,T)$ denotes

the space of all continuous functions mapping from $[0, T]$ into $\mathbb{R}^n$, this action can be written as

$$S_T(\psi) = \begin{cases} \int_0^T L(\psi, \dot{\psi})dt & \text{if } \psi \in C(0,T) \text{ is absolutely continuous and the integral converges,} \\ +\infty & \text{otherwise,} \end{cases} \tag{1.1}$$

where the Lagrangian $L(x, y)$ is given by

$$L(x, y) = \sup_{\theta \in \mathbb{R}^n} (\langle y, \theta \rangle - H(x, \theta)). \tag{1.2}$$

Here $\langle \cdot, \cdot \rangle$ denotes the Euclidean scalar product in $\mathbb{R}^n$ and $H(x, \theta)$ is the Hamiltonian whose specific form depends on the dynamical system at hand.

There are two important classes we shall consider here. The first consists of stochastic differential equations (SDEs) on $\mathbb{R}^n$ with drift vector b and diffusion tensor $a = \sigma\sigma^T$, i.e.,

$$dX^\varepsilon(t) = b(X^\varepsilon(t))dt + \sqrt{\varepsilon}\,\sigma(X^\varepsilon(t))dW(t). \tag{1.3}$$

Their Hamiltonian H and Lagrangian L are given by

$$\begin{aligned} H(x, \theta) &= \langle b(x), \theta \rangle + \tfrac{1}{2}\langle \theta, a(x)\theta \rangle, \\ L(x, y) &= \big\langle y - b(x), a^{-1}(x)(y - b(x)) \big\rangle. \end{aligned} \tag{1.4}$$

Additional restrictions are required on b and σ in order that large deviations theory applies, but these are usually mild—for instance, it suffices that a and b be bounded and uniformly continuous, and that a be uniformly elliptic, i.e., $\exists m > 0\ \forall \xi \in \mathbb{R}^n$: $\langle \xi, a(x)\xi \rangle \geq m|\xi|^2$; see [6, chap. 5.3].

The second class consists of continuous-time Markov jump processes on $\varepsilon\mathbb{Z}^n$ with a generator Q defined for every test function $f : \mathbb{R}^n \to \mathbb{R}$ by

$$(Qf)(x) = \varepsilon^{-1} \sum_{j=1}^{N} \nu_j(x)\big(f(x + \varepsilon e_j) - f(x)\big), \tag{1.5}$$

where $\nu_j : \mathbb{R}^n \to (0, \infty)$, $j = 1, \ldots, N$, are the rates (or propensities) and $e_j \in \mathbb{Z}^n$, $j = 1, \ldots, N$, are the change (or stoichiometric) vectors. The Hamiltonian H for this type of dynamics is given by

$$H(x, \theta) = \sum_{j=1}^{N} \nu_j(x)(e^{\langle \theta, e_j \rangle} - 1), \tag{1.6}$$

and L must be obtained via (1.2)—in this case, no closed-form expression for L is available in general. Here, too, some mild restrictions are necessary in order that large deviations theory applies, e.g., that ν_j be uniformly bounded away from 0 and $+\infty$ [17].

Large-deviations theory gives a rough estimate for the probability that the trajectory $X^\varepsilon(t)$, $t \in [0, T]$, $T < \infty$, of the random dynamical system—be it the

SDE (1.3), the Markov chain with generator (1.5), or any other system whose action functional can be expressed as (1.1)—lies in a small neighborhood around a given path $\psi \in C(0, T)$. The theory asserts that, for δ and ε sufficiently small,

$$\mathbb{P}_x\Big\{\sup_{0\le t\le T}|X^\varepsilon(t)-\psi(t)|\le\delta\Big\}\approx\exp(-\varepsilon^{-1}S_T(\psi)), \tag{1.7}$$

where $\mathbb{P}_x$ denotes the probability conditional on $X^\varepsilon(0) = x$ and we assumed that $\psi(0) = x$. Estimate (1.7) can be made precise in terms of lower and upper bounds on the probability [6, 17, 19], but for our purpose here it suffices to say that it implies that the probability of various events can be evaluated by constrained minimization. For instance, if B is a Borel subset of $\mathbb{R}^n$, we have

$$\mathbb{P}_x\{X^\varepsilon(T)\in B\}\asymp\exp(-\varepsilon^{-1}\inf_{\psi}S_T(\psi)) \tag{1.8}$$

where $f(\varepsilon) \asymp g(\varepsilon)$ if and only if $\log f(\varepsilon)/\log g(\varepsilon) \to 1$ as $\varepsilon \to 0$, and the infimum is taken over all paths ψ such that $\psi(0) = x$ and $\psi(T) \in B$. The minimizer of $S_T(\psi)$ in (1.8) is then the path of maximum likelihood by which the process X^ε ends in B at time T starting from x.

1.2 The Role of the Quasi-Potential

In (1.8), T is finite, but large deviations theory can be generalized to make predictions on long-time intervals $[0, T(\varepsilon)]$, with $T(\varepsilon) \asymp \exp(\varepsilon^{-1}C)$ and $C > 0$. On these time scales, the effects of the noise become ubiquitous in the sense that events are likely to occur that are otherwise prohibited by the deterministic dynamics. For this reason these are often the natural time scales over which to analyze the dynamics, and these are the time scales on which we shall mostly focus in this paper. To understand what happens then, the relevant object is the quasi-potential

$$V(x_1,x_2)=\inf_{T>0}\inf_{\psi\in\bar C_{x_1}^{x_2}(0,T)}S_T(\psi), \tag{1.9}$$

where $\bar C_{x_1}^{x_2}(0, T)$ denotes the space of all absolutely continuous functions $f : [0, T] \to \mathbb{R}^n$ such that $f(0) = x_1$ and $f(T) = x_2$.

A detailed exposition of the significance of the quasi-potential is beyond the scope of this paper and can be found in [6, chap. 6]. Let us simply say that the quasi-potential roughly measures the difficulty to go from point x_1 to point x_2, as made apparent by the following alternative definition (see [6, p. 161]):

$$V(x_1,x_2)=\lim_{T\to\infty}\lim_{\delta\to0}\lim_{\varepsilon\to0}(-\varepsilon\log\mathbb{P}_{x_1}\{\tau_{\delta,x_2}(X^\varepsilon)\le T\}) \tag{1.10}$$

where

$$\tau_{\delta,x_2}(X^\varepsilon):=\inf\{t>0\mid X^\varepsilon(t)\in B_\delta(x_2)\} \tag{1.11}$$

denotes the first time at which the process X^ε starting from x_1 enters the ball $B_\delta(x_2)$ of radius δ around x_2.

The quasi-potential allows one to understand the limiting dynamics over exponentially long intervals of time. For instance, suppose that the deterministic systems associated with (1.3) and (1.5), that is,

$$\dot{X}(t) = b(X(t)) \tag{1.12}$$

and, according to Kurtz's theorem [17],

$$\dot{X}(t) = \sum_{j=1}^{N} \nu_j(X(t))e_j, \tag{1.13}$$

respectively, possess exactly two stable equilibrium points x_1 and x_2, the basins of attraction of which form a complete partition of $\mathbb{R}^n$. Then on large time intervals the dynamics can be reduced to that of a continuous-time Markov chain on the state space $\{x_1, x_2\}$ with rates

$$k_{1,2} \asymp \exp(-\varepsilon^{-1}V(x_1, x_2)), \quad k_{2,1} \asymp \exp(-\varepsilon^{-1}V(x_2, x_1)). \tag{1.14}$$

These are reminiscent of the Arrhenius law. Similar reductions are possible when (1.12) and (1.13) possess more than two stable equilibrium points or even other stable equilibrium structures such as limit cycles [6]. The quasi-potential $V(x_1, x_2)$ is also the key object to characterize the equilibrium distribution of the process in the limit as $\varepsilon \to 0$. For instance, if x_1 is the only stable equilibrium point of (1.12) or (1.13) and it is globally attracting, then

$$\mu^\varepsilon(B) \asymp \exp(-\varepsilon^{-1} \inf_{x_2 \in B} V(x_1, x_2)) \tag{1.15}$$

where B is any Borel set in $\mathbb{R}^n$ and μ^ε is the equilibrium distribution of the process. (1.15) is reminiscent of the Gibbs distribution associated with a potential. Similar statements can again be made in more general situations [6].

1.3 Geometric Reformulation

One of the main theoretical results of this paper is to show that the variational problem (1.9) that defines the quasi-potential admits a geometric reformulation. This reformulation will prove quite useful for numerical purposes. Since it is actually quite simple to understand in the context of SDEs, let us outline the argument in this case (a similar argument is given in [18] in the different context of quantum tunneling, and it is also at the core of [6, lemma 3.1, p. 120]). For an SDE like (1.3), (1.9) reduces to (using (1.1) and (1.4))

$$V(x_1, x_2) = \frac{1}{2} \inf_{T>0} \inf_{\psi \in \bar{C}^{x_2}_{x_1}(0,T)} \int_0^T |\dot{\psi}(t) - b(\psi(t))|^2_{a(\psi)}\, dt, \tag{1.16}$$

where, for any $u, v, x \in \mathbb{R}^n$, $\langle u, v\rangle_{a(x)} = \langle u, a^{-1}(x)v\rangle$ is the inner product that is associated with the diffusion tensor $a = \sigma\sigma^T$ and $|u|_{a(x)} = \langle u, u\rangle^{1/2}_{a(x)}$ is the

associated norm. Clearly, expanding the square under the integral in (1.16) and using $|u|^2_{a(x)} + |v|^2_{a(x)} \geq 2|u|_{a(x)}|v|_{a(x)}$, we deduce that

$$\begin{aligned} &V(x_1, x_2) \\ &\quad \geq \inf_{T,\psi} \int_0^T \big(|\dot\psi(t)|_{a(\psi)}\, |b(\psi(t))|_{a(\psi)} - \langle \dot\psi(t), b(\psi(t))\rangle_{a(\psi)}\big) dt \\ &\quad = 2 \inf_{T,\psi} \int_0^T |\dot\psi(t)|_{a(\psi)}\, |b(\psi(t))|_{a(\psi)} \sin^2 \frac{1}{2}\, \eta(t) dt, \end{aligned} \tag{1.17}$$

where $\eta(t)$ is the angle between $\dot\psi(t)$ and $b(\psi(t))$ in the metric that is induced by $\langle \cdot, \cdot \rangle_{a(\psi(t))}$. On the other hand, there is a matching upper bound since equality between the integrals at the right-hand sides of (1.16) and (1.17) is achieved in the special case when ψ is constrained so that $|\dot\psi(t)| = |b(\psi(t))|$. Thus, the inequality sign in (1.17) can be replaced by an equality sign (this conclusion is proven rigorously in Section 2).

Now, the key observation is that the integral in (1.17) has become independent of the particular way in which ψ is parametrized by time. In other words, (1.17) offers a geometric expression for the quasi-potential as

$$V(x_1, x_2) = 2 \inf_\gamma \int_\gamma |b|_a \sin^2 \frac{1}{2}\, \eta\, ds, \tag{1.18}$$

where the integral at the right-hand side is the line integral along the curve γ (ds being the arc length element along this curve), η is the angle between γ and b at location s along the curve, and the infimum is taken over all curves γ connecting x_1 to x_2.

As shown below, (1.18) can be generalized to dynamical systems with action functional (1.1) that are not SDEs (such as Markov jump processes with generator (1.5)). In these cases, too, the key idea is to reformulate (1.9) geometrically in terms of curves $\gamma = \{\varphi(\alpha) \mid \alpha \in [0,1]\}$, where $\varphi : [0,1] \to \mathbb{R}^n$ is an arbitrary parametrization of the curve γ. Our main result in this direction is that the quasi-potential (1.9) can be expressed as

$$V(x_1, x_2) = \inf_{\varphi \in \bar C^{x_2}_{x_1}(0,1)} \hat S(\varphi) \quad \text{with } \hat S(\varphi) = \sup_{\substack{\vartheta:[0,1]\to\mathbb{R}^n \\ H(\varphi,\vartheta)\equiv 0}} \int_0^1 \langle \varphi', \vartheta \rangle d\alpha \tag{1.19}$$

(see Proposition 2.1 below for a precise statement and other representations of $\hat S(\varphi)$).

The action $\hat S(\varphi)$ in (1.19) is parametrization free; i.e., it is left invariant under reparametrization of φ, so it can be interpreted as an action on the space of

curves. Compared to (1.9), the minimizer of (1.19) over all φ exists in more general circumstances (for reasons to be explained later), and this makes (1.19) also more suitable for computations, as explained next. The curve $\gamma^\star$ associated with the minimizer $\varphi^\star$ of (1.19) can then be interpreted as the curve of maximum likelihood by which transitions from x_1 to x_2 occur (see Proposition 2.3).

1.4 Numerical Aspects

One of our main points of focus in this paper is the numerical counterpart to Freidlin-Wentzell theory; i.e., how can one efficiently compute the quasi-potential $V(x_1, x_2)$ in (1.19) and the corresponding minimizer $\varphi^\star$ (the maximum likelihood transition curve)?

The Shooting Method

Perhaps the simplest way to minimize the Freidlin-Wentzel action is to use a shooting method (see, e.g., [10]) to solve as an initial value problem the boundary value problem for the Hamilton equation associated with the minimization problem in (1.8) or (1.9). Working with the Hamiltonian is an advantage since it is typically known explicitly. On the other hand, in practice this approach quickly becomes inefficient when the dimension of the system increases, and it can be inapplicable in infinite dimension. In addition, the shooting method may lead to additional difficulties when T is optimized upon as well.

The Original MAM and the String Method

In [4], a numerical technique, termed minimum action method (MAM), was introduced for situations where the minimization of $S_T(\psi)$ is sought over a fixed time interval of length T. The MAM is a relaxation method and is a generalization of previous techniques, such as the one used in [15]. The MAM, however, is not very well suited for the double minimization problem over ψ and T required to compute the quasi-potential $V(x_1, x_2)$ defined in (1.9). The main reason is that the functional may have no minimizer because the infimum is only "achieved" when $T \to \infty$. (In fact, this will always happen in the typical case in which the prescribed start and end points x_1 and x_2 are critical points of the deterministic dynamics (1.12) or (1.13); see Lemma 2.8(ii) below.)

In the special case of an SDE (1.3) in which b is minus the gradient of some potential, $b = -\nabla U$, and σ is the identity, the string method (introduced in [3] and generalizing the nudged elastic band method introduced in [9]) circumvents this problem by taking advantage of the fact that for such systems transition paths are always parallel to the drift $b = -\nabla U$. This allows for a geometric reformulation of the problem and leads to a numerical algorithm in which a discretized curve (or string) is evolved by iterating over the following two-step procedure: in the first step the discretization points along the curve are evolved independently in the direction of the flow $b = -\nabla U$; in the second step the curve is reparametrized by redistributing the discretization points at equally spaced positions along the curve

(an idea which we will borrow in our approach). Unfortunately, for a generic SDE, transition paths are generally not parallel to the drift, and therefore the string method is not applicable.

The gMAM

The geometric minimum action method (gMAM) that is presented in this paper merges and further develops ideas from both the original MAM and the string method. It also has the advantage that it is formulated in terms of the Hamiltonian $H(x, \theta)$. The gMAM resolves the problem of infinite T analytically, leading to the equivalent minimization problem (1.19), which can then be performed in various ways. Here we will use what is, in essence, a preconditioned steepest-descent algorithm (that is, it is based on a semi-implicit spatiotemporal discretization of the Euler-Lagrange equation for (1.19)). The only nonstandard aspects of the procedure are that (i) it requires performing first the maximization over ϑ, which we do in an inner loop using a quadratically convergent version of a Newton-Raphson-like algorithm, and (ii) it requires controlling the parametrization of the curve φ since the latter is nonunique. Here we opt for parametrizing φ by normalized arc length (as it was done in the string method), meaning that φ satisfies $|\varphi'| = cst$ a.e. on $[0, 1]$.

The gMAM can be applied to generic SDEs, continuous-time Markov chains, and other types of dynamics whose Hamiltonians are known analytically and fulfill Assumptions 1–3 below. The gMAM can also be applied to SPDEs, as illustrated here, and the underlying strategy may even apply to the minimization of integrals whose integrand is not the Legendre transform of a Hamiltonian (see Remark 2.6).

1.5 Organization, Notation, and Assumptions

The remainder of this paper, which is also the core of the thesis [8], is organized as follows. In Section 2 we first establish and discuss the theoretical results mentioned above, and we also show how to recover the optimal time parametrization once the minimizing curve $\gamma^\star$ is found. In Section 3, we propose and discuss the gMAM algorithm for computing $V(x_1, x_2)$ and the maximum-likelihood transition curve $\gamma^\star$. In Section 4 we illustrate these algorithms on several examples. In Section 4.1 we consider an example with bistable behavior first analyzed in [12] in the context of an SDE; in Section 4.2 we consider an SPDE generalization of this example; and in Section 4.3 we consider a Markov chain used in [1, 16] that arises in the context of the genetic toggle switch. Finally, we draw some conclusions in Section 5.

For the reader's convenience, our most technical calculations and proofs are deferred to several appendices, which we recommend skipping on first reading. We do, however, recommend reading the proof of Proposition 2.1 in Section 2.3, since it provides valuable insights into the workings of our method. Note also that the appendices are sorted by their order of dependence and should thus be read in order.

Notation and Assumptions

Throughout this paper we make the following assumptions on the Hamiltonian $H(x,\theta) : D \times \mathbb{R}^n \to \mathbb{R}$ in (1.2), where the domain D is an open connected subset of $\mathbb{R}^n$ (in the introduction we used $D = \mathbb{R}^n$ for simplicity):

ASSUMPTION 1 *For every $x \in D$ we have $H(x,0) \leq 0$.*

ASSUMPTION 2 *$H(\cdot,\cdot)$ is twice continuously differentiable.*

ASSUMPTION 3 *$H_{\theta\theta}(x,\cdot)$ is uniformly elliptic on compact sets; i.e., there exists a function $m(x)$ such that for $\forall \xi, \theta \in \mathbb{R}^n : \langle \xi, H_{\theta\theta}(x,\theta)\xi\rangle \geq m(x)|\xi|^2$, and for every compact set $K \subset D$ we have $m_K := \inf_{x\in K} m(x) > 0$.*

REMARK 1.1 Equivalently, one can rephrase these assumptions in terms of the Lagrangian $L(x,y)$ defined in (1.2) by requiring that $L(x,y) \geq 0$ for every $x \in D$ and $y \in \mathbb{R}^n$, and that Assumptions 2 and 3 hold with H replaced by L.

For every $T > 0$ we denote by $C(0,T)$ the space of all continuous functions $f : [0,T] \to D$ equipped with the supremum norm $|f|_{[0,T]} := \sup_{t\in[0,T]} |f(t)|$, and by $\bar{C}(0,T)$ the subspace of all such functions that are absolutely continuous. For every $x_1, x_2 \in D$ we further define the subspaces

$$\bar{C}_{x_1}(0,T) = \{f \in \bar{C}(0,T) \mid f(0) = x_1\},$$
$$\bar{C}_{x_1}^{x_2}(0,T) = \{f \in \bar{C}(0,T) \mid f(0) = x_1,\ f(T) = x_2\}.$$

For every function $f \in \bar{C}(0,T)$ we denote its graph as

$$\gamma(f) := \{f(t) \mid t \in [0,T]\}.$$

We say that two functions $f_1 \in \bar{C}(0,T_1)$ and $f_2 \in \bar{C}(0,T_2)$ traverse the same curve and write

$$\gamma(f_1) = \gamma(f_2)$$

if there exists a (necessarily unique) curve $\varphi \in \bar{C}(0,1)$ with $|\varphi'| \equiv cst$ a.e. and two absolutely continuous rescalings $\alpha_1 : [0,T_1] \to [0,1]$ and $\alpha_2 : [0,T_2] \to [0,1]$ with $\alpha_1', \alpha_2' \geq 0$ a.e. such that

$$\varphi(\alpha_1(t)) = f_1(t) \quad \text{for every } t \in [0,T_1],$$
$$\varphi(\alpha_2(t)) = f_2(t) \quad \text{for every } t \in [0,T_2].$$

We denote the space of all functions g traversing the curve of a given function $f \in \bar{C}(0,T_f)$ within a fixed time T by

$$\bar{C}_f(0,T) := \{g \in \bar{C}(0,T) \mid \gamma(g) = \gamma(f)\}.$$

To express the distance between two functions $f_1 \in \bar{C}(0,T_1)$ and $f_2 \in \bar{C}(0,T_2)$, we either use the pointwise distance $|f_1 - f_2|_{[0,T_1]}$ (if $T_1 = T_2$), or for more geometrical statements we use the Fréchet distance defined as

$$\rho(f_1,f_2) = \inf_{\substack{t_1:[0,1]\to[0,T_1]\\ t_2:[0,1]\to[0,T_2]}} \left|f_1 \circ t_1 - f_2 \circ t_2\right|_{[0,1]}, \tag{1.20}$$

where the infimum is taken over all weakly increasing, continuous, surjective reparametrizations t_1 and t_2 only. (One can quickly check that $\rho(f_1, f_2) = 0$ if $\gamma(f_1) = \gamma(f_2)$.)

We use subscripts to denote differentiation, i.e., $H_\theta(x, \theta) = \frac{\partial H}{\partial \theta}$, etc., and regard all vectors (including gradients) as column vectors.

We introduce the following notation for the Lagrangian:

$$L(x, y) = \sup_{\theta \in \mathbb{R}^n} \big(\langle y, \theta \rangle - H(x, \theta)\big) \tag{1.21}$$

$$= \langle y, \theta^*(x, y) \rangle - H(x, \theta^*(x, y)), \tag{1.22}$$

where the maximizer $\theta^*(x, y)$ is implicitly (and due to Assumption 3 uniquely) defined by

$$H_\theta(x, \theta^*(x, y)) = y. \tag{1.23}$$

Finally, we call a point $x \in D$ a critical point if

$$H(x, 0) = 0 \quad \text{and} \quad H_\theta(x, 0) = 0. \tag{1.24}$$

REMARK 1.2 Note that in the examples treated in this paper, i.e., for the Hamiltonians (1.4) and (1.6), we actually have equality in Assumption 1 so that the requirement $H(x, 0) = 0$ in (1.24) is redundant. However, the weaker Assumption 1 allows for a broader class of applications, as we will show in the conclusions of this paper (Section 5). In fact, in the example in Section 5, it is the *first* condition in (1.24) that is the decisive one, whereas the second one is fulfilled by every point $x \in D$. Our motivation to define critical points in the general case via (1.24) will become clear later in Lemmas 2.2 and 2.8 (see Remark 2.9).

2 Theoretical Background

2.1 A Large-Deviations Action on the Space of Curves

We collect our main theoretical results regarding the quasi-potential $V(x_1, x_2)$ defined in (1.9), with S_T given by (1.1), in the following proposition, whose proof will be carried out in Section 2.3.

PROPOSITION 2.1

(i) *Under Assumptions* 1–3 *the following two representations of the quasi-potential are equivalent*:

$$V(x_1, x_2) = \inf_{T>0} \inf_{\psi \in \bar{C}^{x_2}_{x_1}(0,T)} S_T(\psi), \tag{2.1}$$

$$V(x_1, x_2) = \inf_{\varphi \in \bar{C}^{x_2}_{x_1}(0,1)} \hat{S}(\varphi), \tag{2.2}$$

where for every $\varphi \in \bar{C}(0,1)$ *the action* $\hat{S}(\varphi)$ *is given by any of the following four equivalent expressions*:

$$\hat{S}(\varphi) = \inf_{T>0} \inf_{\psi \in \bar{C}_\varphi(0,T)} S_T(\psi), \tag{2.3}$$

$$\hat{S}(\varphi) = \sup_{\substack{\vartheta:[0,1]\to\mathbb{R}^n \\ H(\varphi,\vartheta)\equiv 0}} \int_0^1 \langle \varphi', \vartheta \rangle d\alpha, \tag{2.4}$$

$$\hat{S}(\varphi) = \int_0^1 \langle \varphi', \hat{\vartheta}(\varphi,\varphi') \rangle d\alpha, \tag{2.5}$$

$$\hat{S}(\varphi) = \int_0^1 \frac{L(\varphi, \lambda\varphi')}{\lambda}\, d\alpha, \quad \lambda = \lambda(\varphi,\varphi'). \tag{2.6}$$

Here $L(x,y)$ *is the Lagrangian associated with the Hamiltonian* $H(x,\theta)$ *through* (1.21)*, and the functions* $\hat{\vartheta}(x,y)$ *and* $\lambda(x,y)$ *are implicitly defined for all* $x \in D$ *and* $y \in \mathbb{R}^n \setminus \{0\}$ *as the unique solution* $(\hat{\vartheta}, \lambda) \in \mathbb{R}^n \times [0,\infty)$ *of the system*

$$H(x,\hat{\vartheta}) = 0, \quad H_\theta(x,\hat{\vartheta}) = \lambda y, \quad \lambda \geq 0. \tag{2.7}$$

When $\varphi' = 0$ *or* $\lambda(\varphi,\varphi') = 0$*, the integrands in* (2.5) *and* (2.6) *are interpreted as* 0.

(ii) *The functional* $\hat{S}(\varphi)$ *is invariant under reparametrization of* φ *in the sense that* $\hat{S}(\varphi_1) = \hat{S}(\varphi_2)$ *if* $\gamma(\varphi_1) = \gamma(\varphi_2)$*. Thus the infimum in* (2.2) *may be taken subject to some additional constraint on the parametrization of* φ*, e.g., that* $|\varphi'| = cst$ *almost everywhere.*

(iii) *Assume that the sequence* $((T_k, \psi_k))_{k\in\mathbb{N}}$*,* $T_k > 0$*,* $\psi_k \in \bar{C}^{x_2}_{x_1}(0,T_k)$ *for every* $k \in \mathbb{N}$*, is a minimizing sequence of* (2.1) *and that the lengths of the curves of* ψ_k *are uniformly bounded, i.e.,*

$$\lim_{k\to\infty} S_{T_k}(\psi_k) = V(x_1,x_2) \quad \textit{and} \quad \sup_{k\in\mathbb{N}} \int_0^{T_k} |\dot{\psi}_k| dt < \infty. \tag{2.8}$$

Then the infimum in (2.2) *has a minimizer* $\varphi^\star$*, and for some subsequence* $(\psi_{k_l})_{l\in\mathbb{N}}$ *we have that*

$$\lim_{l\to\infty} \rho(\psi_{k_l}, \varphi^\star) = 0, \tag{2.9}$$

where ρ *denotes the Fréchet distance. If* $\varphi^\star$ *is unique up to reparametrization (i.e., if* $\gamma(\tilde{\varphi}) = \gamma(\varphi^\star)$ *for every minimizer* $\tilde{\varphi}$ *of* $\hat{S}$*), then the full sequence* $(\psi_k)_{k\in\mathbb{N}}$ *converges to* $\varphi^\star$ *in the Fréchet distance.*

At the end of this section we specialize the results in this proposition to the case of diffusions and derive expression (1.18). The probabilistic interpretation of Proposition 2.1 is discussed in Section 2.2.

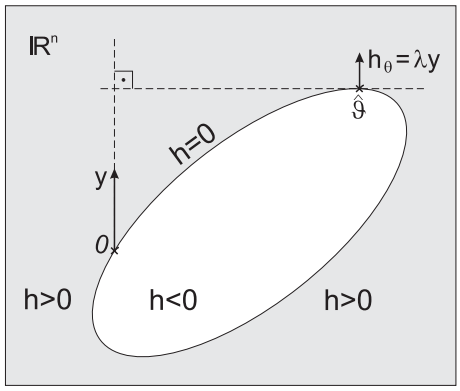

FIGURE 2.1. Illustration of the system of equations (2.7) for fixed x and y, with $h(\theta) := H(x,\theta)$: $\hat{\vartheta}$ is the extremal point of $\{\theta \in \mathbb{R}^n \mid h(\theta) \le 0\}$ in direction y; λ is then the value such that $h_\theta(\hat{\vartheta}) = \lambda y$.

We comment on the meaning of the various quantities entering Proposition 2.1, starting with the action $\hat{S}(\varphi)$. The function $\hat{S}(\varphi)$ can be viewed as the rate function on the space of curves (constructed in a way reminiscent of the contraction principle of large deviations theory; see (2.3)). Indeed, $\hat{S}(\varphi)$ is invariant under reparametrization of φ (this is part (ii) of Proposition 2.1, which is a consequence of (2.3)), and one should think of the integrals (2.4)–(2.6) as line integrals such as

$$\hat{S}(\varphi) = \int_{\gamma(\varphi)} \langle \hat{\vartheta}(z, \hat{\tau}_z), dz \rangle = \int_{\gamma(\varphi)} \frac{L(z, \hat{\tau}_z \lambda)}{\lambda}\, ds, \quad \lambda = \lambda(z, \hat{\tau}_z), \tag{2.10}$$

where $\hat{\tau}_z$ denotes the unit tangent vector along the curve. Note that this invariance also means that in order to make the minimizer $\varphi^\star$ (as opposed to $\gamma(\varphi^\star)$) unique, one has to decide for a constraint on its parametrization, such as $|\varphi'| = cst$ almost everywhere.

Consider now the other two important quantities in Proposition 2.1, $\hat{\vartheta}(x,y)$ and $\lambda(x,y)$. The meaning of the system of equations (2.7) that defines the functions $\hat{\vartheta}(x,y)$ and $\lambda(x,y)$ can be understood as follows: $\hat{\vartheta}(x,y)$ is the extremal point of the set $\{\theta \in \mathbb{R}^n \mid H(x,\theta) \le 0\}$ in the direction y (see the illustration in Figure 2.1); therefore $H_\theta(x,\hat{\vartheta})$ is parallel to y, and $\lambda(x,y)$ is the factor such that $H_\theta(x,\hat{\vartheta}) = \lambda y$. One can quickly check the properties

$$\hat{\vartheta}(x,cy) = \hat{\vartheta}(x,y) \quad \text{and} \quad c\lambda(x,cy) = \lambda(x,y) \quad \text{for } \forall c > 0, \tag{2.11}$$

which are used to show that the representations (2.5) and (2.6) of $\hat{S}$ are invariant under reparametrization of φ (Proposition 2.1(ii); see also Lemma A.1 in Appendix A).

Two further interpretations of λ are: (i) $\lambda(x,y)y$ is the optimal speed for moving in a given direction y starting from point x (this will become clear in the proof

of Proposition 2.1), and (ii) λ is the Lagrange multiplier used to enforce the constraint in (2.4). λ can also be used as an indicator that tells us where the curve passes a critical point, as part (i) of the following lemma shows.

LEMMA 2.2

(i) *Let $y \neq 0$. Then x is a critical point if and only if $\lambda(x, y) = 0$.*
(ii) *If x is a critical point and $y \neq 0$, then $\hat{\vartheta}(x, y) = 0$.*
(iii) *If x is a critical point, then for $\forall y \in \mathbb{R}^n$: $\lim_{\lambda \to 0^+} L(x, \lambda y)/\lambda = 0$.*
(iv) *Thus the local action of $\hat{S}$, given by any of the integrands in* (2.4)–(2.6) (*in* (2.4) *including the pointwise supremum over ϑ), vanishes as φ passes a critical point.*

The proof of Lemma 2.2 is carried out in Appendix B. Note also that parts (i) and (iii) explain why we have to interpret the integrand in (2.6) as 0 if $\lambda = 0$.

The Case of Diffusion Processes

$L(x, y)$ is available explicitly (see (1.4)) if we specialize to diffusion processes whose dynamics is given by (1.3), and this allows us to give a closed-form formula also for $\hat{S}(\varphi)$. A quick calculation shows that in this case

$$\hat{\vartheta}(x, y) = a^{-1}(x)\left(\frac{|b(x)|_a}{|y|_a} y - b(x)\right), \tag{2.12}$$

$$\lambda(x, y) = \frac{|b(x)|_a}{|y|_a}. \tag{2.13}$$

As a result, $\hat{S}(\varphi)$ as given by (2.5), and (2.6) reduces to

$$\hat{S}(\varphi) = \int_0^1 (|\varphi'|_a |b(\varphi)|_a - \langle \varphi', b(\varphi) \rangle_a) d\alpha \quad \text{(SDE)}, \tag{2.14}$$

consistent with (1.18).

2.2 Probabilistic Interpretation

The minimizing curve $\gamma(\varphi^\star)$ in Proposition 2.1(iii) also has a probabilistic interpretation: Let $\{(X_t^\varepsilon)_{t \geq 0},\ \varepsilon > 0\}$ be a family of processes that for every fixed $T > 0$ in the limit $\varepsilon \to 0$ satisfy a large deviations principle with respect to the metric induced by $|\cdot|_{[0,T]}$, and let the associated rate function S_T be of the form (1.1), where the Hamiltonian H fulfills Assumptions 1–3. Then the statement in Proposition 2.3 holds.

Put simply, Proposition 2.3 says the following (under certain technical assumptions): Given that a transition from x_1 to a small ball around x_2 occurs before some finite time T close to some $T^\star = T^\star(\varphi^\star)$, the probability that the process follows $\gamma(\varphi^\star)$ throughout this transition goes to 1 as $\varepsilon \to 0$. ($T^\star$ can be interpreted as the "maximum likelihood transition time," and we will show later that $T^\star = \infty$ if x_1 or x_2 is a critical point; see Section 2.4.)

The precise statement is as follows:

PROPOSITION 2.3 *Assume that the action $\hat{S}$ has a minimizer $\varphi^\star$ among all curves leading from $x_1 \in D$ to $x_2 \in D$, and that this minimizer is unique up to reparametrization. Define $T^\star := \int_0^1 1/\lambda(\varphi^\star, \varphi^{\star\prime})d\alpha \in (0,\infty]$, and for any $\delta > 0$ and any path $\psi : [0,T] \to D$, $T > 0$, let $\tau_\delta(\psi)$ denote the first time the path ψ hits the closed ball $B_\delta(x_2)$.*

Further, assume that for all $\delta, T > 0$ sufficiently close to 0 and $T^\star$, respectively, there exists a unique path $\psi_{\delta,T} \in \bar{C}_{x_1}(0,T)$ such that

$$S_T(\psi_{\delta,T}) = \inf_{\substack{\psi \in \bar{C}_{x_1}(0,T) \\ \tau_\delta(\psi) \le T}} S_T(\psi),$$

and such that the length and the endpoint of this path fulfill

$$\limsup_{\substack{\delta \to 0^+ \\ T \to T^\star}} \int_0^T |\dot{\psi}_{\delta,T}| dt < \infty \quad \text{and} \quad \lim_{\substack{\delta \to 0^+ \\ T \to T^\star}} \psi_{\delta,T}(T) = x_2. \tag{2.15}$$

Then for every $\eta > 0$ we have

$$\lim_{\substack{\delta \to 0^+ \\ T \to T^\star}} \liminf_{\varepsilon \to 0} \mathbb{P}\big(\rho\big(X^\varepsilon|_{[0,\tau_\delta(X^\varepsilon)]}, \varphi^\star\big) \le \eta \;\big|\; \tau_\delta(X^\varepsilon) \le T\big) = 1, \tag{2.16}$$

where ρ is the Fréchet distance. Equation (2.16) *remains true if $X^\varepsilon|_{[0,\tau_\delta(X^\varepsilon)]}$ is replaced by $X^\varepsilon|_{[0,T]}$.*

REMARK 2.4

(i) The form of equation (2.16) was chosen to resemble formula (1.10). We actually prove a stronger statement, namely, that for δ and T fixed and sufficiently close to 0 and $T^\star$, respectively, the lim inf in (2.16) as $\varepsilon \to 0$ is *equal* to 1.

(ii) The second condition in (2.15) can be shown to hold whenever x_1 is a critical point, or under other technical assumptions (such as bounded lengths of the paths $\psi_{\delta,T}$ *in phase space* if $T^\star$ is finite). We decided not to go any further here in order to keep the length of the proof within reasonable limits.

SKETCH OF PROOF: The proof of this proposition relies on three rather technical statements (Steps 1–3 below) whose proofs can be found in Appendix D. Note that the proof of Step 2 requires techniques that we will only develop in the proof of Proposition 2.1 in Section 2.3.

First we would like to estimate the probability in (2.16) below by the same expression with $X^\varepsilon|_{[0,\tau_\delta(X^\varepsilon)]}$ replaced by $X^\varepsilon|_{[0,T]}$ (and then show that the resulting expression still converges to 1). Since replacing $X^\varepsilon|_{[0,\tau_\delta(X^\varepsilon)]}$ by $X^\varepsilon|_{[0,T]}$ can potentially decrease the Fréchet distance and thus increase the probability, we have to decrease η at the same time. This is done as follows:

Step 1. There exists an $\tilde{\eta} > 0$ such that for small enough δ

$$\rho(X^\varepsilon|_{[0,T]}, \varphi^\star) \le \tilde{\eta} \text{ and } \tau_\delta(X^\varepsilon) \le T \quad \Rightarrow \quad \rho(X^\varepsilon|_{[0,\tau_\delta(X^\varepsilon)]}, \varphi^\star) \le \eta. \tag{2.17}$$

We then want to replace $\varphi^\star$ by $\psi_{\delta,T}$ since we expect X^ε to be close to $\psi_{\delta,T}$ (even pointwise). This can be achieved by showing

Step 2. $\lim_{(T,\delta)\to(T^\star,0^+)} \rho(\psi_{\delta,T},\varphi^\star) = 0$.

Putting both steps together, we find that if δ is small enough so that (2.17) is true, and if δ and T are also close enough to 0 and $T^\star$ so that $\rho(\psi_{\delta,T},\varphi^\star) \le \frac{1}{2}\tilde\eta$, then we have

$$\begin{aligned} 1 &\ge \mathbb{P}\big(\rho(X^\varepsilon|_{[0,\tau_\delta(X^\varepsilon)]},\varphi^\star) \le \eta \mid \tau_\delta(X^\varepsilon) \le T\big) \\ &\ge \mathbb{P}\big(\rho(X^\varepsilon|_{[0,T]},\varphi^\star) \le \tilde\eta \mid \tau_\delta(X^\varepsilon) \le T\big) \\ &\ge \mathbb{P}\big(\rho(X^\varepsilon|_{[0,T]},\psi_{\delta,T}) \le \tfrac{1}{2}\tilde\eta \mid \tau_\delta(X^\varepsilon) \le T\big) \\ &\ge \mathbb{P}\big(|X^\varepsilon - \psi_{\delta,T}|_{[0,T]} \le \tfrac{1}{2}\tilde\eta \mid \tau_\delta(X^\varepsilon) \le T\big). \end{aligned} \tag{2.18}$$

Now it suffices to show

Step 3. For all $T,\delta > 0$ the set of paths $\{\psi \in \bar C_{x_1}(0,T) \mid \tau_\delta(\psi) \le T\}$ is regular with respect to S_T (i.e., the minimal action on the closure of that set is the same as the one on its interior; see [6, p. 85]). Then, since $\psi_{\delta,T}$ is the unique minimizer of the action S_T on the set of paths $\{\psi \in \bar C_{x_1}(0,T) \mid \tau_\delta(\psi) \le T\}$, by [6, p. 86, theorem 3.4] the lower bound in (2.18) converges to 1 as $\varepsilon \to 0$, thus terminating the proof. □

2.3 Lower Semicontinuity of $\hat S$ and Proof of Proposition 2.1

The proof of part (iii) of Proposition 2.1 relies on parts (ii) and (iii) of the following lemma, which states some important technical properties of the action $\hat S(\varphi)$. The proof of this lemma will be carried out in Appendix C.

LEMMA 2.5

(i) *For every $M > 0$ and every compact set $X \subset D$, the set*

$$C_{X,M} := \{\varphi \in \bar C(0,1) \mid \varphi(0) \in X,\ |\varphi'| \le M \text{ a.e.}\} \tag{2.19}$$

is a compact subset of $C(0,1)$.

(ii) *For every $x_1, x_2 \in D$ and every $M > 0$, the set*

$$C_M^{x_1,x_2} := \{\varphi \in \bar C_{x_1}^{x_2}(0,1) \mid |\varphi'| \le M \text{ a.e.}\} \tag{2.20}$$

is a compact subset of $C(0,1)$.

(iii) *For every $M > 0$ and every compact $X \subset D$, the functional $\hat S : C_{X,M} \to \mathbb{R}$ defined by* (2.3)–(2.6) *is lower-semicontinuous with respect to uniform convergence.*

(iv) *$\hat S$ attains its infimum on every nonempty closed subset of $C_{X,M}$. Specifically, it attains its infimum on the sets $C_M^{x_1,x_2}$.*

We can now begin with the proof of Proposition 2.1, which generalizes the heuristic argument given in Section 1.3 for the case of diffusions.

PROOF OF PROPOSITION 2.1:

(i) and (ii): The main idea of the proof is to rewrite the quasi-potential as

$$\begin{aligned} V(x_1,x_2) &= \inf_{T>0} \inf_{\psi\in\bar{C}_{x_1}^{x_2}(0,T)} S_T(\psi) \\ &= \inf_{T>0} \inf_{\varphi\in\bar{C}_{x_1}^{x_2}(0,1)} \inf_{\psi\in\bar{C}_{\varphi}(0,T)} S_T(\psi) \\ &= \inf_{\varphi\in\bar{C}_{x_1}^{x_2}(0,1)} \Big(\inf_{T>0} \inf_{\psi\in\bar{C}_{\varphi}(0,T)} S_T(\psi)\Big) \\ &=: \inf_{\varphi\in\bar{C}_{x_1}^{x_2}(0,1)} \hat{S}(\varphi), \end{aligned} \tag{2.21}$$

where $\hat{S}(\varphi)$ is defined by (2.3). Note that it is clear from definition (2.3) that $\hat{S}(\varphi)$ actually depends only on the curve that φ traverses and not on the specific parametrization of φ (which already proves part (ii)). Therefore, to prove that $\hat{S}(\varphi)$ as defined in (2.3) can also be written in the forms (2.4)–(2.6), it is enough to restrict ourselves to all those functions $\varphi \in \bar{C}_{x_1}^{x_2}(0,1)$ with the additional property that $|\varphi'| \equiv cst$ almost everywhere, and then to show that the representations (2.4)–(2.6) are invariant under reparametrization as well.

To do so, let $\varphi \in \bar{C}_{x_1}^{x_2}(0,1)$ be given with $|\varphi'| \equiv cst$ almost everywhere. To get a lower bound for $\hat{S}(\varphi)$, we estimate, for any $T>0$ and any path $\psi \in \bar{C}_{\varphi}(0,T)$,

$$\begin{aligned} S_T(\psi) = \int_0^T L(\psi,\dot{\psi})dt &= \int_0^T \sup_{\theta\in\mathbb{R}^n} (\langle\dot{\psi},\theta\rangle - H(\psi,\theta))dt \\ &\geq \int_0^T \sup_{\substack{\theta\in\mathbb{R}^n \\ H(\psi,\theta)=0}} (\langle\dot{\psi},\theta\rangle - H(\psi,\theta))dt \\ &= \int_0^T \sup_{\substack{\theta\in\mathbb{R}^n \\ H(\psi,\theta)=0}} \langle\dot{\psi},\theta\rangle dt = \int_0^1 \sup_{\substack{\theta\in\mathbb{R}^n \\ H(\varphi,\theta)=0}} \langle\varphi',\theta\rangle d\alpha, \end{aligned}$$

where in the last step we applied Lemma A.1 in Appendix A, with $\ell(x,y) := \sup_{\theta\in\mathbb{R}^n,\, H(x,\theta)=0}\langle y,\theta\rangle$. Since the last expression depends only on φ, this shows that the representations (2.4) and (2.5) are lower bounds for $\hat{S}(\varphi)$:

$$\begin{aligned} \hat{S}(\varphi) &= \inf_{T>0} \inf_{\psi\in\bar{C}_{\varphi}(0,T)} S_T(\psi) \\ &\geq \int_0^1 \sup_{\substack{\theta\in\mathbb{R}^n \\ H(\varphi,\theta)=0}} \langle\varphi',\theta\rangle d\alpha \geq \int_0^1 \langle\varphi',\hat{\vartheta}(\varphi,\varphi')\rangle d\alpha, \end{aligned} \tag{2.22}$$

where we used the first equation in (2.7). To obtain an upper bound on $\hat{S}(\varphi)$, define a minimizing sequence $((T_k, \psi_k))_{k\in\mathbb{N}}$ as follows: For every $k \in \mathbb{N}$ let

$$\begin{aligned}
\lambda_k(\alpha) &:= \max\left\{\lambda(\varphi(\alpha), \varphi'(\alpha)), \frac{1}{k}\right\}, \quad \alpha \in [0,1],\\
G_k(\alpha) &:= \int_0^\alpha \frac{1}{\lambda_k}\, da, \qquad\qquad \alpha \in [0,1],\\
T_k &:= G_k(1),\\
\psi_k(t) &:= \varphi(G_k^{-1}(t)), \qquad\qquad t \in [0, T_k].
\end{aligned} \tag{2.23}$$

Since for the rescaling $\alpha(t) := G_k^{-1}(t)$ we have $\alpha'(t) = \lambda_k(\alpha(t))$ and thus $1/k \le \alpha'(t) \le |\lambda_k|_\infty < \infty$ for every $t \in [0, T_k]$ (see Lemma A.3 in Appendix A), $\alpha(t)$ is absolutely continuous. Therefore we see from (2.23) that $\gamma(\psi_k) = \gamma(\varphi)$, i.e., $\psi_k \in \bar{C}_\varphi(0, T_k)$.

To compute $S_{T_k}(\psi_k)$, we perform the change of variables $t = t(\alpha) = G_k(\alpha)$ so that $dt = d\alpha/\lambda_k$, $\varphi(\alpha) = \psi_k(G_k(\alpha))$, and

$$\varphi'(\alpha) = \dot{\psi}_k(t) G_k'(\alpha) = \dot{\psi}_k(t)/\lambda_k(\alpha),$$

and we find that

$$S_{T_k}(\psi_k) = \int_0^{T_k} L(\psi_k, \dot{\psi}_k) dt = \int_0^1 \frac{L(\varphi, \varphi'\lambda_k)}{\lambda_k}\, d\alpha. \tag{2.24}$$

Since the integrand on the right-hand side is uniformly bounded in k (see again Lemma A.3), to compute the limit of (2.24) as $k \to \infty$, we can exchange limit and integral and obtain the upper bound

$$\begin{aligned}
\hat{S}(\varphi) &= \inf_{T>0} \inf_{\psi\in\bar{C}_\varphi(0,T)} S_T(\psi)\\
&\le \lim_{k\to\infty} S_{T_k}(\psi_k) = \int_0^1 \frac{L(\varphi, \varphi'\lambda)}{\lambda}\, d\alpha, \quad \lambda = \lambda(\varphi, \varphi'),
\end{aligned} \tag{2.25}$$

which is representation (2.6), where we interpret $L(\varphi, \varphi'\lambda)/\lambda = 0$ if $\lambda = 0$, due to Lemma 2.2(i) and (iii).

To show that the integrands of the lower bound in (2.22) and the upper bound in (2.25) are the same, consider first the case $\lambda > 0$. The maximizing θ in the expression

$$\frac{L(\varphi, \varphi'\lambda)}{\lambda} = \sup_{\theta\in\mathbb{R}^n} \left(\langle \varphi', \theta\rangle - \frac{H(\varphi, \theta)}{\lambda}\right)$$

has to fulfill the first- and second-order conditions that

$$\varphi' - \frac{H_\theta(\varphi, \theta)}{\lambda} = 0 \quad \text{and} \quad -\frac{H_{\theta\theta}(\varphi, \theta)}{\lambda} \text{ is negative definite.}$$

By Assumption 3 and the second equation in (2.7), both conditions are fulfilled by $\theta = \hat{\vartheta}(\varphi, \varphi')$, so that in fact

$$\frac{L(\varphi, \varphi'\lambda)}{\lambda} = \langle \varphi', \hat{\vartheta} \rangle - \frac{H(\varphi, \hat{\vartheta})}{\lambda} = \langle \varphi', \hat{\vartheta} \rangle, \quad \hat{\vartheta} = \hat{\vartheta}(\varphi, \varphi'), \tag{2.26}$$

by also using the first relation in (2.7). When $\lambda = 0$, equation (2.26) holds as well because then $\hat{\vartheta} = 0$ due to Lemma 2.2(i) and (ii) and since we agreed on interpreting the left-hand side of (2.26) as 0 if $\lambda = 0$.

Therefore the lower bound in (2.22) and the upper bound in (2.25) are the same, and thus all four representations (2.3)–(2.6) of $\hat{S}(\varphi)$ are equal if $|\varphi'| \equiv cst$ almost everywhere.

To end the proof of part (i), it now remains only to show that the expressions (2.4)–(2.6) are invariant under reparametrization; i.e., for $\hat{S}$ given by any of the representations (2.4)–(2.6) and for any $\tilde{\varphi} \in \bar{C}_{\varphi}(0,1)$, we have $\hat{S}(\tilde{\varphi}) = \hat{S}(\varphi)$. But this is a direct consequence of Lemma A.1, the observations (2.11), and our agreement in the statement of Proposition 2.1 to interpret the integrands in (2.5) and (2.6) as 0 if $\varphi' = 0$.

(iii): The proof of part (iii) of Proposition 2.1 follows a standard argument based on the lower-semicontinuity of the functional $\hat{S}$ and the compactness of an appropriate set of functions, both of which were established in parts (ii) and (iii) of Lemma 2.5.

Let a sequence $((T_k, \psi_k))$ be given with the properties stated in Proposition 2.1(iii), and define the functions $\varphi_k \in \bar{C}_{\psi_k}(0,1)$ such that they traverse the curves $\gamma(\psi_k)$ at normalized unit speed, i.e., $|\varphi_k'| \equiv L_k$ a.e., where L_k is the length of the curve ψ_k, as follows:

Let $\alpha_k : [0, T_k] \to [0,1]$ be defined as $\alpha_k(t) := (1/L_k) \int_0^t |\dot{\psi}_k(\tau)| d\tau$, where $L_k = \int_0^{T_k} |\dot{\psi}_k(\tau)| d\tau$. Define its "inverse" as $\alpha_k^{-1}(\alpha) := \inf\{t \in [0,1] \mid \alpha_k(t) \geq \alpha\}$, and set $\varphi_k := \psi_k \circ \alpha_k^{-1}$. Then we have $\varphi_k(\alpha_k(t)) = \psi_k(t)$ for all $t \in [0, T_k]$, and both α_k and φ_k are absolutely continuous, with $\alpha_k' = |\dot{\psi}_k|/L_k$ and $|\varphi'| = (|\dot{\psi}_k|/\alpha_k') \circ \alpha_k^{-1} \equiv L_k$. Therefore we have $\gamma(\varphi_k) = \gamma(\psi_k)$, i.e., $\psi_k \in \bar{C}_{\varphi_k}(0, T_k)$.

Using (2.3), this gives us the estimate

$$\inf_{\varphi \in \bar{C}_{x_1}^{x_2}(0,1)} \hat{S}(\varphi) \leq \hat{S}(\varphi_k) = \inf_{T>0} \inf_{\psi \in \bar{C}_{\varphi_k}(0,T)} S_T(\psi) \leq S_{T_k}(\psi_k)$$

for every $k \in \mathbb{N}$. In the limit as $k \to \infty$, the right-hand side converges to the left-hand side, and it follows that

$$\lim_{k \to \infty} \hat{S}(\varphi_k) = \inf_{\varphi \in \bar{C}_{x_1}^{x_2}(0,1)} \hat{S}(\varphi). \tag{2.27}$$

Since $M := \sup_k |\varphi_k'| = \sup_k L_k < \infty$, the sequence $(\varphi_k)_{k \in \mathbb{N}}$ lies in the compact set $C_M^{x_1, x_2}$ defined in Lemma 2.5(ii), and thus there exists a subsequence (φ_{k_l}) that

converges uniformly to some limiting function $\varphi^\star \in C_M^{x_1,x_2}$. Now since $C_M^{x_1,x_2} \subset C_{\{x_1\},M}$, by Lemma 2.5(iii) and equation (2.27), we have

$$\hat{S}(\varphi^\star) \le \liminf_{l\to\infty} \hat{S}(\varphi_{k_l}) = \inf_{\varphi\in\bar{C}_{x_1}^{x_2}(0,1)} \hat{S}(\varphi),$$

and thus $\hat{S}(\varphi^\star) = \inf_\varphi \hat{S}(\varphi)$; i.e., $\varphi^\star$ is a minimizer of $\hat{S}$.

Since the functions φ_{k_l} are time-rescaled versions of the functions ψ_{k_l} and converge uniformly to $\varphi^\star$, this implies that

$$\rho(\psi_{k_l},\varphi^\star) = \rho(\varphi_{k_l},\varphi^\star) \le |\varphi_{k_l} - \varphi^\star|_{[0,1]} \to 0 \quad \text{as } l\to\infty,$$

which proves the first statement of part (iii).

To prove the second statement, assume now that the minimizer of $\hat{S}$ is unique up to reparametrization, let $\varphi^\star$ be the limit of some converging subsequence of (ψ_k) from the first part of the proof, and suppose that $\rho(\psi_k,\varphi^\star) \not\to 0$ as $k\to\infty$. Then we could construct a subsequence (ψ_{k_l}) such that

$$\inf_{l\in\mathbb{N}} \rho(\psi_{k_l},\varphi^\star) > 0. \tag{2.28}$$

But by the same arguments as above, this subsequence would have a subsubsequence $(\psi_{k_{l_m}})$ that converges in the Fréchet metric to some limit $\tilde{\varphi}$ that is a minimizer of $\hat{S}$. Now the uniqueness of the minimizer implies that $\gamma(\tilde{\varphi}) = \gamma(\varphi^\star)$, and thus we have $\rho(\psi_{k_{l_m}},\varphi^\star) = \rho(\psi_{k_{l_m}},\tilde{\varphi}) \to 0$ as $m\to\infty$, contradicting (2.28). □

REMARK 2.6 The formulas for $\hat{S}$, $\hat{\vartheta}$, and λ can also be derived as follows: Every $\psi \in \bar{C}_{x_1}^{x_2}(0,T)$ can be written as $\psi = \varphi\circ G^{-1}$, where $\varphi \in \bar{C}_{x_1}^{x_2}(0,1)$ follows the path of ψ at constant speed, and $G : [0,1] \to [0,T]$ is an appropriately chosen time rescaling. Minimizing over all ψ and T is therefore equivalent to minimizing over all functions φ and G. But after a change of variables we see that

$$S_T(\psi) = \int_0^T L(\psi,\dot{\psi})dt = \int_0^1 L(\varphi,\varphi'/g)g\,d\alpha,$$

where $g = G' : [0,1] \to (0,\infty)$. The second expression can now easily be minimized over all g (and thus over all G) by setting the derivative of the integrand equal to 0, which leads us directly to representations (2.5) and (2.6) and equations (2.7) for $\hat{\vartheta}$ and $\lambda := 1/g$.

This trick may also be useful for problems that do not directly fit into the framework of this paper.

2.4 Recovering the Time Parametrization

Since $\hat{S}(\varphi)$ is parametrization free, its minimizer $\varphi^\star$ only gives us information about the graph of the minimizer $\psi^\star$ of the original action $S_T(\psi)$ over both ψ and T (assuming that $\psi^\star$ exists), but not its parametrization by time. However, if the minimizing $T^\star$ is finite, we can recover $T^\star$ and the path $\psi^\star$ parametrized by

physical time afterwards by defining $G(\alpha) := \int_0^\alpha 1/\lambda(\varphi^\star, \varphi^{\star\prime})d\alpha$ for $\alpha \in [0,1]$, $T^\star := G(1)$, and setting $\psi^\star(t) := \varphi^\star(G^{-1}(t))$ for $t \in [0, T^\star]$, since then we have

$$S_{T^\star}(\psi^\star) = \int_0^{T^\star} L(\psi^\star, \psi^{\star\prime})dt = \int_0^1 \frac{L(\varphi^\star, \varphi^{\star\prime}\lambda)}{\lambda}\, d\alpha$$
$$= \hat{S}(\varphi^\star) = \inf_{\varphi \in \bar{C}^{x_2}_{x_1}(0,1)} \hat{S}(\varphi) = \inf_{T>0} \inf_{\psi \in \bar{C}^{x_2}_{x_1}(0,T)} S_T(\psi),$$

where we performed the change of variables $t = G(\alpha)$ and used (2.1) and (2.2).

If $T^\star = \int_0^1 1/\lambda(\varphi^\star, \varphi^{\star\prime})d\alpha = \infty$ (i.e., if "the minimizing $T^\star$ is infinite"), then no minimizer $(T^\star, \psi^\star)$ of the original action $S_T(\psi)$ exists, but we can still extract information from $\lambda(\varphi^\star, \varphi^{\star\prime})$ by splitting the curve into pieces on which λ is nonzero (i.e., into pieces that do not contain any critical points): The following proposition says that if we recover the parametrization on any such piece as above, then the resulting path will give us the optimal way to move from the starting point to the end point of that piece.

PROPOSITION 2.7 *Let $\varphi^\star$ be a minimizer of the functional $\hat{S}(\varphi)$ defined by* (2.3)–(2.6)*, parametrized such that $|\varphi^{\star\prime}| \equiv cst$ almost everywhere. Let $\alpha_1, \alpha_2 \in [0,1]$ be such that there is no critical point on $\gamma(\varphi^\star)$ between $\tilde{x}_1 := \varphi^\star(\alpha_1)$ and $\tilde{x}_2 := \varphi^\star(\alpha_2)$.*

Define the rescaling $G(\alpha) := \int_{\alpha_1}^\alpha 1/\lambda(\varphi^\star, \varphi^{\star\prime})da$, $\alpha \in [\alpha_1, \alpha_2]$, and then set $\tilde{\psi}^\star(t) := \varphi^\star(G^{-1}(t))$ for $t \in [0, \tilde{T}^\star]$, $\tilde{T}^\star := G(\alpha_2)$. Then we have

$$V(\tilde{x}_1, \tilde{x}_2) = \inf_{T>0} \inf_{\psi \in \bar{C}^{\tilde{x}_2}_{\tilde{x}_1}(0,T)} S_T(\psi) = S_{\tilde{T}^\star}(\tilde{\psi}^\star). \tag{2.29}$$

Proposition 2.7, which is proven at the end of this section, is relevant because $T^\star = \int_0^1 1/\lambda(\varphi^\star, \varphi^{\star\prime})d\alpha$ is infinite in most cases of interest, e.g., if at least one end point of the path is a critical point or if the path has to pass a critical point to connect the two given states: Part (ii) in the following lemma, which is a slightly stronger statement than Lemma 2.2(i), tells us that the minimizing path needs infinite time to leave, pass through, or reach any critical point of the system:

LEMMA 2.8 *Suppose that φ is parametrized such that $|\varphi'| \equiv cst$ a.e., and let $\alpha_c \in [0,1]$ be such that $\varphi(\alpha_c)$ is a critical point. Then*

(i) *$\lambda = \lambda(\varphi, \varphi')$ is Lipschitz-continuous at α_c in the sense that there exists a constant $C > 0$ such that for a.e. $\alpha \in [0,1]$, we have $\lambda\big(\varphi(\alpha), \varphi'(\alpha)\big) \le C|\alpha - \alpha_c|$.*

(ii) *$1/\lambda$ is not locally integrable at α_c. In particular, if the curve $\gamma(\varphi)$ contains a critical point, then $T^\star = \int_0^1 1/\lambda\, d\alpha = \infty$.*

The proof of this lemma is technical and is carried out in Appendix B.

REMARK 2.9 Recall in this context that for SDEs and continuous-time Markov chains, critical points are those points x with vanishing drift, $H_\theta(x,0) = 0$. For other Hamiltonians (see, e.g., Section 5), this may not be enough: In general, the point x also needs to fulfill $H(x,0) = 0$ to be a critical point, and then it takes infinite time to pass x. If, however, the point x fulfills $H(x,0) < 0$, then by Lemma 2.2 we have $\lambda(x,y) \neq 0$ for any direction $y \neq 0$, and therefore the point x is passed in finite time. This finally justifies our definition of critical points via (1.24): A point fulfills the properties (1.24) if and only if it is passed in infinite time.

PROOF OF PROPOSITION 2.7: First, note that since $\lambda(x,y)$ is continuous (even differentiable; see Lemma E.1 in Appendix E), we have

$$\operatorname*{ess\,inf}_{\alpha_1 \le \alpha \le \alpha_2} \lambda(\varphi^\star, \varphi^{\star\prime}) > 0,$$

and thus G is well-defined.

Now assume that (2.29) does not hold. Then there exist $\hat{T} > 0$ and $\hat{\psi} \in \bar{C}^{\tilde{x}_2}_{\tilde{x}_1}(0,\hat{T})$ such that $S_{\hat{T}}(\hat{\psi}) < S_{\tilde{T}^\star}(\tilde{\psi}^\star)$, i.e., $\eta := S_{\tilde{T}^\star}(\tilde{\psi}^\star) - S_{\hat{T}}(\hat{\psi}) > 0$. Observe that

$$\begin{aligned}
S_{\tilde{T}^\star}(\tilde{\psi}^\star) &= \int_0^{\tilde{T}^\star} L(\tilde{\psi}^\star, \tilde{\psi}^{\star\prime}) dt \\
&= \int_{\alpha_1}^{\alpha_2} \frac{L(\varphi^\star, \varphi^{\star\prime}\lambda)}{\lambda}\, d\alpha, \quad \lambda = \lambda(\varphi^\star, \varphi^{\star\prime}) \\
&= \int\limits_{\gamma(\varphi^\star|_{[\alpha_1,\alpha_2]})} \frac{L(z, \hat{\tau}_z\lambda)}{\lambda}\, ds, \quad \lambda = \lambda(z, \hat{\tau}_z) \\
&= \inf_{T>0} \inf_{\psi \in \bar{C}_{\varphi^\star|_{[\alpha_1,\alpha_2]}}(0,T)} S_T(\psi).
\end{aligned}$$

We will now use the path $\hat{\psi}$ to construct a contradiction to the minimizing property of $\varphi^\star$. To do so, define the sequence $((\psi_k, T_k))$ with $\psi_k \in \bar{C}_{\varphi^\star}(0,T_k)$ for all $k \in \mathbb{N}$ and with $\lim_{k\to\infty} S_{T_k}(\psi_k) = \hat{S}(\varphi^\star)$, as in the proof of Proposition 2.1(i). Now let T_1^k and T_2^k be such that $\psi_k(T_1^k) = \tilde{x}_1$ and $\psi_k(T_1^k + T_2^k) = \tilde{x}_2$, set $T_3^k := T_k - T_1^k - T_2^k$, and define the pieces ψ_1^k, ψ_2^k, and ψ_3^k by

$$\begin{aligned}
\psi_1^k(t) &= \psi_k(t), && t \in [0, T_1^k], \\
\psi_2^k(t) &= \psi_k(T_1^k + t), && t \in [0, T_2^k], \\
\psi_3^k(t) &= \psi_k(T_1^k + T_2^k + t), && t \in [0, T_3^k].
\end{aligned}$$

Finally, define the sequence $(\bar{T}_k, \bar{\psi}_k)$ by replacing the piece of ψ_k between $\tilde{x}_1$ and $\tilde{x}_2$ by $\hat{\psi}$ in order to reduce its action; i.e., let

$$\bar{\psi}_k(t) := \begin{cases} \psi_1^k(t), & t \in [0, T_1^k], \\ \hat{\psi}(t - T_1^k), & t \in [T_1^k, T_1^k + \hat{T}], \\ \psi_3^k(t - T_1^k - \hat{T}), & t \in [T_1^k + \hat{T}, T_1^k + \hat{T} + T_3^k], \end{cases}$$

and $\bar{T}_k := T_1^k + \hat{T} + T_3^k$. For this path we have

$$\begin{aligned} S_{\bar{T}_k}(\bar{\psi}_k) &= S_{T_1^k}(\psi_1^k) + S_{\hat{T}}(\hat{\psi}) + S_{T_3^k}(\psi_3^k) \\ &= S_{T_1^k}(\psi_1^k) + S_{\tilde{T}^\star}(\tilde{\psi}^\star) - \eta + S_{T_3^k}(\psi_3^k) \\ &= S_{T_1^k}(\psi_1^k) + \inf_{T>0} \inf_{\psi \in \bar{C}_{\varphi^\star|_{[\alpha_1,\alpha_2]}}(0,T)} S_T(\psi) - \eta + S_{T_3^k}(\psi_3^k) \\ &\le S_{T_1^k}(\psi_1^k) + S_{T_2^k}(\psi_2^k) - \eta + S_{T_3^k}(\psi_3^k) \\ &= S_{T_k}(\psi_k) - \eta \\ &\to \hat{S}(\varphi^\star) - \eta = \inf_{\varphi \in \bar{C}_{x_1}^{x_2}(0,1)} \hat{S}(\varphi) - \eta \\ &= \inf_{T>0} \inf_{\psi \in \bar{C}_{x_1}^{x_2}(0,T)} S_T(\psi) - \eta \end{aligned}$$

as $k \to \infty$. But this means that for sufficiently large k we have

$$S_{\bar{T}_k}(\bar{\psi}_k) < \inf_{T>0} \inf_{\psi \in \bar{C}_{x_1}^{x_2}(0,T)} S_T(\psi),$$

and since $\bar{\psi}_k \in \bar{C}_{x_1}^{x_2}(0, T_k)$ for every $k \in \mathbb{N}$, we have a contradiction. □

3 Numerical Algorithms

The main objective of this section is to design a numerical algorithm to compute the quasi-potential $V(x_1, x_2)$ via minimization of $\hat{S}(\varphi)$ and identify the minimizer $\varphi^\star$ such that

$$V(x_1, x_2) = \inf_{\varphi \in \bar{C}_{x_1}^{x_2}(0,1)} \hat{S}(\varphi) = \hat{S}(\varphi^\star), \tag{3.1}$$

where $\hat{S}(\varphi)$ is the action functional given by (2.3)–(2.6). We are primarily interested in cases where x_1 and x_2 in (3.1) are stable equilibrium points of the deterministic dynamics, $\dot{X}(t) = H_\theta(X(t), 0)$, although the algorithm presented below can also be applied to situations where x_1 and/or x_2 are not critical points.

Several strategies can be used for the minimization problem in (3.1). Here, we will proceed as follows: In Section 3.1, starting from the representation (2.5) we

will derive the Euler-Lagrange equation associated with the minimization of $\hat{S}(\varphi)$, assuming that $\hat{\vartheta}(\varphi, \varphi')$ is known. In Section 3.2 we will then design a (preconditioned) steepest-descent algorithm for the solution of the Euler-Lagrange equation. If no explicit formula for $\hat{\vartheta}(x, y)$ is available, this algorithm will compute $\hat{\vartheta}(x, y)$ in an inner loop, using an efficient quadratically convergent routine that is derived in Section 3.4. The steepest-descent algorithm is based on a proper discretization of the Euler-Lagrange equation and uses an interpolation-reparametrization step, similar to the one used in the string method [3], to enforce exactly a constraint on the parametrization of φ, such as $|\varphi'| = cst$. (As we mentioned in Section 2.1, such a constraint is necessary to make the minimizer $\varphi^\star$ of $\hat{S}$ unique.)

We note that the strategy above may not be the most efficient one: for instance, the nonlinear minimization problem in (2.2) could be tackled by discretizing the action $\hat{S}(\varphi)$ first, then using techniques other than steepest descent (like, e.g., a quasi-Newton method such as BFGS or conjugate gradient, or a multigrid method; cf. [14]). However, the approach that we take here has the advantage that it gives some insight into the nature of the action $\hat{S}(\varphi)$. It was also sufficient for our purpose: even the problem considered in Section 4.2, which involves a stochastic partial differential equation (in which case the path φ is not defined in $\mathbb{R}^n$ but rather in some Hilbert space), can be handled by our algorithm in a few minutes using Matlab on a standard workstation.

3.1 The Euler-Lagrange Equation and the Steepest-Descent Flow

We have the following result, whose proof is carried out in Appendix E:

PROPOSITION 3.1 *The Euler-Lagrange equation associated with the minimization problem in* (2.2) *can be written in the following two ways*:

$$\begin{cases} 0 = P_{\varphi'}(-\lambda^2\varphi'' + \lambda H_{\theta x}\varphi' - H_{\theta\theta}H_x) \\ \quad = -\lambda^2\varphi'' + \lambda H_{\theta x}\varphi' - H_{\theta\theta}H_x - \lambda\lambda'\varphi', \\ \varphi(0) = x_1,\ \varphi(1) = x_2, \end{cases} \tag{3.2}$$

$$\text{where} \quad \lambda = \frac{\langle H_\theta, \varphi'\rangle}{|\varphi'|^2} \quad \text{and} \quad P_{\varphi'} = I - \frac{\varphi' \otimes H_{\theta\theta}^{-1}\varphi'}{\langle \varphi', H_{\theta\theta}^{-1}\varphi'\rangle},$$

and where H_x, $H_{\theta x}$, *and* $H_{\theta\theta}$ *are evaluated at* $(\varphi, \hat{\vartheta}(\varphi, \varphi'))$.

The right-hand side in (3.2) is in fact $\lambda H_{\theta\theta} D\hat{S}(\varphi)$, where $D\hat{S}(\varphi)$ is the gradient of $\hat{S}(\varphi)$ with respect to the L^2 inner product. Note that by taking the Euclidean inner product of (3.2) with $\lambda^{-1}H_{\theta\theta}^{-1}\varphi'$, one can see that $\langle D\hat{S}(\varphi), \varphi'\rangle = 0$ for all α; i.e., the variation $D\hat{S}(\varphi)$ is everywhere perpendicular to the path with respect to the Euclidean metric. This is a simple consequence of the fact that $\hat{S}(\varphi)$ is

parametrization free: if id denotes the identity mapping on $[0, 1]$, then for any test function $\eta \in C_c^\infty(0,1)$ and sufficiently small $h > 0$ we have

$$\begin{aligned} 0 &= h^{-1}\big[\hat{S}(\varphi \circ (\mathrm{id} + h\eta)) - \hat{S}(\varphi)\big] \\ &= h^{-1}\big[\hat{S}(\varphi + h\eta\varphi' + o(h)) - \hat{S}(\varphi)\big] \\ &\to \langle D\hat{S}(\varphi), \eta\varphi'\rangle_{L^2([0,1];\,\mathbb{R}^n)} = \big\langle \langle D\hat{S}(\varphi), \varphi'\rangle, \eta\big\rangle_{L^2([0,1];\,\mathbb{R})} \quad \text{as } h \to 0. \end{aligned}$$

The algorithm presented in Section 3.2 finds the solution of (3.2) using a relaxation method based on a discretized version of the equation:

$$\text{(3.3)} \qquad \begin{cases} \dot{\varphi} = P_{\varphi'}\big(\lambda^2\varphi'' - \lambda H_{\theta x}\varphi' + H_{\theta\theta}H_x\big) + \mu\varphi' \\ \quad = \lambda^2\varphi'' - \lambda H_{\theta x}\varphi' + H_{\theta\theta}H_x + \lambda\lambda'\varphi' + \mu\varphi', \\ \varphi(\tau, 0) = x_1, \quad \varphi(\tau, 1) = x_2, \quad \varphi(0, \alpha) = \varphi^0(\alpha), \end{cases}$$

for $\alpha \in [0, 1]$ and $\tau \geq 0$. Here $\varphi = \varphi(\tau, \alpha)$ where τ is the artificial relaxation time, $\dot{\varphi} = \partial\varphi/\partial\tau$, $\varphi' = \partial\varphi/\partial\alpha$, $\varphi'' = \partial^2\varphi/\partial\alpha^2$, and $\mu\varphi'$ is a Lagrange multiplier term added to enforce some constraint on the parametrization of φ, e.g., by normalized arc length (in which case $|\varphi'(\tau, \cdot)| = cst(\tau)$ and the initial condition $\varphi(0, \alpha) = \varphi^0(\alpha)$ must be consistent with this constraint). Adding the term $\mu\varphi'$ has no effect on the graph $\gamma(\varphi)$ of the solution since $\hat{S}(\varphi)$ is parametrization free.

The simple form of (3.3) is a result of us building the flow on $\lambda H_{\theta\theta} D\hat{S}(\varphi)$ rather than $D\hat{S}(\varphi)$ alone, which is legitimate since $H_{\theta\theta}$ is a positive definite matrix by Assumption 1 and $\lambda \geq 0$. As we shall show in Section 4 where we analyze examples, this choice allows us to design an algorithm that achieves a good balance among speed, stability, and accuracy.

To further understand the properties of this flow, let us note that (3.3) can also be derived independently of the theory developed in Section 2:

REMARK 3.2 Another interpretation of the right-hand side of (3.3) is the following. Suppose that ψ is a minimizer of the original action $S_T(\psi)$ for fixed T; i.e., it satisfies the Hamiltonian system of ODEs, $\dot{\psi} = H_\theta(\psi, \theta)$, $\dot{\theta} = -H_x(\psi, \theta)$, subject to some boundary conditions. Let $\varphi(\alpha) = \psi(G(\alpha))$ and differentiate it twice in α to get

$$\lambda\varphi' = \dot{\psi} \circ G \quad \text{and} \quad \lambda^2\varphi'' + \lambda\lambda'\varphi' = \ddot{\psi} \circ G,$$

where $\lambda := 1/G'$. Now use the Hamilton equations for ψ to obtain the following second-order ODE for φ:

$$\begin{aligned} \ddot{\psi} &= H_{\theta x}\dot{\psi} + H_{\theta\theta}\dot{\theta} \\ &= H_{\theta x}\dot{\psi} - H_{\theta\theta}H_x \qquad \text{(3.4)} \\ \Leftrightarrow \quad \lambda^2\varphi'' + \lambda\lambda'\varphi' &= H_{\theta x}\lambda\varphi' - H_{\theta\theta}H_x \\ \Leftrightarrow \quad \lambda^2\varphi'' - \lambda H_{\theta x}\varphi' + H_{\theta\theta}H_x + \lambda\lambda'\varphi' &= 0. \qquad \text{(3.5)} \end{aligned}$$

The derivatives of H have to be evaluated at (φ, θ), which has to fulfill $H(\varphi, \theta) = cst$ and $H_\theta(\varphi, \theta) = \dot{\psi} = \lambda\varphi'$.

This shows the following property of the steady state solutions of (3.3):

LEMMA 3.3 *The flow in* (3.3) *has reached steady state if and only if*

(i) $\mu \equiv 0$ *and*
(ii) *the functions* ψ *corresponding to* (φ, λ) *in the sense of Proposition* 2.7 (*i.e., defined by pieces of* (φ, λ) *on which* $\lambda \neq 0$) *solve the second-order Hamiltonian ODE given by* H *on the energy level* $H = 0$; *i.e., they fulfill* (3.4) *and* $H \equiv 0$, *where* H *and all its derivatives are evaluated at* $(\psi, \theta^*(\psi, \dot{\psi}))$.

PROOF: Looking at the first representation of the flow in (3.3), we multiply the equation by $P_{\varphi'}$ and by $I - P_{\varphi'}$ to conclude that at steady state we must have $\mu\varphi' \equiv 0$ (and thus $\mu \equiv 0$) and

$$P_{\varphi'}(\lambda^2\varphi'' - \lambda H_{\theta x}\varphi' + H_{\theta\theta}H_x) = 0.$$

But as shown in Proposition 3.1, this equation is the same as (3.5), which by Remark 3.2 is equivalent to the second-order Hamiltonian ODE (3.4) for $\psi(t) = \varphi(G^{-1}(t))$, where $G' = 1/\lambda$ with

$$\lambda = \frac{\langle \varphi', H_\theta(\varphi, \hat{\vartheta}(\varphi, \varphi'))\rangle}{|\varphi'|^2} = \frac{\langle \varphi', \lambda(\varphi, \varphi')\varphi'\rangle}{|\varphi'|^2} = \lambda(\varphi, \varphi'),$$

as in the construction of Proposition 2.7. The energy level is 0 because we have

$$H(\psi, \theta^*(\psi, \dot{\psi})) \circ G = H(\varphi, \theta^*(\varphi, \varphi'\lambda)) = H(\varphi, \hat{\vartheta}(\varphi, \varphi')) \equiv 0.$$

□

The fact that at steady state we have $\mu \equiv 0$ also eliminates possible inaccuracies in the result of an algorithm based on discretizing (3.3), and it opens the door to methods for achieving second-order accuracy in α or higher even if the curve passes through critical points; see Section 3.3.

Also note that one could have designed the algorithm without the discussion in Section 2, solely on the basis of the observation in Remark 3.2. Within that approach, however, to show that (3.3) converges we would then have to look for a corresponding Lyapunov function for this equation, which is in fact given by $\hat{S}(\varphi)$.

3.2 The Outer Loop

To solve (3.3) in practice, we discretize first $\varphi(\tau, \alpha)$ both in τ and α; i.e., we define $\varphi_i^k = \varphi(k\triangle\tau, i\triangle\alpha)$, $k \in \mathbb{N}_0$, $i = 0, \ldots, N$, where $\triangle\tau$ is the time step and $\triangle\alpha = 1/N$ if we discretize the curve into $N + 1$ points. Then we discretize the initial condition $\varphi(0, \alpha)$ to obtain $\{\varphi_i^0\}_{i=0,\ldots,N}$ and, for $k \geq 0$, use the following two-step method to update these points:

(1) Given φ_i^k, compute $\varphi_i'^k = (\varphi_{i+1}^k - \varphi_{i-1}^k)/(2/N)$, $\hat{\vartheta}_i^k = \hat{\vartheta}(\varphi_i^k, \varphi_i'^k)$, and $\lambda_i^k = \langle H_\theta(\varphi_i^k, \hat{\vartheta}_i^k), \varphi_i'^k\rangle/|\varphi_i'^k|^2$ for $i = 1, \dots, N-1$, and set $\lambda_0^k = 3\lambda_1^k - 3\lambda_2^k + \lambda_3^k$ and $\lambda_N^k = 3\lambda_{N-1}^k - 3\lambda_{N-2}^k + \lambda_{N-3}^k$. Finally, compute $\lambda_i'^k = (\lambda_{i+1}^k - \lambda_{i-1}^k)/(2/N)$ for $i = 1, \dots, N-1$.

(2) Let $\{\tilde{\varphi}_i\}_{i=0,\dots,N}$ be the solution of the linear system

$$\begin{cases} \dfrac{\tilde{\varphi}_i - \varphi_i^k}{\triangle\tau} = (\lambda_i^k)^2 \dfrac{\tilde{\varphi}_{i+1} - 2\tilde{\varphi}_i + \tilde{\varphi}_{i-1}}{1/N^2} - \lambda_i^k H_{\theta x}\varphi_i'^k \\ \qquad\qquad + H_{\theta\theta}H_x + \lambda_i^k\lambda_i'^k\varphi_i'^k, \quad i = 1, \dots, N-1, \\ \tilde{\varphi}_0 = x_1, \\ \tilde{\varphi}_N = x_2, \end{cases} \tag{3.6}$$

where $H_{\theta x}$, $H_{\theta\theta}$, and H_x are evaluated at $(\varphi_i^k, \hat{\vartheta}_i^k)$.

(3) Interpolate a curve across $\{\tilde{\varphi}_i\}_{i=0,\dots,N}$ and discretize this curve to find $\{\varphi_i^{k+1}\}_{i=0,\dots,N}$ so that the prescribed constraint on the parametrization of φ is satisfied.

(4) Repeat until some stopping criterion is fulfilled.

Step 1 requires the computation of $\hat{\vartheta}(\varphi, \varphi')$. In the case of a diffusion, $\hat{\vartheta}(\varphi, \varphi')$ is given by (2.12). If $\hat{\vartheta}(\varphi, \varphi')$ is not available explicitly, it is computed using the algorithm given in Section 3.4 in an inner loop. Note that if x_1 or x_2 are critical points, then the calculations can be simplified by using that the corresponding values of $\hat{\vartheta}_{0,N}^k$ and $\lambda_{0,N}^k$ are 0.

Step 2 uses semi-implicit updating for stability: as will be shown via the examples in Section 4, proceeding this way makes the time step $\triangle\tau$ required for stability independent of $\triangle\alpha = 1/N$ (in contrast, an explicit step would require $\triangle\tau = O(\triangle\alpha^2)$). As a result, it accelerates the convergence rate (see the discussion in Section 3.3) and, in effect, amounts to preconditioning appropriately the steepest-descent scheme [13, 14]. In practice, it turns out that it is not necessary to treat the term $\lambda\lambda'\varphi'$ (which, when written out, contains the term φ'' as well) implicitly, since changes of the curve φ in the direction of φ' do not carry any information. Notice also that Step 2 is computationally straightforward since λ_i^k is scalar: hence the linear system can be solved component by component using, e.g., Thomas algorithm [13]. Finally, notice that a simple modification of (3.6) in Step 2 can be used to have the two end points of the curve fall into the nearest stable state by setting

$$\frac{\tilde{\varphi}_i - \varphi_i^k}{\triangle\tau} = H_\theta(\varphi_i^k, 0), \quad i = 0, N. \tag{3.7}$$

Step 3 is the interpolation-reparametrization step used to enforce the constraint on the parametrization of the curve $\gamma(\varphi)$. For instance, if we parametrize the curve by normalized arc length so that $|\varphi'| = cst$, this step amounts to redistributing the images along the interpolated curve in such a way that the points $\varphi_i^k, i = 0, \dots, N$,

be equidistant. Consistent with the order of accuracy at which we discretize the derivatives φ', φ'', etc., Step 3 can be done using linear interpolation that is second-order accurate if $\varphi \in C^1(0,1)$ (see the discussion about accuracy in Section 3.3).

Finally, the stopping criterion in Step 4 can be based on a slowdown in the movement of φ or in the decay of the action $\hat{S}(\varphi)$. Plotting the function $\alpha \mapsto \lambda(\varphi(\alpha), \varphi'(\alpha))$ at each iteration can further help to determine whether the algorithm has already converged: if one knows that the curve that one is looking for has to pass a saddle point, then λ must have a root in $(0,1)$ by Lemma 2.2(i) (see also Figure 4.3 in Section 4.1).

All in all, this algorithm is a blend between the original MAM [4] and the string method [3].

3.3 Recovering the Parametrization and Evaluating the Action

Other quantities of interest include the actual value of the action, the optimal transition time $T^\star$, and the path $\psi^\star$ parametrized by physical time. To compute those, one can then add the following steps:

(5) Given $\{\varphi_i^k\}_{i=0,\dots,N}$, compute $\varphi_i'^k$, $\hat{\vartheta}_i^k$, and λ_i^k as in Step 1 for every $i = 0,\dots,N$.
(6) Return the action

$$\hat{S} = \frac{1}{N}\left(\frac{3}{2}\langle \varphi_1'^k, \hat{\vartheta}_1^k\rangle + \sum_{i=2}^{N-2}\langle \varphi_i'^k, \hat{\vartheta}_i^k\rangle + \frac{3}{2}\langle \varphi_{N-1}'^k, \hat{\vartheta}_{N-1}^k\rangle\right).$$

(7) Set $t_0 = 0$ and

$$t_i = \frac{1}{2\lambda_0^k} + \frac{1}{\lambda_1^k} + \cdots + \frac{1}{\lambda_{i-1}^k} + \frac{1}{2\lambda_i^k}$$

for $i = 1,\dots,N$.
(8) Return the transition time $T^\star = t_N$.
(9) To add $D+1$ points at equidistant times to the graph of φ (if $T^\star < \infty$), interpolate the function $G^{-1}(t)$ given by the points $(t, G^{-1}(t)) = (t_i, i/N)$, $i = 0,\dots,N$, at the values $\tilde{t}_d = (d/D)T^\star$, $d = 0,\dots,D$, to obtain values $\alpha_d = G^{-1}(\tilde{t}_d)$, and then discretize the curve interpolated from $\{\varphi_i^k\}_{i=0,\dots,N}$ at those values α_d.

If $T^\star$ is infinite or very large (i.e., if $\lambda_i^k \approx 0$ for some index i), Step 9 can be performed on trimmed values $\tilde{\lambda}_i^k := \max\{\lambda_i^k, \eta\}$ (for some small $\eta > 0$): Proposition 2.7 shows that this will still lead to representative dots away from the critical points (where $\lambda \geq \eta$); only close to the critical points (where $\lambda < \eta$) will this simply lead to dots that are equidistant *in space*.

Accuracy and Efficiency of the Outer Loop

A rigorous discussion of the accuracy and efficiency of the gMAM is beyond the scope of the present paper. However, we find it useful to make a few heuristic comments.

The discussion is complicated by the fact that the minimum action path (i.e., the steady state solution $\varphi^\star$ of (3.3) that is also the minimizer of $\hat{S}(\varphi)$) will, in general, go through critical points, and the path may not be smooth at these points. We first discuss the case when this does not happen, i.e., when $\varphi^\star$ is smooth, and then explain what to do if that is not the case.

If $\varphi^\star$ is smooth, we expect the algorithm to identify $\varphi^\star$ and $\hat{S}(\varphi^\star)$ with second-order accuracy in $\triangle\alpha = 1/N$. This is because the derivatives of φ and λ are computed with second-order accuracy, and the linear interpolation in Step 3 and the formula for $\hat{S}$ in Step 6 are second-order accurate as well. This was confirmed in the example below. As long as we achieve stability (which requires taking a small enough value for $\triangle\tau$, but one that is independent of N), we observe that the error on the curve can be made $O(\triangle\alpha^2) = O(1/N^2)$, in the sense that

$$\rho(\varphi_{\text{interp}}, \varphi^\star) \le C N^{-2} \tag{3.8}$$

for some constant $C > 0$, where φ_{interp} is the curve linearly interpolated from $\{\varphi_i^k\}_{i=0,\dots,N}$ after convergence. Assuming linear convergence in time, the number of steps until convergence is then $O(\log N)$, which gives a total cost, measured in the number of operations until convergence, scaling as

$$\text{cost} = O(N \log N). \tag{3.9}$$

Notice that this estimate takes into account that the interpolation step requires $O(N)$ operations if there are $N + 1$ discretization points along the curve. The estimate (3.9) was confirmed in our numerical examples; see Section 4.

Consider now what happens if the steady state solution of (3.3) (i.e., the solution of (3.2)) goes through one or more critical points and is not smooth at these points. Notice first that this leads to no problem with (3.2). Indeed, by Lemma 2.2(i), if the point $\varphi(\alpha_c)$ is a critical point for some $\alpha_c \in [0, 1]$, then $\lambda \to 0$ as $\alpha \to \alpha_c$. All the terms in (3.2) involving φ', φ'', and λ' are multiplied by λ or λ^2, and so these products tend to 0 as $\alpha \to \alpha_c$. Furthermore, because of the Lipschitz continuity of λ, their discretizations still approximate the correct value 0 at the critical point. However, they will do so only up to first-order accuracy, $O(\triangle\alpha) = O(1/N)$, unless one makes sure that one discretization point of the curve falls onto the critical point (in which case we obtain the exact value 0).

In the algorithm, this problem is also aggravated by the interpolation-reparametrization Step 3. The nondifferentiability of the curve will reduce the order of accuracy of the linear interpolation procedure to first-order as well unless we take some extra care of how we handle the critical points on the curve.

One possible way to solve these problems and restore the second-order accuracy is to identify the location(s) of the critical point(s) along the curve and treat the

pieces on each side separately by the same basic algorithm as above. This can be done on the fly using the following procedure: Specify a small threshold value for λ, say $\lambda_0 > 0$, such that if $\lambda < \lambda_0$ there is likely to be a critical point in the vicinity. Then let the curve evolve as above, but as soon as $\lambda < \lambda_0$ at some point, say $\varphi_{i\star}^k$, split the curve into the two pieces at the left and right of $\varphi_{i\star}^k$. Continue the algorithm with modified Steps 2 and 3: in Step 2 replace the equation for $\varphi_{i\star}^k$ in (3.6) by

$$\frac{\tilde{\varphi}_{i\star} - \varphi_{i\star}^k}{\triangle\tau} = -H_{x\theta}H_\theta - HH_x \quad \big(= -\tfrac{1}{2}\nabla_x(|H_\theta|^2 + H^2)\big), \tag{3.10}$$

with all functions on the right evaluated at $(\varphi_{i\star}^k, 0)$, so that $\varphi_{i\star}^k$ is attracted by the critical point where $H_\theta(x,0)$ and $H(x,0)$ vanish; in Step 3 redistribute the points on both parts of the curve separately, without changing $\tilde{\varphi}_{i\star}$ (i.e., $\varphi_{i\star}^{k+1} = \tilde{\varphi}_{i\star}$). Observe that in the cases of an SDE or an SPDE with unit noise, the modification (3.10) can be achieved by *setting* $\lambda_{i\star}^k = 0$ after completion of Step 1 (to see this, set $\lambda = 0$ in (4.3) and (4.10) below).

This procedure, which we found to work well on all examples treated in Section 4 and which is further discussed in Section 4.1, restores the second-order accuracy in $\triangle\alpha = 1/N$ even if there are critical points along the curve. Note that there is no a priori difficulty in designing more accurate schemes by using a higher-order stencil for the derivatives, choosing a higher-order interpolation method, and taking care of the critical points along the curve as explained above.

3.4 The Inner Loop (Computing $\hat{\vartheta}(\varphi, \varphi')$)

In order to compute $\hat{\vartheta}(\varphi, \varphi')$ from (2.7) we must solve the following problem: Given the strictly convex and twice-differentiable function $h(\cdot) = H(\varphi, \cdot)$ with $h(0) \le 0$, and given a direction φ', we want to find the unique point $\hat{\vartheta}$ with

$$h(\hat{\vartheta}) = 0 \quad \text{and} \quad h_\theta(\hat{\vartheta}) = \lambda\varphi' \quad \text{for some } \lambda \ge 0. \tag{3.11}$$

This problem has a simple geometric interpretation, as was illustrated before in Figure 2.1 (with $y = \varphi'$): it amounts to finding the point of the convex zero-level set of h where the outer normal to that level set is parallel to and points in the same direction as φ'.

Since the region $\{\theta \in \mathbb{R}^n \mid h(\theta) \le 0\}$ can potentially be very thin and long, one must make use of the underlying geometry of the problem. One very efficient strategy for finding a smart update for an initial guess $\hat{\vartheta}^0$ is a procedure similar in spirit to a higher-order version of the standard Newton-Raphson algorithm. However, while the Newton-Raphson method typically computes in each iteration the exact solution of the first-order approximation of the problem, we *must* use a second-order approximation since the solution of our problem is only well-defined for strictly convex functions h.

The procedure is thus as follows. For $p \ge 0$:

(1) Compute $h(\hat{\vartheta}^p)$, $h_\theta(\hat{\vartheta}^p)$, and $h_{\theta\theta}(\hat{\vartheta}^p)$.
(2) Find the unique quadratic function $f(\theta)$ such that

$$f(\hat{\vartheta}^p) = h(\hat{\vartheta}^p), \quad f_\theta(\hat{\vartheta}^p) = h_\theta(\hat{\vartheta}^p), \quad \text{and} \quad f_{\theta\theta}(\hat{\vartheta}^p) = h_{\theta\theta}(\hat{\vartheta}^p).$$

(3) If the region $\{\theta \in \mathbb{R}^n \mid f(\theta) < 0\}$ is nonempty, let $\hat{\vartheta}^{p+1}$ be the solution of

$$f(\hat{\vartheta}) = 0 \quad \text{and} \quad f_\theta(\hat{\vartheta}) = \lambda\varphi' \quad \text{for some } \lambda \geq 0,$$

i.e., of (3.11) with h replaced by its approximation f. Otherwise, let $\hat{\vartheta}^{p+1} := \operatorname{argmin}_\theta f(\theta)$.
(4) Repeat until convergence.

Steps 1–3 in this procedure can be done analytically, and so it provides us with a closed-form update formula. The computation is carried out in Appendix F and gives

$$\hat{\vartheta}^{p+1} := \hat{\vartheta}^p + h_{\theta\theta}^{-1}\big(\tilde{\lambda}(\hat{\vartheta}^p)\varphi' - h_\theta\big) \quad \text{with } \tilde{\lambda}(\hat{\vartheta}^p) := \left(\frac{\langle h_\theta, h_{\theta\theta}^{-1} h_\theta\rangle - 2h}{\langle \varphi', h_{\theta\theta}^{-1}\varphi'\rangle}\right)_+^{1/2}, \tag{3.12}$$

where $w_+^{1/2} = \sqrt{w}$ if $w \geq 0$ and $w_+^{1/2} = 0$ otherwise, and where h, h_θ, and $h_{\theta\theta}$ are evaluated at $\hat{\vartheta}^p$. Note also that by definition of the algorithm, if h is quadratic to begin with, then the algorithm converges after only one iteration (since then $f = h$). This will happen if the underlying process is a diffusion process.

Once $\hat{\vartheta}$ has been determined, the value of λ in (3.11) can then be computed as a simple function of $\hat{\vartheta}$ via

$$\lambda = \frac{\langle h_\theta(\hat{\vartheta}), \varphi'\rangle}{|\varphi'|^2} = \frac{\langle H_\theta(\varphi, \hat{\vartheta}), \varphi'\rangle}{|\varphi'|^2}. \tag{3.13}$$

Next we show that the sequence generated by (3.12) has $\hat{\vartheta}$ as its unique fixed point and is quadratically convergent if h is smooth enough. The latter is not surprising since the standard Newton-Raphson algorithm has the same rate of convergence.

LEMMA 3.4 (Uniqueness of Fixed Point $\hat{\vartheta}$) *We have $\hat{\vartheta}^{p+1} = \hat{\vartheta}^p$ if and only if $\hat{\vartheta}^p = \hat{\vartheta}$, i.e., if $\hat{\vartheta}^p$ is the solution of system* (3.11). *In that case, the value of λ in* (3.11) *is given by $\tilde{\lambda}(\hat{\vartheta}^p)$.*

PROOF:
"⇐": If $h(\hat{\vartheta}^p) = 0$ and $h_\theta(\hat{\vartheta}^p) = \lambda\varphi'$ for some $\lambda \geq 0$, then

$$\begin{aligned}\tilde{\lambda}(\hat{\vartheta}^p)\varphi' &= \left(\frac{\langle h_\theta, h_{\theta\theta}^{-1} h_\theta\rangle - 2h}{\langle \varphi', h_{\theta\theta}^{-1}\varphi'\rangle}\right)_+^{1/2}\varphi' \\ &= \left(\frac{\langle h_\theta, h_{\theta\theta}^{-1} h_\theta\rangle}{\langle \varphi', h_{\theta\theta}^{-1}\varphi'\rangle}\right)_+^{1/2}\varphi' = \lambda\varphi' = h_\theta(\hat{\vartheta}^p),\end{aligned}$$

so that $\hat{\vartheta}^{p+1} = \hat{\vartheta}^p$.

"$\Rightarrow$": Now let $\hat{\vartheta}^{p+1} = \hat{\vartheta}^p$. Then $h_\theta(\hat{\vartheta}^p) = \tilde{\lambda}(\hat{\vartheta}^p)\varphi'$ and clearly $\tilde{\lambda}(\hat{\vartheta}^p) \geq 0$, so it remains to show that $h(\hat{\vartheta}^p) = 0$. If $\beta := \langle h_\theta, h_{\theta\theta}^{-1} h_\theta \rangle - 2h \geq 0$ (where here and in the next line h, h_θ, and $h_{\theta\theta}$ are evaluated at $\hat{\vartheta}^p$), then we can compute that

$$\langle h_\theta, h_{\theta\theta}^{-1} h_\theta \rangle = \tilde{\lambda}(\hat{\vartheta}^p)^2 \langle \varphi', h_{\theta\theta}^{-1} \varphi' \rangle = \langle h_\theta, h_{\theta\theta}^{-1} h_\theta \rangle - 2h \quad \Rightarrow \quad h(\hat{\vartheta}^p) = 0.$$

If $\beta \leq 0$, then $\tilde{\lambda}(\hat{\vartheta}^p) = 0$ and thus $h_\theta(\hat{\vartheta}^p) = 0$; i.e., $\hat{\vartheta}^p$ is the minimum of h. Since we know that $h(0) \leq 0$, this implies $h(\hat{\vartheta}^p) \leq 0$. On the other hand, $0 \geq \beta = -2h(\hat{\vartheta}^p)$, so $h(\hat{\vartheta}^p)$ must be 0. □

LEMMA 3.5 (Quadratic Convergence) *If $h \in C^4(\mathbb{R}^n)$, then there exists a neighborhood $U_\epsilon(\hat{\vartheta})$ of the solution $\hat{\vartheta}$ and a constant $c > 0$ such that for $\forall \hat{\vartheta}^p \in U_\epsilon(\hat{\vartheta})$ we have*

$$|\hat{\vartheta}^{p+1} - \hat{\vartheta}| \leq c|\hat{\vartheta}^p - \hat{\vartheta}|^2.$$

PROOF: Starting from (3.12), we write

$$\left|h_{\theta\theta}(\hat{\vartheta}^p)(\hat{\vartheta}^{p+1} - \hat{\vartheta})\right| = \left|h_{\theta\theta}(\hat{\vartheta}^p)(\hat{\vartheta}^p - \hat{\vartheta}) + \tilde{\lambda}(\hat{\vartheta}^p)\varphi' - h_\theta(\hat{\vartheta}^p)\right|. \tag{3.14}$$

We approximate the expression $\tilde{\lambda}(\hat{\vartheta}^p)\varphi' - h_\theta(\hat{\vartheta}^p)$ by its first-order Taylor expansion around $\hat{\vartheta}$ and estimate the remainder involving its second derivative (and thus the fourth derivative of h) by $O(|\hat{\vartheta}^p - \hat{\vartheta}|^2)$. Since the zeroth-order term vanishes, i.e., $\tilde{\lambda}(\hat{\vartheta})\varphi' - h_\theta(\hat{\vartheta}) = 0$ (this was shown in the first part of the proof of Lemma 3.4), the right-hand side of (3.14) is equal to

$$\left|h_{\theta\theta}(\hat{\vartheta}^p)(\hat{\vartheta}^p - \hat{\vartheta}) + (\varphi' \otimes \nabla\tilde{\lambda}(\hat{\vartheta}) - h_{\theta\theta}(\hat{\vartheta}))(\hat{\vartheta}^p - \hat{\vartheta})\right| + O(|\hat{\vartheta}^p - \hat{\vartheta}|^2).$$

We show below that $\nabla\tilde{\lambda}(\hat{\vartheta}) = 0$, so that

$$\begin{aligned}\left|h_{\theta\theta}(\hat{\vartheta}^p)(\hat{\vartheta}^{p+1} - \hat{\vartheta})\right| &= \left|(h_{\theta\theta}(\hat{\vartheta}^p) - h_{\theta\theta}(\hat{\vartheta}))(\hat{\vartheta}^p - \hat{\vartheta})\right| + O(|\hat{\vartheta}^p - \hat{\vartheta}|^2) \\ &= O(|\hat{\vartheta}^p - \hat{\vartheta}|^2).\end{aligned}$$

Since $|\hat{\vartheta}^{p+1} - \hat{\vartheta}| \leq |h_{\theta\theta}^{-1}(\hat{\vartheta}^p)|\,|h_{\theta\theta}(\hat{\vartheta}^p)(\hat{\vartheta}^{p+1} - \hat{\vartheta})|$, we are done.

To show that $\nabla\tilde{\lambda}(\hat{\vartheta}) = 0$, consider first the case $\lambda > 0$. Pick any $i \in \{1, \dots, n\}$ and use that at $\theta = \hat{\vartheta}$ we have $h = 0$ and $h_\theta = \lambda\varphi'$:

$$
\begin{aligned}
&\partial_{\theta_i}\left(\frac{\langle h_\theta, h_{\theta\theta}^{-1}h_\theta\rangle - 2h}{\langle\varphi', h_{\theta\theta}^{-1}\varphi'\rangle}\right)^{1/2}\Bigg|_{\theta=\hat{\vartheta}} \\
&= \left(\frac{1}{2(\dots)^{1/2}}\,\partial_{\theta_i}\frac{\langle h_\theta, h_{\theta\theta}^{-1}h_\theta\rangle - 2h}{\langle\varphi', h_{\theta\theta}^{-1}\varphi'\rangle}\right)\Bigg|_{\theta=\hat{\vartheta}} \\
&= \frac{1}{2\lambda}\langle\varphi', h_{\theta\theta}^{-1}\varphi'\rangle^{-2}\Big[\Big(\langle h_\theta, (\partial_{\theta_i}h_{\theta\theta}^{-1})h_\theta\rangle \; + \underbrace{2h_\theta^T h_{\theta\theta}^{-1}h_{\theta\theta_i} - 2h_{\theta_i}}_{=0}\Big)\langle\varphi', h_{\theta\theta}^{-1}\varphi'\rangle \\
&\qquad\qquad - \Big(\langle h_\theta, h_{\theta\theta}^{-1}h_\theta\rangle - \underbrace{2h}_{=0}\Big)\langle\varphi', (\partial_{\theta_i}h_{\theta\theta}^{-1})\varphi'\rangle\Big]\Big|_{\theta=\hat{\vartheta}} \\
&= \frac{1}{2\lambda}\langle\varphi', h_{\theta\theta}^{-1}\varphi'\rangle^{-2}\Big[\langle h_\theta, (\partial_{\theta_i}h_{\theta\theta}^{-1})h_\theta\rangle\langle\varphi', h_{\theta\theta}^{-1}\varphi'\rangle \\
&\qquad\qquad - \langle h_\theta, h_{\theta\theta}^{-1}h_\theta\rangle\langle\varphi', (\partial_{\theta_i}h_{\theta\theta}^{-1})\varphi'\rangle\Big]\Big|_{\theta=\hat{\vartheta}} \\
&= 0.
\end{aligned}
$$

The case $\lambda = 0$ can be treated by checking that the function $\langle h_\theta, h_{\theta\theta}^{-1}h_\theta\rangle - 2h$ as well as its first two derivatives vanish at $\theta = \hat{\vartheta}$, so that its square root is of order $o(|\hat{\vartheta}^p - \hat{\vartheta}|)$. □

4 Examples

4.1 SDE: The Maier-Stein Model

As a first test for our method, we use the following example of a diffusion process (SDE) first proposed by Maier and Stein [12]:

$$
\begin{cases} du = (u - u^3 - \beta u v^2)dt + \sqrt{\varepsilon}\, dW_u(t) \\ dv = -(1 + u^2)v\, dt + \sqrt{\varepsilon}\, dW_v(t) \end{cases} \tag{4.1}
$$

where W_u and W_v are independent Wiener processes and $\beta > 0$ is a parameter. (In [12], Maier and Stein use two parameters: μ, which we set to 1 in this treatment, and α, which we call β in order to avoid confusion with the variable used to parametrize the path $\varphi(\alpha)$.)

For all values of $\beta > 0$, the SDE (4.1) has two stable equilibrium points at $(u, v) = (\pm 1, 0)$ and an unstable equilibrium point at $(u, v) = (0, 0)$ (see Figure 4.1). The drift vector field

$$
b(u, v) = \begin{pmatrix} u - u^3 - \beta u v^2 \\ -(1 + u^2)v \end{pmatrix} \tag{4.2}
$$

is the gradient of a potential if and only if $\beta = 1$.

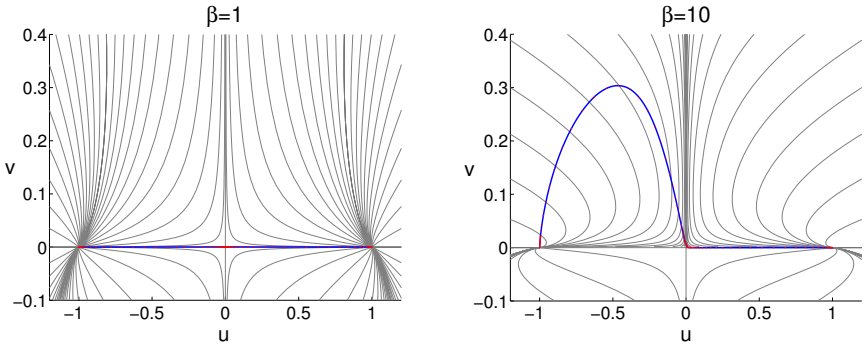

FIGURE 4.1. The minimum action paths from $(u, v) = (-1, 0)$ to $(u, v) = (1, 0)$ for the Maier-Stein model (4.1) shown on the top of the flow lines of the deterministic velocity field (gray lines). The parameters are $\beta = 1$ (left panel) and $\beta = 10$ (right panel). When $\beta = 1$, the minimum action path is simply the heteroclinic orbit joining $(\pm 1, 0)$ via $(0, 0)$; when $\beta = 10$, nongradient effects take over, and the minimum action path is different from the heteroclinic orbit.

When the noise amplitude ε is small, (4.1) displays bistability. Any initial condition with $u < 0$ is rapidly attracted toward a small neighborhood of $(u, v) = (-1, 0)$, whereas any initial condition with $u > 0$ is rapidly attracted toward a small neighborhood of $(u, v) = (1, 0)$. As a result, the equilibrium distribution of the process defined by (4.1) is concentrated in small neighborhoods around $(\pm 1, 0)$ and the process switches between these two regions only rarely. When it does so, large deviations theory tells us that, with probability 1 in the limit as $\varepsilon \to 0$, the trajectory remains in an arbitrarily small tube around the miminizer $\varphi^\star$ of $\hat{S}(\varphi)$ connecting $(u, v) = (-1, 0)$ to $(u, v) = (1, 0)$ or the other way around—in other words, the minimum action curve $\varphi^\star$ is the maximum-likelihood pathway of switching (see Section 2.2). In addition, large deviations theory tells us that the frequency of these hopping events is roughly $\exp(-\varepsilon^{-1}\hat{S}(\varphi^\star))$.

Maier and Stein studied (4.1) for various values of β. They noted that the minimum action path from $(u, v) = (-1, 0)$ to $(u, v) = (1, 0)$ is the heteroclinic orbit joining these two points via $(u, v) = (0, 0)$ when $\beta \le \beta_{\text{crit}} = 4$ (this is consistent with the system not being too far from the gradient regime in these cases). However, when $\beta > \beta_{\text{crit}} = 4$, the piece of the minimum action path in the region $u < 0$ (i.e., in the basin of attraction of $(u, v) = (-1, 0)$ by the deterministic dynamics) stops being the heteroclinic orbit. Some intuition for why this change of behavior occurs can be gained by looking at the deterministic flow lines shown in Figure 4.1. Here we confirm these results using our method to find the minimum action path, as shown in Figure 4.1.

Before discussing the accuracy, stability, and efficiency of our method in the context of the Maier-Stein model in detail, let us note that when applying our technique to a diffusion process such as (4.1) where the diffusion tensor is the identity, we can use the following explicit formulas for $\hat{\vartheta}$ and λ:

$$\hat{\vartheta} = \lambda\varphi' - b(\varphi), \quad \lambda = \frac{|b(\varphi)|}{|\varphi'|}.$$

Since $H(x,\theta) = \langle b(x),\theta\rangle + \frac{1}{2}|\theta|^2$, at $(x,\theta) = (x,\hat{\vartheta})$ we also have

$$H_{\theta x} = \nabla b, \quad H_{\theta\theta} = I, \quad H_x = (\nabla b)^T\hat{\vartheta} = (\nabla b)^T(\lambda\varphi' - b),$$

and so equation (3.3) can be written explicitly as

$$\dot{\varphi} = \lambda^2\varphi'' - \lambda(\nabla b - (\nabla b)^T)\varphi' - (\nabla b)^T b + \lambda\lambda'\varphi' + \mu\varphi'. \tag{4.3}$$

Equation (4.3) can be integrated using a straightforward modification of the algorithm presented in Section 3.2. If b is a gradient field, $b = -\nabla U$, then $\nabla b - (\nabla b)^T = 0$ and the right-hand side simplifies further:

$$\dot{\varphi} = \lambda^2\varphi'' - \nabla\nabla U\,\nabla U + \lambda\lambda'\varphi' + \mu\varphi'. \tag{4.4}$$

The steady state of this equation is the minimum energy path, i.e., the path such that $\nabla U^{\perp} = 0$ along it. Using gMAM to integrate (4.4) may represent a useful alternative to the string method [3].

Stability, Accuracy, and Efficiency

We discuss the case $\beta = 10$ when the minimum action path is nontrivial. To obtain a benchmark solution, we first ran the algorithm with $N = 10^5$ discretization points at decreased step size to obtain a curve that we regarded as the true solution connecting $(-1,0)$ and $(1,0)$ (to get this benchmark, we actually ran the code between $(-1,0)$ and $(0,0)$ and then extended the path by the straight line between $(0,0)$ and $(1,0)$ since we know that piece exactly).

Next we ran the code for 300 iterations for $N = 100, 200, \ldots, 900, 1000, 2000, \ldots, 10\,000$ at a fixed time step $\triangle\tau = 0.1$, to find both the minimum action path connecting $(-1,0)$ to $(0,0)$ and the one connecting $(-1,0)$ to $(1,0)$ via the critical point $(0,0)$. For the initial condition, we used a semicircle in the upper half-plane connecting the critical points $(-1,0)$ and $(0,0)$ in the first case or $(-1,0)$ and $(1,0)$ in the second case. The error was estimated by computing the maximum distance of each of the curves interpolated between the points to the benchmark curve obtained before. (Note that we took as many as 300 iterations because we are interested in measuring the accuracy of the algorithm here, but convergence is already achieved up to an error of 10^{-6} in the action after less than 20 iterations; see Figure 4.4.)

Since the left part of the path is smooth (there is no critical point along the path), we expect that the unmodified algorithm of Section 3.2 to be second-order accurate in N if we seek for the minimum action path connecting $(-1,0)$ to $(0,0)$: this is

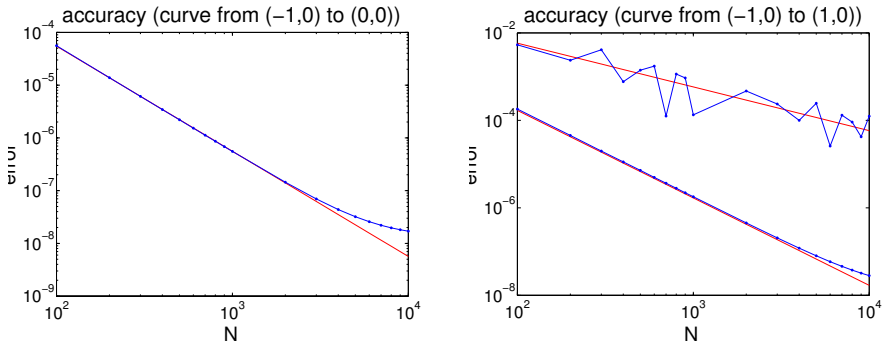

(a) (b)

FIGURE 4.2. The accuracy measurements for the Maier-Stein model on a double-logarithmic scale, for the left path (a) and the whole path (b), which uses the modified and the unmodified algorithm. The fitted straight lines have slope -1 (upper curve in (b)) and -2, indicating accuracies of order $O(1/N)$ and $O(1/N^2)$, respectively. The noise in the measurements of the unmodified algorithm on the whole path (upper curve in (b)) is due to the fact that the error strongly depends on whether a grid point happens to lie close to the unstable equilibrium point; however, modifying the algorithm as explained in Section 3.3 restores the second-order accuracy.

confirmed by results shown in Figure 4.2(a). On the other hand, since the path connecting $(-1, 0)$ to $(1, 0)$ has to pass the critical point $(0, 0)$ and is not differentiable at that point, we expect the unmodified algorithm of Section 3.2 to be only first-order accurate for these runs, and this is confirmed by the upper curve in Figure 4.2(b). However, when we modified the algorithm as proposed in Section 3.3 and ran it for an additional 300 steps with the reparametrization step treating the right and the left side separately, second-order accuracy was restored, as shown by the lower curve in Figure 4.2(b).

To check convergence of the curve between $(-1, 0)$ and $(1, 0)$, we also plotted $\lambda(\varphi(\alpha), \varphi'(\alpha))$; see Figure 4.3. As expected, after convergence it has one root in the interval $(0, 1)$, corresponding to the critical point on the curve φ. The plot also confirms Lemma 2.8(i), which says that λ is Lipschitz-continuous at that point. Furthermore, we observed that with the unmodified algorithm the value of λ at that point only reaches $O(N^{-1})$ (since the points of the discretized curve φ only approximate the critical point to that order), whereas our method to achieve second-order accuracy brings it all the way down to 0 (up to machine precision).

The time step to achieve stability in all the runs was found to be largely independent of the choice of N. For the grid sizes N as above, the maximum value for $\triangle\tau$ before visible oscillations occurred stayed constant at about 0.3.

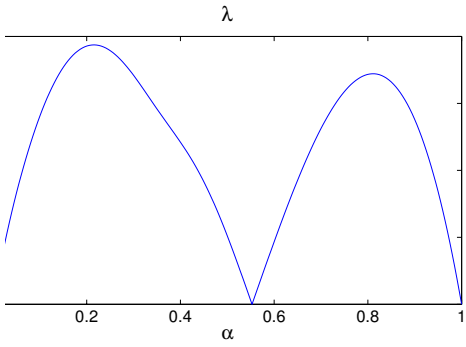

FIGURE 4.3. The function $\lambda(\varphi(\alpha), \varphi'(\alpha))$. The root in the middle corresponds to the value α where $\varphi(\alpha)$ is a critical point.

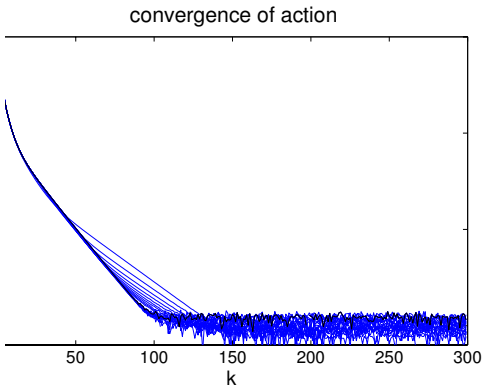

FIGURE 4.4. The error in the action plotted in function of the number of iterations on semilogarithmic scale, for various values of N between 100 and 10 000. The black curve corresponds to $N = 10\,000$. These graphs indicate linear convergence, with a rate that is independent of N since the time step $\triangle\tau$ is independent of N.

The required number of iterations at $\triangle\tau = 0.2$ until the change of the action per iteration became less than 10^{-7} varied insignificantly between 31 and 33 for the grid sizes N as above. For fixed N, the action decreases exponentially to its limiting value, as can be seen in Figure 4.4, which shows the decay for the various values of N in a semilogarithmic plot. The runtime for 100 iterations for various grid sizes is plotted in Figure 4.5. It shows linear dependency on N, which is due to the fact that all of our operations have a cost of order $O(N)$, including solving the linear system in Step 2 and the linear interpolation in Step 3. These observations are consistent with estimate (3.9) for the cost.

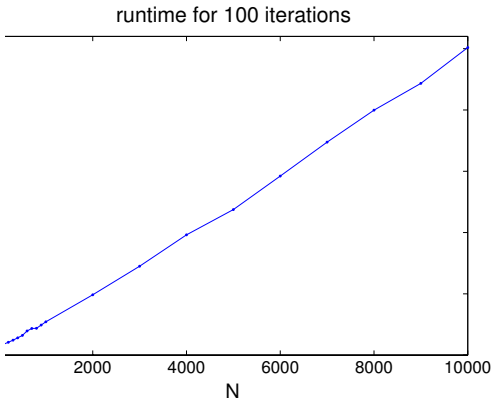

FIGURE 4.5. The runtime for 100 iterations at various grid sizes (using MATLAB 6.5 running under Windows XP on a 1.5-GHz Pentium 4), showing linear dependency in N.

4.2 SPDE: An Infinite-Dimensional Generalization of the Maier-Stein Model

As a natural generalization of the SDE (4.1), we consider the following infinite-dimensional analogue of this equation (here written as a standard PDE for the sake of clarity):

$$\begin{cases} u_t = \kappa u_{xx} + u - u^3 - \beta u v^2 + \sqrt{\varepsilon}\,\eta_u(x,t), \\ v_t = \kappa v_{xx} - (1+u^2)v + \sqrt{\varepsilon}\,\eta_v(x,t). \end{cases} \tag{4.5}$$

Here $x \in [0,1]$ and we assume periodic boundary conditions. $\kappa > 0$ is an additional parameter, and $\eta_u(x,t)$ and $\eta_v(x,t)$ are spatiotemporal white noises (i.e., the space-time derivatives of Brownian sheets, $W_u(x,t)$ and $W_v(x,t)$, defined on $(x,t) \in [0,1] \times [0,\infty)$). System (4.5) is formal, but it can be shown (see [5]) by rewriting it in integral form that its solutions are well-defined and Hölder-continuous and define a Markov process adapted to the filtrations of $W_u(t,x)$ and $W_v(t,x)$. In addition, it was shown in [5] that (4.5) satisfies a large deviations principle with action functional

$$S_T(u,v) = \frac{1}{2}\int_0^T \int_0^1 \big((u_t - \kappa u_{xx} - u + u^3 + \beta u v^2)^2 + \big(v_t - \kappa v_{xx} + (1+u^2)v\big)^2\big)dx\,dt. \tag{4.6}$$

Thus, like its finite-dimensional analogue (4.1), (4.5) will display bistability in the limit as $\varepsilon \to 0$ in the sense that the invariant measure of the process defined by (4.5) is concentrated in a small neighborhood around the two stable equilibrium solutions of the deterministic equation obtained by setting $\varepsilon = 0$ in (4.5): these are $(u_\pm(x), v_\pm(x)) \equiv (\pm 1, 0)$. Here we are interested in analyzing the pathways of

transition between these points which, with probability 1 as $\varepsilon \to 0$, are located in a small tube around the minimizer of the action (4.6) over both $(u(t,x), v(t,x))$ and T.

By analogy with what happens in the finite-dimensional system, we expect that when the system is not too far from gradient, i.e., when β is small enough, the minimum action path will follow the graph of a heteroclinic orbit connecting (u_-, v_-) and (u_+, v_+). The only difference with the finite-dimensional situation is then that, if the coefficient κ in (4.5) is small enough, $\kappa < \kappa_{\text{crit}} = 1/(4\pi^2) \approx 0.0253$, there are many such orbits because (4.5) has many unstable equilibrium points. As a result there will be several minimum action paths (one global minimizer and several local minimizers). How to identify these unstable critical points as a way to benchmark the results from the minimum action method is explained below.

On the other hand, if the system is far from gradient, i.e., if β is large enough, then we expect that the piece of the minimum action path connecting the stable equilibrium point (u_-, v_-) to an unstable equilibrium point will be different from the heteroclinic orbit connecting these points. Our results below confirm this intuition.

It is worth pointing out that traditional shooting methods to solve the Hamilton equations associated with the minimization of (4.6) are inapplicable here. The reason is that, unlike their finite-dimensional analogue, these equations are only well-posed as a boundary value problem in time, which prohibits the use of the shooting method. Hence, the technique used by Maier and Stein in [12] in the context of the finite-dimensional diffusion (4.1) cannot be used to obtain the minimizers of (4.6). Next we show that the gMAM is the right alternative to do this minimization.

The gMAM in Infinite Dimensions

We want to apply our algorithm to find the minimum action path connecting the stable states (u_-, v_-) and (u_+, v_+). In order to do so, we first recast our theoretical results to the present infinite-dimensional setting. Basically, this amounts to changing the finite-dimensional inner product $\langle \cdot, \cdot \rangle_a$ by its analogue in function space, and the only result we actually need is the equivalent of (2.2) and (2.14), which we state without proof:

$$V((u_-, v_-), (u_+, v_+)) = \inf_{\varphi} \hat{S}(\varphi) \tag{4.7}$$

where the infimum is taken over all spatially periodic functions $\varphi(x, \alpha) : [0,1] \times [0,1] \to \mathbb{R}^2$ subject to $\varphi(\cdot, 0) \equiv (-1, 0)$ and $\varphi(\cdot, 1) \equiv (1, 0)$, and where

$$\hat{S}(\varphi) = \int_0^1 \big(\|\varphi'\|_{L^2} \, \|B(\varphi)\|_{L^2} - \langle \varphi', B(\varphi) \rangle_{L^2} \big) d\alpha. \tag{4.8}$$

Here

$$B(\varphi) := b(\varphi) + \kappa \varphi_{xx}, \tag{4.9}$$

where b is given by (4.2).

The steepest-descent flow associated with (4.7) is the analogue of (4.3). It can be written in compact form as

$$\dot{\varphi} = \lambda^2\varphi'' - \lambda(\partial B - (\partial B)^*)\varphi' - (\partial B)^* B + \lambda\lambda'\varphi' + \mu\varphi', \tag{4.10}$$

where $\lambda = \|B(\varphi)\|_{L^2}/\|\varphi'\|_{L^2}$, ∂B is the operator

$$\partial B = \nabla b(\varphi) + \kappa\partial_x^2, \tag{4.11}$$

and $(\partial B)^*$ is its adjoint. Explicitly, (4.10) is

$$\begin{aligned}\dot{\varphi} = {} & \lambda^2\varphi'' - \lambda(\nabla b - (\nabla b)^T)\varphi' - (\nabla b)^T b - \kappa(\nabla b + (\nabla b)^T)\varphi_{xx} \\ & - \kappa^2\varphi_{xxxx} - \kappa\begin{pmatrix}\langle\varphi_x, \nabla\nabla b_1\,\varphi_x\rangle \\ \langle\varphi_x, \nabla\nabla b_2\,\varphi_x\rangle\end{pmatrix} + \lambda\lambda'\varphi' + \mu\varphi'.\end{aligned} \tag{4.12}$$

(4.12) can be solved by discretizing $\varphi(x, \alpha, \tau)$ in x, α, and τ and using a generalization of the algorithm in Section 3.2. There is, however, an additional difficulty caused by the presence of the spatial derivatives such as φ_{xxxx}. To stabilize the code with respect to those, we may use an FFT-based pseudospectral code in x and Duhamel's principle to solve $\dot{\varphi} + \kappa^2\varphi_{xxxx} =$ (remaining terms) explicitly. However, having tried this approach, we found that a slightly more efficient alternative was to not go pseudospectral but rather split each iteration step into two, the first one being the equivalent of the semi-implicit Step 2 (evaluating φ'' at the new time step) in which the term $\kappa^2\varphi_{xxxx}$ at the right-hand side of (4.12) was excluded, and the second one being an implicit step with that term only. In this approach all spatial derivatives of φ were estimated by finite differences.

To apply the gMAM, we initialized the transition path as the linear interpolation between (u_-, v_-) and (u_+, v_+) and added a bump to break the degeneracy due to the periodicity in x; i.e., we set

$$\varphi(\tau = 0, x, \alpha) := \big(-1 + 2\alpha + 2\sin^2(\pi\alpha)\sin^2(\pi x), 0\big).$$

We chose the grid sizes $\triangle x = 1/128$ and $\triangle\alpha = 1/100$, and set the step size to $\triangle\tau = 0.1$. We then started the algorithm with the model parameters $\beta = 1$ and $\kappa = 0.01$, and after 40 seconds and about 120 iterations we obtained an approximate solution. Using a continuation method, we decreased κ to $\kappa = 0.003$ and then to $\kappa = 0.001$, each time running the algorithm starting from the previous solution. The whole sequence of operations took about two minutes using MATLAB 6.5 running under Windows XP on a 1.5-GHz Pentium 4. Then we started the process over again, this time increasing κ until it reached $\kappa = 0.026 > \kappa_{\text{crit}}$.

Results

Figure 4.6 shows plots for $\beta = 1$ and various values of κ. Each of them shows the first components of the functions $\varphi(\cdot, \alpha)$ for equidistant values of α as blue lines. To check our results, we added in each figure the lowest-energy saddle point of the system as a red line, determined independently using the method explained below. One can see that the transition paths found by our algorithm indeed pass

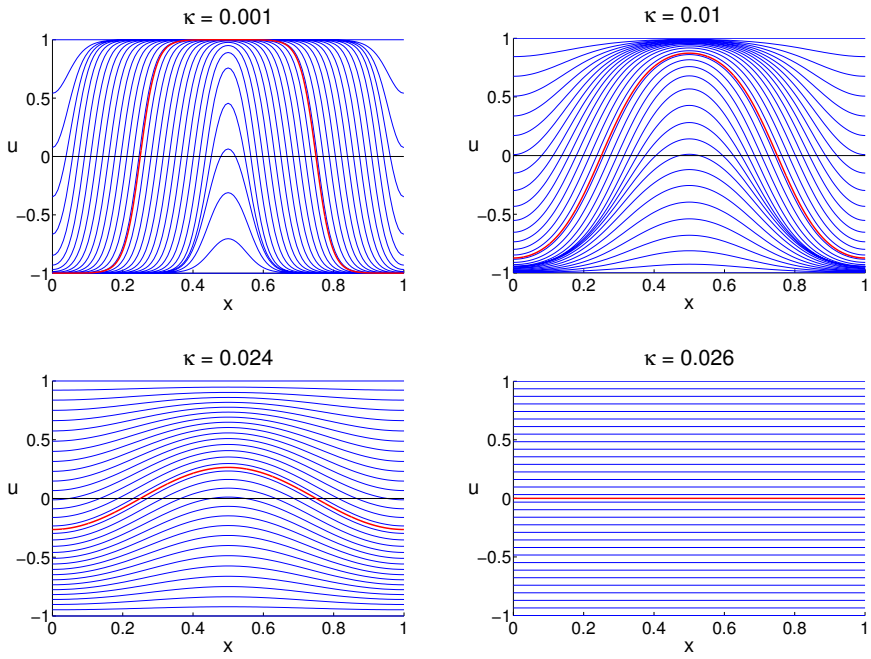

FIGURE 4.6. Snapshots along the minimum action path from (u_-, v_-) to (u_+, v_+) for the SPDE generalization of the Maier-Stein model. The parameters are $\beta = 1$ and $\kappa = 0.001, 0.01, 0.024, 0.026$. The highlighted lines are the unstable equilibrium points.

through these saddle points to very satisfying accuracy. Figure 4.7 shows a three-dimensional representation of the solution for $\kappa = 0.01$.

We then added a little bump to the v-field (the second component of φ), set $\beta = 10$, and restarted the algorithm. For this value of β, by analogy with what happens in the finite-dimensional Maier-Stein model, we expected that the field v would assist in the transition during the uphill path. The gMAM confirmed this intuition, as shown in Figure 4.8. Now as u makes a transition similar to the previous one, v also increases around $x = \frac{1}{2}$ but vanishes again as the saddle point is reached.

Figure 4.9 shows the plot for $\kappa = 0.001$. As we can see, smaller values for κ lead to steeper domain walls. Finally, Figure 4.10 shows an example for a two-periodic local minimizer, obtained by starting from a two-periodic initial curve.

Notice that the minimum action paths in this example are degenerate due to the spatial periodicity (i.e., if $\varphi(\tau, x, \alpha)$ is a minimizer of the action, so is $\varphi(\tau, x+c, \alpha)$ for any $c \in \mathbb{R}$). This degeneracy, however, was broken by our choice of initial condition and does not appear to affect the convergence of the algorithm.

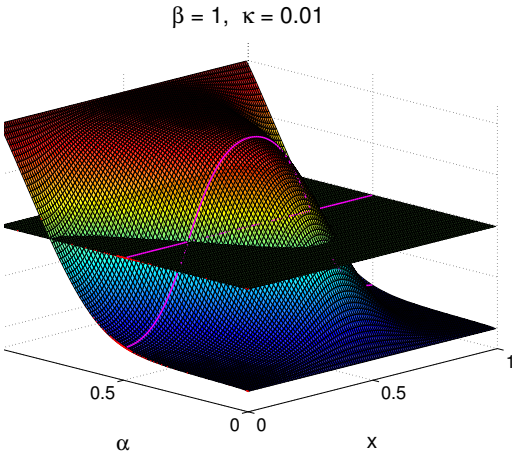

FIGURE 4.7. The minimum action path from (u_-, v_-) to (u_+, v_+) for $\kappa = 0.01$ and $\beta = 1$. The two surfaces represent the two components u and v of the minimizer $\varphi^\star$, the pink line shows the saddle point, and the red dots at the side mark points at equidistant times.

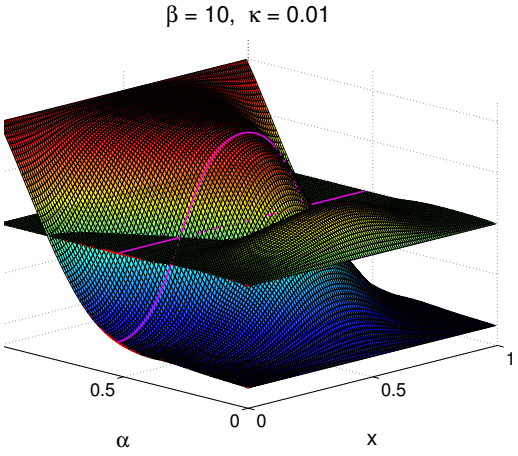

FIGURE 4.8. Same as in Figure 4.7, for $\kappa = 0.01$ and $\beta = 10$. For those parameters the field v assists in the transition.

Finding Saddle Points

Since we know that the minimum action paths must go through critical points (such as saddle points), to check our results we computed these critical points using the following strategy. Any critical point of the form $(u(x), 0)$ must fulfill the equation

$$0 = B_1((u,0)) = b_1((u,0)) + \kappa u_{xx} = u - u^3 + \kappa u_{xx}. \tag{4.13}$$

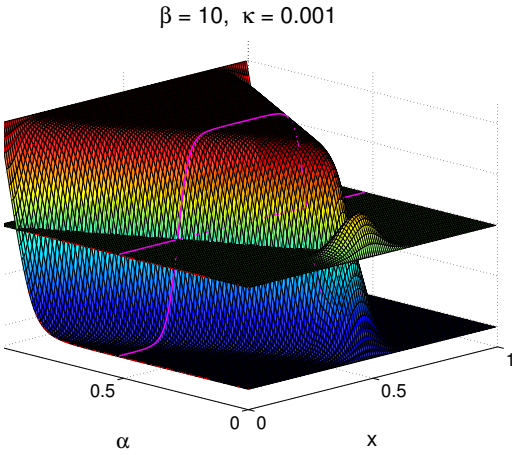

FIGURE 4.9. Same as in Figure 4.7, for $\beta = 10$ and $\kappa = 0.001$. Compared with Figure 4.8 we observe that smaller values for κ lead to steeper domain walls.

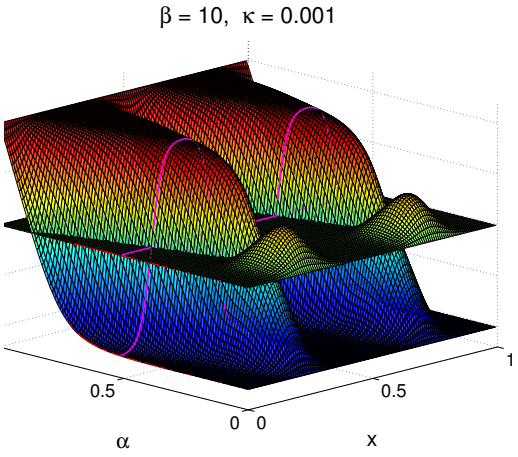

FIGURE 4.10. A local minimizer with period $\frac{1}{2}$ for $\beta = 10$ and $\kappa = 0.001$.

This equation has three constant solutions $u_k(x) \equiv (k, 0)$ for $k = -1, 0, +1$. The functions $(u_{\pm 1}, 0)$ can be shown to be stable states, whereas $(u_0, 0)$ is an unstable critical point. To find nonconstant solutions of (4.13), multiply this equation by u_x and integrate to obtain

$$-\frac{1}{4}(1-u^2)^2 + \frac{1}{2}\kappa u_x^2 = cst =: -\frac{1}{4}E^2,$$

$E \in [0, 1]$, or equivalently

$$|u_x(u)| = \kappa^{-1/2} \sqrt{\frac{1}{2}(1-u^2)^2 - \frac{1}{2}E^2}.$$

Additional solutions can thus be obtained by inverting the function

$$x(u) = \int_{u_-}^{u} \frac{1}{u_x(u')}\, du', \quad u_- \le u \le u_+, \tag{4.14}$$

where $u_\pm$ are the locations at which $u_x = 0$, i.e., $u_\pm = \pm\sqrt{1-E}$, and then setting $u(x) := u(2x(u_+) - x)$ for $x(u_+) \le x \le 2x(u_+)$. For every choice of E this leads to a solution with period $p(E) = 2x(u_+)$, but we are only interested in those values for which $1/p(E) \in \mathbb{N}$ since $u(x)$ must be periodic on the original domain $x \in [0, 1]$. These values of E can be found from (4.14):

$$p(E) = 2\int_{u_-}^{u_+} \frac{1}{u_x(u)}\, du = 2\sqrt{\kappa} \int_0^1 u^{-1/2} f_E(u) du,$$

where

$$f_E(u) = \left(1 - \frac{1}{2}u\right)^{-1/2} \left(\left(\frac{1}{2}(1-E)u + 2E \right)^{-1/2} + \left((1-E)\left(1 - \frac{1}{2}u\right) + 2E \right)^{-1/2} \right).$$

We can compute the integral for $p(E)$ numerically for several values of $E \in [0, 1]$ and then determine for which E_0 we have $p(E_0) = 1$. Finally, we can invert the solution $x(u)$ for $E = E_0$ to find the corresponding $u_{E_0}(x)$.

As a final remark, note that $p(E)$ can be shown to take its minimum at $E = 1$, and its value there is

$$\begin{aligned} p(1) &= 2\sqrt{2\kappa} \int_0^1 u^{-1/2} \left(1 - \frac{u}{2}\right)^{-1/2} du \\ &= 4\sqrt{\kappa} \int_0^{1/2} u^{-1/2}(1-u)^{-1/2}\, du \\ &= 2\sqrt{\kappa} \int_0^1 u^{-1/2}(1-u)^{-1/2}\, du = 2\pi\sqrt{\kappa}. \end{aligned}$$

Therefore, if $\kappa > \kappa_{\text{crit}} := 1/(4\pi^2)$, then for every $E \in [0, 1]$ we have $p(E) \ge p(1) = 2\pi\sqrt{\kappa} > 1$, i.e., $1/p(E) \notin \mathbb{N}$, and there is no nonconstant critical point (with $v = 0$).

4.3 Continuous-Time Markov Chain: The Genetic Switch

As a last example, we apply our technique to a birth-death process with a positive feedback loop that results in two stable states. The model was first defined by Roma et al. [16] (see also [7, 20]) and describes a mechanism in molecular biology called the genetic switch, illustrated in Figure 4.11.

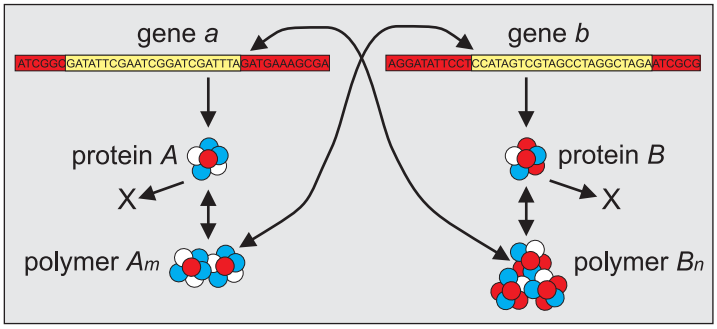

FIGURE 4.11. The mechanism of the genetic switch.

A bacterial cell contains plasmids with two gene sites a and b that can be transcribed and translated into proteins A and B. Those in turn can form polymers that bind to the operator site of the respective other gene, preventing further production of the corresponding protein. Other reactions are to reverse polymer formation or protein binding, and the degradation of proteins.

This setup leads to bistable behavior: If the cell is in a state with many proteins A and only few proteins B, then there are likely also many polymers A_m, the operator site of gene b will be blocked most of the time, and thus only few new proteins B will be produced. Since there are only few proteins B, it is unlikely that a polymer B_n will bind to the operator site of gene a, and the production rate of new proteins A will stay high. Therefore there will be a stable state with many proteins A and few proteins B, and by symmetry of the mechanism there is another stable state with few proteins A and many proteins B. Bistability arises because the fluctuations leading to a switch from one stable state to the other are rare events.

A simplifying description of this process keeps track only of the numbers of the proteins of the two types, (X_a, X_b), and models polymer formation and binding to the DNA only by defining the production rate as a function of the number of proteins of the respective other type, the precise form of which is motivated by the Hill equation [21]. It thus consists of only four reactions, as listed in Table 4.1.

Here, Ω is the system size parameter (such as the total number of proteins in the cell), $(x_a, x_b) := (X_a/\Omega, X_b/\Omega)$ is the protein density, a_1 and a_2 are rate

Reaction Type	Rate	State Change of (X_a, X_b)
protein production	$\Omega a_1(1 + x_b^n)^{-1}$	$(1, 0)$
	$\Omega a_2(1 + x_a^m)^{-1}$	$(0, 1)$
protein degradation	$\Omega \mu_1 x_a$	$(-1, 0)$
	$\Omega \mu_2 x_b$	$(0, -1)$

TABLE 4.1. The reactions of the genetic switch model by Roma et al. [16].

parameters that combine the rates for transcription into RNA and their translation into proteins, and m and n are the cooperativity parameters that represent the numbers of proteins per polymer. In the simulations below, we use the same model parameters as Roma et al. [16], namely, $a_1 = 156$, $a_2 = 30$, $\mu_1 = \mu_2 = 1$, $m = 1, n = 3$.

Under this kind of scaling the stochastic system for $x := (x_a, x_b)$ satisfies a large deviations principle as $\varepsilon = 1/\Omega \to 0$, with Hamiltonian

$$H(x,\theta) = \frac{a_1}{1+x_b^n}(e^{\theta_a}-1) + \mu_1 x_a(e^{-\theta_a}-1) + \frac{a_2}{1+x_a^m}(e^{\theta_b}-1) + \mu_2 x_b(e^{-\theta_b}-1) \tag{4.15}$$

(see [17]), which we used in the gMAM algorithm presented in Section 3.

Figure 4.12 shows the transition path obtained with gMAM, for the full path and only for the uphill path. They match those found in [16] using a shooting method based on the Hamilton equations associated with the Hamiltonian (4.15). While in general for continuous-time Markov chains no explicit expression for $\hat{\vartheta}(x, y)$ exists, for the simple Hamiltonian (4.15) we could indeed find one. Comparing the curve obtained from gMAM using the explicit formula for $\hat{\vartheta}(x, y)$ with the one using the algorithm from Section 3.4 in an inner loop, we found that both curves matched exactly. When we applied the technique to obtain second-order accuracy as described in Section 3.3, the corner of the path at the saddle point was sharp, and λ at that point vanished up to machine precision.

Table 4.2 shows the results of our performance tests on this model. For various grid sizes N it lists the optimal step size $\triangle\tau$, the number of steps necessary until the change in the action $\hat{S}(\varphi)$ per iteration drops below 10^{-7}, and the corresponding runtime. We observe again that the maximum step size $\triangle\tau$ is roughly independent of the grid size N, and that the runtime is close to linear in N.

Grid Size n	Step Size $\triangle\tau$	# Iterations	Runtime
100	0.22	20	0.5 sec
300	0.27	15	0.6 sec
1,000	0.26	18	1.3 sec
3,000	0.26	18	3.1 sec
10,000	0.27	19	11.6 sec

TABLE 4.2. Algorithm performance for the Roma model.

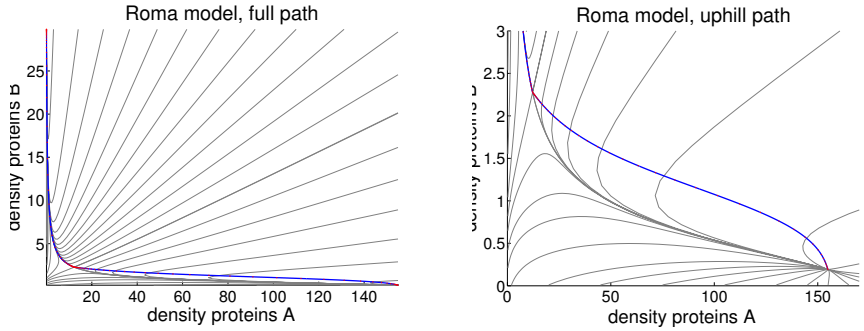

FIGURE 4.12. The minimum action path for the Roma model. The x- and y-axes denote the densities of the proteins of type A and B, respectively. The left panel shows the full path from the right stable state to the left stable state; the right panel shows the piece of the path from the right stable state to the saddle point.

5 Conclusions

Summarizing, we have proposed a variant of the MAM, the geometric minimum action method (gMAM), which is tailored to the double minimization problem required to compute the quasi-potential $V(x_1, x_2)$ in the Freidlin-Wentzell theory of large deviations. The key idea behind the gMAM is to reformulate the Freidlin-Wentzell action functional on the space of curves. With this reformulation, we guarantee that the new action will have minimizers (that is, curves) in a broader class of situations, in particular when the points x_1 and x_2 in $V(x_1, x_2)$ are stable equilibrium points of the deterministic dynamics (in contrast, the original action minimized over both the paths and their length in time fails to have a minimizer in this case). The corresponding minimizer of the action is the curve of maximum likelihood by which the transitions between these stable equilibrium points occur due to the presence of the small noise.

The gMAM is an algorithm to evolve curves with arbitrary parametrization in order to find the minimizer of the reformulated Freidlin-Wentzell action functional. Here the algorithm was tested on several examples: a finite-dimensional diffusion (SDE) with a nongradient drift, an infinite-dimensional generalization of this SDE (i.e., an SPDE for which traditional methods based on a shooting algorithm are inapplicable) and a Markov jump process. However, the potential range of applicability of the gMAM is broader than these illustrative examples.

In particular, Proposition 2.1 relies only on Assumptions 1–3 for the Hamiltonian $H(x, \theta)$. This makes the results in this paper applicable to a wider class of problems than those arising in the context of large deviations theory. One such problem is the determination of the instanton by which quantum tunneling arises

(for background on this problem, see, e.g., [11, 18]). The relevant action in this case is

$$V(x_1, x_2) = \inf_{T>0} \inf_{\psi \in \bar{C}^{x_2}_{x_1}(0,T)} \int_0^T \left(\frac{1}{2} |\dot{\psi}(t)|^2 + U(\psi(t)) \right) dt. \tag{5.1}$$

Here x_1 and x_2 are minima of the potential $U \geq 0$, and it is assumed that $U(x_1) = U(x_2) = 0$. Hence x_1 and x_2 are critical points according to our definition (1.24).

It is well-known [18] that this minimization problem can be recast into a geodesic problem in terms of the Agmon distance; i.e., $V(x_1, x_2)$ can be expressed as

$$V(x_1, x_2) = \inf_{\varphi \in \bar{C}^{x_2}_{x_1}(0,1)} \int_0^1 \sqrt{2U(\varphi(\alpha))}\, |\varphi'(\alpha)| d\alpha. \tag{5.2}$$

The instanton is the minimizer of this action. The new MAM can be straightforwardly applied to (5.2) since the corresponding Hamiltonian $H(x, \theta) = \frac{1}{2}|\theta|^2 - U(x)$ fulfills Assumptions 1–3 of our paper. The gMAM can also be applied to similar problems involving finding geodesics in high-dimensional space with the Riemannian metric.

Appendix A: Three Technical Lemmas

The goal in this appendix is to prove Lemmas A.1 and A.3, which are needed in the proof of Proposition 2.1(i).

LEMMA A.1 *Let $\psi_1 \in \bar{C}(0, T_1)$ and $\psi_2 \in \bar{C}(0, T_2)$ with $\gamma(\psi_1) = \gamma(\psi_2)$, and let the local action $\ell : D \times \mathbb{R}^n \to [0, \infty)$ have the property that for all $x \in D$, $y \in \mathbb{R}^n$, and $c \geq 0$, we have $\ell(x, cy) = c\ell(x, y)$. Then*

$$\int_0^{T_1} \ell(\psi_1, \psi_1') dt = \int_0^{T_2} \ell(\psi_2, \psi_2') dt.$$

PROOF: Let $\psi_1(t) = \varphi(\alpha(t))$ for all $t \in [0, T_1]$, some $\varphi \in \bar{C}(0, 1)$ with $|\varphi'| \equiv cst$ a.e., and for some absolutely continuous rescaling $\alpha : [0, 1] \to [0, T_1]$ with $\alpha' \geq 0$ almost everywhere. Then for all $t \in [0, T_1]$ we have $\dot{\psi}_1(t) = \varphi'(\alpha(t))\alpha'(t)$, and we can compute

$$\begin{aligned} \int_0^{T_1} \ell(\psi_1, \dot{\psi}_1) dt &= \int_0^{T_1} \ell\big(\varphi(\alpha(t)), \varphi'(\alpha(t))\alpha'(t)\big) dt \\ &= \int_0^{T_1} \ell\big(\varphi(\alpha(t)), \varphi'(\alpha(t))\big)\alpha'(t) dt \\ &= \int_0^1 \ell\big(\varphi(\alpha), \varphi'(\alpha)\big) d\alpha. \end{aligned}$$

Since the same calculation can be made for ψ_2, we are done. □

To prepare for the proof of Lemma A.3, we need to show some technical properties of H and θ^* first.

LEMMA A.2

(i) *The following equalities hold*:

$$L_y(x, y) = \theta^*(x, y), \tag{A.1}$$

$$\theta^*_y(x, y) = H^{-1}_{\theta\theta}(x, \theta^*(x, y)) = L_{yy}(x, y). \tag{A.2}$$

(ii) *Assumption* 3 *implies the limits*

$$\lim_{\theta\to\infty} H(x, \theta) = \infty, \tag{A.3}$$

$$\lim_{y\to\infty} \theta^*(x, y) = \infty, \tag{A.4}$$

uniformly in x *on compact sets.*

PROOF:

(i) By differentiating (1.22) with respect to y and using (1.23), we obtain

$$L_y(x, y) = \theta^*(x, y) + \big(\theta^*_y(x, y)\big)^T \big(y - H_\theta(x, \theta^*(x, y))\big) = \theta^*(x, y).$$

Differentiating (1.23) with respect to y leads us to

$$H_{\theta\theta}(x, \theta^*(x, y))\theta^*_y(x, y) = I$$

and thus

$$H^{-1}_{\theta\theta}(x, \theta^*(x, y)) = \theta^*_y(x, y) = L_{yy}(x, y).$$

(ii) Denoting $\hat{e}_\theta := \theta/|\theta|$, for any compact set $K \subset D$ Assumption 3 implies that

$$\begin{aligned}\langle H_\theta(x, \theta), \hat{e}_\theta\rangle &= \int_0^{|\theta|} \langle \hat{e}_\theta, H_{\theta\theta}(x, \tau\hat{e}_\theta)\hat{e}_\theta\rangle d\tau + \langle H_\theta(x, 0), \hat{e}_\theta\rangle \\ &\geq m(x)|\theta| - \sup_{x\in K} |H_\theta(x, 0)| \geq m_K|\theta| - C_K.\end{aligned} \tag{A.5}$$

Performing one more integration, we find

$$\begin{aligned}H(x, \theta) &= \int_0^{|\theta|} \langle H_\theta(x, \tau\hat{e}_\theta), \hat{e}_\theta\rangle d\tau + H(x, 0) \\ &\geq \int_0^{|\theta|} (m_K\tau - C_K)d\tau - C'_K = \frac{1}{2} m_K|\theta|^2 - C_K|\theta| - C'_K,\end{aligned}$$

proving (A.3).

To prove (A.4), assume that it is not true. Then there exists a sequence (y_k) with $y_k \to \infty$ and a bounded sequence (x_k) such that the sequence $(\theta^*(x_k, y_k))$ is bounded. But continuity of $H_\theta(\cdot, \cdot)$ then implies that $y_k = H_\theta(x_k, \theta^*(x_k, y_k))$ stays bounded, and we have a contradiction. □

Now we are ready to prove Lemma A.3.

LEMMA A.3 *For the functions λ_k defined in the proof of Proposition* 2.1*, we have* $|\lambda_k|_\infty < \infty$ *and*

$$\sup_{k\in\mathbb{N}} \left| \frac{L(\varphi, \varphi'\lambda_k)}{\lambda_k} \right|_\infty < \infty, \tag{A.6}$$

where $|\cdot|_\infty$ *denotes the* L^∞ *norm on* $[0,1]$.

PROOF: First let us show that $M := |\lambda(\varphi,\varphi')|_\infty < \infty$. To do so, suppose $M = \infty$. Then for every $l \in \mathbb{N}$ the set $\{\alpha \in [0,1] \mid \lambda(\varphi,\varphi') > l\}$ would have nonzero measure, and we could construct a sequence (α_l) such that $\lim_{l\to\infty} \lambda(\varphi(\alpha_l), \varphi'(\alpha_l)) = \infty$ and $|\varphi'(\alpha_l)| = L_\varphi$ for every $l \in \mathbb{N}$, where $L_\varphi > 0$ is the constant such that $|\varphi'| \equiv L_\varphi$ almost everywhere. Now comparing (1.23) with (2.7), we see that $\hat{\vartheta}(\varphi,\varphi') = \theta^*(\varphi,\varphi'\lambda)$, so that

$$0 \equiv H(\varphi, \hat{\vartheta}(\varphi,\varphi'))\big|_{\alpha=\alpha_l} = H(\varphi, \theta^*(\varphi,\varphi'\lambda))\big|_{\alpha=\alpha_l} \to \infty \quad \text{as } l \to \infty$$

by Lemma A.2(ii), and we would have a contradiction. This shows that $M < \infty$, and thus also that $|\lambda_k|_\infty \le \max\{M, 1/k\} < \infty$.

Now we can begin our estimate by showing that

$$\begin{aligned}
|H(\varphi,\theta^*(\varphi,\varphi'\lambda_k))| &\le |H(\varphi,\theta^*(\varphi,\varphi'\lambda))| + \int_\lambda^{\lambda_k} |\partial_\tau H(\varphi,\theta^*(\varphi,\tau\varphi'))| d\tau \\
&= 0 + \int_\lambda^{\lambda_k} \left|\left\langle H_\theta\big(\varphi,\theta^*(\varphi,\tau\varphi')\big), \theta_y^*(\varphi,\tau\varphi')\varphi'\right\rangle\right| d\tau \\
&= \int_\lambda^{\lambda_k} \tau \left|\left\langle \varphi', H_{\theta\theta}^{-1}(\varphi,\theta^*(\varphi,\tau\varphi'))\varphi'\right\rangle\right| d\tau \\
&\le \frac{L_\varphi^2}{m_K} \int_\lambda^{\lambda_k} \tau\, d\tau = \frac{L_\varphi^2}{2m_K}(\lambda_k^2 - \lambda^2) \le \frac{L_\varphi^2 \lambda_k^2}{2m_K},
\end{aligned}$$

where in the third and fourth step we have used (1.23), (A.2), and Assumption 3 with $K := \gamma(\varphi)$ and $\xi = H_{\theta\theta}^{-1/2}\varphi'$. Thus

$$\left| \frac{H(\varphi,\theta^*(\varphi,\varphi'\lambda_k))}{\lambda_k} \right| \le \frac{L_\varphi^2 \lambda_k}{2m_K} \le \frac{L_\varphi^2 \max\{1,M\}}{2m_K} =: C < \infty,$$

and we obtain the bound

$$\begin{aligned}
\left| \frac{L(\varphi,\varphi'\lambda_k)}{\lambda_k} \right| &\le |\langle \theta^*(\varphi,\varphi'\lambda_k), \varphi'\rangle| + \left| \frac{H(\varphi,\theta^*(\varphi,\varphi'\lambda_k))}{\lambda_k} \right| \\
&\le L_\varphi \max\left\{ |\theta^*(x,y)| \mid x \in \gamma(\varphi),\ |y| \le L_\varphi \max\{1,M\} \right\} + C \\
&< \infty.
\end{aligned}$$

□

Appendix B: Proofs of Lemmas 2.2 and 2.8

PROOF OF LEMMA 2.2:

(i) and (ii) If $\lambda(x, y) = 0$, then the second equation in (2.7) tells us that $\hat{\vartheta}(x, y)$ is a minimizer of $H(x, \cdot)$ (which by Assumption 3 is unique). Because of the first equation in (2.7), we thus have $\inf_{\theta\in\mathbb{R}^n} H(x, \theta) = 0$, and together with Assumption 1 this implies that $H(x, 0) = 0$. But this means that 0 minimizes $H(x, \cdot)$, so we must have $\hat{\vartheta}(x, y) = 0$. Now the second equation in (2.7) finally says that $H_\theta(x, 0) = 0$, and x must be a critical point.

To show the reverse direction, observe that if x is a critical point, then $(\lambda, \hat{\vartheta}) = (0, 0)$ solves (2.7).

(iii) Let $x \in D$ be a critical point. By Definition (1.23) of θ^*, $H_\theta(x, 0) = 0$ tells us that $\theta^*(x, 0) = 0$. Therefore x fulfills $L(x, 0) = \langle\theta^*(x, 0), 0\rangle - H(x, \theta^*(x, 0)) = 0 - H(x, 0) = 0$, and we can apply l'Hospital's rule and use (A.1) to find the limit

$$\lim_{\lambda\to 0^+} \frac{L(x, \lambda y)}{\lambda} = \langle y, L_y(x, 0)\rangle = \langle y, \theta^*(x, 0)\rangle = 0.$$

(iv) For the representation (2.5) this follows from part (ii); for the representation (2.6), it follows from parts (i) and (iii) combined. For the representation (2.4), observe that if φ is a critical point, then $\vartheta = 0$ is the minimum of $H(\varphi, \cdot)$, and thus we have $H(\varphi, \vartheta) = 0$ only for $\vartheta = 0$. □

PROOF OF LEMMA 2.8:

(i) Let L_φ be the constant such that $|\varphi'| \equiv L_\varphi$ a.e., and let $\alpha \in [0, 1]$ such that $|\varphi'(\alpha)| = L_\varphi$. Denote $\varphi := \varphi(\alpha)$, $\varphi' := \varphi'(\alpha)$, $\hat{\vartheta} := \hat{\vartheta}(\varphi, \varphi')$, $\lambda := \lambda(\varphi, \varphi')$, and finally $\varphi_c := \varphi(\alpha_c)$.

Since φ_c is a critical point, we have $H_\theta(\varphi_c, 0) = 0$ and $H(\varphi_c, 0) = 0$, and the latter equality together with Assumption 1 tells us that also $H_x(\varphi_c, 0) = 0$. Thus if we expand $H(\varphi, \hat{\vartheta})$, which is 0 by definition of $\hat{\vartheta}$, around the point $(x, \theta) = (\varphi_c, 0)$, the zeroth- and first-order terms vanish, and we obtain

$$\begin{aligned} 0 &= H(\varphi, \hat{\vartheta}) \\ &= \frac{1}{2}\langle\varphi - \varphi_c, H_{xx}(\tilde{x}, \tilde{\theta})(\varphi - \varphi_c)\rangle + \langle\hat{\vartheta}, H_{\theta x}(\tilde{x}, \tilde{\theta})(\varphi - \varphi_c)\rangle \\ &\quad + \frac{1}{2}\langle\hat{\vartheta}, H_{\theta\theta}(\tilde{x}, \tilde{\theta})\hat{\vartheta}\rangle \end{aligned}$$

for some point $(\tilde{x}, \tilde{\theta})$ on the straight line between $(\varphi_c, 0)$ and $(\varphi, \hat{\vartheta})$. Note that φ is in the compact set $\gamma(\varphi)$, and so equation (A.3) of Lemma A.2 and the first equation in (2.7) tell us that $\hat{\vartheta}$ must also lie within some compact set independent of α. Since $|\tilde{x} - \varphi_c| \le |\varphi - \varphi_c|$ and $|\tilde{\theta}| \le |\hat{\vartheta}|$, this means that $(\tilde{x}, \tilde{\theta})$ is also within

some compact set $K \times K' \subset D \times \mathbb{R}^n$ independent of α. Applying Assumptions 2 and 3 we find

$$\begin{aligned}\frac{1}{2}m_K|\hat{\vartheta}|^2 &\leq \frac{1}{2}\langle\hat{\vartheta}, H_{\theta\theta}(\tilde{x},\tilde{\theta})\hat{\vartheta}\rangle \\ &= -\frac{1}{2}\langle\varphi-\varphi_c, H_{xx}(\tilde{x},\tilde{\theta})(\varphi-\varphi_c)\rangle - \langle\hat{\vartheta}, H_{\theta x}(\tilde{x},\tilde{\theta})(\varphi-\varphi_c)\rangle \\ &\leq C(|\varphi-\varphi_c|^2 + |\varphi-\varphi_c|\,|\hat{\vartheta}|) \\ &\leq C\left(|\varphi-\varphi_c|^2 + \frac{C}{m_K}|\varphi-\varphi_c|^2 + \frac{m_K}{4C}|\hat{\vartheta}|^2\right)\end{aligned}$$

by Cauchy's inequality. Therefore we have $|\hat{\vartheta}| \leq C'|\varphi-\varphi_c|$ for some constant $C' > 0$, and expanding around $(\varphi_c, 0)$ again we conclude that

$$\begin{aligned}\lambda &= \frac{1}{L_\varphi}|\lambda\varphi'| = \frac{1}{L_\varphi}|H_\theta(\varphi,\hat{\vartheta})| \\ &= \frac{1}{L_\varphi}\big|\underbrace{H_\theta(\varphi_c,0)}_{=0} + H_{\theta x}(\tilde{x}',\tilde{\theta}')(\varphi-\varphi_c) + H_{\theta\theta}(\tilde{x}',\tilde{\theta}')\hat{\vartheta}\big| \\ &\leq C''(|\varphi-\varphi_c| + |\hat{\vartheta}|) \\ &\leq C''(1+C')|\varphi-\varphi_c| \leq C''(1+C')L_\varphi|\alpha-\alpha_c|.\end{aligned}$$

(ii) This is now a direct consequence of (i) since $\lambda \leq C|\alpha-\alpha_c|$ implies for arbitrarily small $\epsilon > 0$ that

$$\int\limits_{|\alpha-\alpha_c|\leq\epsilon} \frac{d\alpha}{\lambda} \geq \frac{1}{C}\int\limits_{|\alpha-\alpha_c|\leq\epsilon} \frac{d\alpha}{|\alpha-\alpha_c|} = \infty.$$

□

Appendix C: Proof of Lemma 2.5

PROOF OF LEMMA 2.5:

(i) In order to apply the Arzèla-Ascoli theorem, we quickly check that the set $C_{X,M}$ is uniformly bounded and uniformly equicontinuous: For all $\varphi \in C_{X,M}$ and all $\alpha \in [0,1]$ we have

$$|\varphi(\alpha)| = \left|\varphi(0) + \int_0^\alpha \varphi'(a)da\right| \leq |\varphi(0)| + \int_0^\alpha |\varphi'(a)|da \leq \sup_{x\in X}|x| + M$$

and

$$|\varphi(\alpha+h)-\varphi(\alpha)| = \left|\int_\alpha^{\alpha+h}\varphi'(a)da\right| \leq \int_\alpha^{\alpha+h}|\varphi'(a)|da \leq Mh.$$

This proves precompactness of the set $C_{X,M}$. To prove that $C_{X,M}$ is also closed, take any sequence (φ_n) in $C_{X,M}$ that converges uniformly to some $\varphi \in C(0,1)$. We have to show that $\varphi \in C_{X,M}$. Clearly, $\varphi(0) \in X$. Furthermore, for every $a, b \in [0,1]$, $a < b$, we have

$$\begin{aligned}
&\sup_{a\le\alpha_0<\cdots<\alpha_N\le b} \sum_{i=1}^{N} |\varphi(\alpha_i) - \varphi(\alpha_{i-1})| \\
&\quad = \sup_{a\le\alpha_0<\cdots<\alpha_N\le b} \lim_{n\to\infty} \sum_{i=1}^{N} |\varphi_n(\alpha_i) - \varphi_n(\alpha_{i-1})| \\
&\quad \le \liminf_{n\to\infty} \sup_{a\le\alpha_0<\cdots<\alpha_N\le b} \sum_{i=1}^{N} |\varphi_n(\alpha_i) - \varphi_n(\alpha_{i-1})| \\
&\quad = \liminf_{n\to\infty} \int_a^b |\varphi_n'(\alpha)| d\alpha \le M(b-a) < \infty.
\end{aligned}$$

This shows that φ is absolutely continuous and that $|\varphi'| \le M$ almost everywhere. Therefore $C_{X,M}$ is closed, and since it is also precompact, it must be compact.

(ii) This now follows directly from (i) by observing that $C_M^{x,y}$ is a closed subset of $C_{X,M}$, for $X := \{x\}$.

(iii) We want to show that for any sequence (φ_n) in $C_{X,M}$ converging to some $\varphi \in C_{X,M}$ we have $\hat{S}(\varphi) \le \liminf_{n\to\infty} \hat{S}(\varphi_n)$. We can follow exactly the lines of the proof of [17, lemma 5.42], applied to convergence in $|\cdot|_{[0,1]}$ (which in [17] is denoted by d_c), except for two modifications: First, since we do not have the equivalent of [17, lemmas 5.17 and 5.18] (the integrand of $\hat{S}$ increases only linearly in $|\varphi'|$), we have to restrict $\hat{S}$ to $C_{X,M}$, which guarantees uniform equicontinuity of the sequence (φ_n), as shown in part (i). Second, we have to adjust the definition of the lower bound $\ell^\delta(x,y)$ for the local action $\ell(x,y)$ to our case and show that our function ℓ^δ still fulfills the required properties, i.e., weak convexity in y and lower semicontinuity in the limit $(x,y,\delta) \to (x_0, y_0, 0^+)$, although the technique in [17, lemma 5.40] to prove the latter fails in our case (since our equivalent of $g^\delta(x,\theta)$ is not continuous).

For every $x \in D$, $y \in \mathbb{R}^n$, and $\delta > 0$ we define

$$\ell^\delta(x,y) := \sup\{\langle y,\theta\rangle \mid \theta \in \mathbb{R}^n \text{ s.t. } \forall z \in D : |z-x| \le \delta \Rightarrow H(z,\theta) \le 0\}.$$

Then for every $\bar{x} \in D$ with $|\bar{x} - x| \le \delta$ we have

$$\ell^\delta(x,y) \le \sup_{\substack{\theta\in\mathbb{R}^n \\ H(\bar{x},\theta)\le 0}} \langle y,\theta\rangle = \sup_{\substack{\theta\in\mathbb{R}^n \\ H(\bar{x},\theta)=0}} \langle y,\theta\rangle =: \ell(\bar{x},y), \tag{C.1}$$

where ℓ is our local action from representation (2.4).

Clearly, $\ell^\delta(x,y)$ is convex in y as the supremum of linear functions. To show lower semicontinuity of $\ell^\delta(x,y)$, consider first the cases when either x_0 is a critical

point or when $y_0 = 0$. If x_0 is a critical point, then the local action ℓ vanishes at (x_0, y_0) by Lemma 2.2; if $y_0 = 0$ then the local action ℓ vanishes by its definition in (C.1). Thus by Assumption 1 we have

$$\ell^\delta(x, y) \geq \langle y, 0\rangle = 0 = \ell(x_0, y_0) \quad \forall x, y, \delta,$$

so that

$$\liminf_{(x,y,\delta)\to(x_0,y_0,0^+)} \ell^\delta(x, y) \geq \ell(x_0, y_0). \tag{C.2}$$

In all other cases (i.e., x_0 is not a critical point and $y_0 \neq 0$) we have $H_\theta(x_0, \hat\vartheta) = \lambda(x_0, y_0)y_0 \neq 0$ (for $\hat\vartheta := \hat\vartheta(x_0, y_0)$) by Lemma 2.2(i). Since by definition of $\hat\vartheta$ we have $H(x_0, \hat\vartheta) = 0$, for every $\varepsilon > 0$ there exists a $\tilde\theta \in \mathbb{R}^n$ with $|\tilde\theta - \hat\vartheta| < \varepsilon$ such that $H(x_0, \tilde\theta) < 0$. By continuity of $H(\cdot, \tilde\theta)$, there exists an $\eta > 0$ such that for all $z \in D$ with $|z - x_0| \leq \eta$ we have $H(z, \tilde\theta) \leq 0$. Let $\delta + |x - x_0| \leq \eta$. Since

$$|z - x| \leq \delta \;\Rightarrow\; |z - x_0| \leq \delta + |x - x_0| \leq \eta,$$

we then have

$$\begin{aligned}
\ell^\delta(x, y) &\geq \sup\{\langle y, \theta\rangle \mid \theta \in \mathbb{R}^n \text{ s.t. } \forall z \in D : |z - x_0| \leq \eta \Rightarrow H(z, \theta) \leq 0\} \\
&\geq \langle y, \tilde\theta\rangle \\
&= \langle y_0, \hat\vartheta\rangle + \langle y - y_0, \hat\vartheta\rangle + \langle y, \tilde\theta - \hat\vartheta\rangle \\
&\geq \ell(x_0, y_0) - |y - y_0||\hat\vartheta| - |y|\varepsilon,
\end{aligned}$$

where in the last step we used representation (2.5) of the local action $\ell(x_0, y_0)$. Taking the lim inf as $(x, y, \delta) \to (x_0, y_0, 0^+)$ and then letting $\varepsilon \to 0$, we see that (C.2) holds also in this case, terminating the proof of part (iii).

(iv) Let K be a nonempty closed subset of $C_{X,M}$, and let (φ_n) be a sequence in K such that $\lim_{n\to\infty} \hat S(\varphi_n) = \inf_{\varphi\in K} \hat S(\varphi)$. Since $C_{X,M}$ is compact, K is compact as well, and thus there exists a subsequence (φ_{n_k}) that converges uniformly to some $\varphi^\star \in K$ as $k \to \infty$. Because of the lower semicontinuity of $\hat S$, we have

$$\hat S(\varphi^\star) \leq \liminf_{k\to\infty} \hat S(\varphi_{n_k}) = \inf_{\varphi\in K} \hat S(\varphi)$$

and thus $\hat S(\varphi^\star) = \inf_{\varphi\in K} \hat S(\varphi)$. □

Appendix D: Proof of Proposition 2.3

In this appendix we will prove the technical details of Steps 1–3 that we omitted in the proof of Proposition 2.3 in Section 2.2. Let us begin with

Step 1. There exists an $\tilde\eta > 0$ such that for small enough δ

$$\rho(X^\varepsilon|_{[0,T]}, \varphi^\star) \leq \tilde\eta \text{ and } \tau_\delta(X^\varepsilon) \leq T \Rightarrow \rho(X^\varepsilon|_{[0,\tau_\delta(X^\varepsilon)]}, \varphi^\star) \leq \eta. \tag{D.1}$$

PROOF: Without loss of generality we may assume that $|\varphi^{\star\prime}| \equiv cst$ a.e. on $[0,1]$. Let $\alpha_0 \in (0,1)$ be large enough so that $\int_{\alpha_0}^1 |\varphi^{\star\prime}| d\alpha \le \frac{1}{2}\eta$, and let

$$\begin{aligned} 0 < \tilde{\eta} &:= \frac{1}{4} \inf_{0\le\alpha\le\alpha_0} |\varphi^\star(\alpha) - x_2| \\ &\le \frac{1}{4}|\varphi^\star(\alpha_0) - x_2| = \frac{1}{4}\left|\int_{\alpha_0}^1 \varphi^{\star\prime}\, d\alpha\right| \le \frac{1}{4}\int_{\alpha_0}^1 |\varphi^{\star\prime}| d\alpha \le \frac{\eta}{8}. \end{aligned} \tag{D.2}$$

Let $\delta \le \tilde{\eta}$. From the definition of the Fréchet distance, there are two weakly increasing, surjective, continuous functions $t(s) : [0,1] \to [0,T]$ and $\alpha(s) : [0,1] \to [0,1]$ such that

$$|X^\varepsilon(t(s)) - \varphi^\star(\alpha(s))|_{[0,1]} \le 2\tilde{\eta}. \tag{D.3}$$

Let $s_0 \in [0,1]$ be such that $t(s_0) = \tau_\delta := \tau_\delta(X^\varepsilon)$, and define $\tilde{t}(s) := t(s) \wedge \tau_\delta$. (We write $a \vee b$ and $a \wedge b$ to denote the maximum and the minimum of two numbers a and b, respectively.) Then

$$\begin{aligned} \rho(X^\varepsilon|_{[0,\tau_\delta]}, \varphi^\star) &\le |X^\varepsilon(\tilde{t}(s)) - \varphi^\star(\alpha(s))|_{[0,1]} \\ &= |X^\varepsilon(\tilde{t}(s)) - \varphi^\star(\alpha(s))|_{[0,s_0]} \vee |X^\varepsilon(\tilde{t}(s)) - \varphi^\star(\alpha(s))|_{[s_0,1]} \\ &= |X^\varepsilon(t(s)) - \varphi^\star(\alpha(s))|_{[0,s_0]} \vee |X^\varepsilon(\tau_\delta) - \varphi^\star(\alpha(s))|_{[s_0,1]} \\ &\le 2\tilde{\eta} \vee (|X^\varepsilon(\tau_\delta) - x_2| + |\varphi^\star(\alpha(s)) - x_2|_{[s_0,1]}). \end{aligned} \tag{D.4}$$

To estimate the second norm in the last expression, observe that (using $t(s_0) = \tau_\delta$ and (D.3)) we have

$$\begin{aligned} |\varphi^\star(\alpha(s_0)) - x_2| &\le |X^\varepsilon(t(s_0)) - x_2| + |X^\varepsilon(t(s_0)) - \varphi^\star(\alpha(s_0))| \\ &\le \delta + 2\tilde{\eta} \le 3\tilde{\eta} < 4\tilde{\eta} = \inf_{0\le\alpha\le\alpha_0} |\varphi^\star(\alpha) - x_2|, \end{aligned}$$

so that $\alpha(s_0) > \alpha_0$ necessarily. Therefore by monotonicity of $\alpha(\cdot)$, for all $s \in [s_0,1]$ we have $\alpha(s) \ge \alpha(s_0) > \alpha_0$ and thus

$$|\varphi^\star(\alpha(s)) - x_2| = \left|\int_{\alpha(s)}^1 \varphi^{\star\prime}\, d\alpha\right| \le \int_{\alpha_0}^1 |\varphi^{\star\prime}| d\alpha \le \frac{\eta}{2}.$$

We can now continue our estimate (D.4) and conclude that

$$\rho(X^\varepsilon|_{[0,\tau_\delta]}, \varphi^\star) \le 2\tilde{\eta} \vee \left(\delta + \frac{\eta}{2}\right) \le 2\tilde{\eta} \vee \left(\tilde{\eta} + \frac{\eta}{2}\right) \le \frac{\eta}{4} \vee \left(\frac{\eta}{8} + \frac{\eta}{2}\right) < \eta$$

by (D.2), proving Step 1. □

Step 2. $\lim_{(T,\delta)\to(T^\star,0^+)} \rho(\psi_{\delta,T}, \varphi^\star) = 0$.

PROOF: It suffices to show that any sequence $(\psi_k)_{k\in\mathbb{N}} := (\psi_{\delta_k,T_k})_{k\in\mathbb{N}}$, in which $\delta_k \to 0^+$ and $T_k \to T^\star$, has a subsequence $(\psi_{k_l})_{l\in\mathbb{N}}$ such that

$$\lim_{l\to\infty} \rho(\psi_{k_l}, \varphi^\star) = 0.$$

To show this, let (ψ_k) be such a sequence, and let us denote by φ_k the reparametrization of ψ_k (i.e., $\gamma(\varphi_k) = \gamma(\psi_k)$) such that $|\varphi_k'(\alpha)| \equiv cst_k$ for almost every $\alpha \in [0,1]$. The curve $\gamma(\varphi_k)$ starts from x_1, and by the assumption of Proposition 2.3 it has bounded length in the limit,

$$M := \limsup_{k\to\infty} \int_0^1 |\varphi_k'| d\alpha \le \limsup_{(T,\delta)\to(T^\star,0^+)} \int_0^T |\dot\psi_{\delta,T}| dt < \infty,$$

so φ_k is in the compact set $C_{\{x_1\},2M}$ defined in Lemma 2.5(i) if k is sufficiently large. Thus there exists a subsequence $(\varphi_{k_l})_{l\in\mathbb{N}}$ that converges uniformly to some limit $\tilde\varphi^\star \in C_{\{x_1\},2M}$. In particular, we have

$$\rho(\psi_{k_l}, \tilde\varphi^\star) = \rho(\varphi_{k_l}, \tilde\varphi^\star) \le |\varphi_{k_l} - \tilde\varphi^\star|_{[0,1]} \to 0 \quad \text{as } l \to \infty.$$

In the remaining part of the proof we will show that $\gamma(\tilde\varphi^\star) = \gamma(\varphi^\star)$ so that $\rho(\psi_{k_l}, \varphi^\star) = \rho(\psi_{k_l}, \tilde\varphi^\star) \to 0$ as $l \to \infty$. By lower semicontinuity of $\hat S$ we have

$$\begin{aligned}(\text{D.5})\quad \hat S(\tilde\varphi^\star) &\le \liminf_{l\to\infty} \hat S(\varphi_{k_l}) = \liminf_{l\to\infty} \inf_{T>0} \inf_{\psi\in\bar C_{\varphi_{k_l}}(0,T)} S_T(\psi) \\ &\le \liminf_{l\to\infty} S_{T_{k_l}}(\psi_{k_l}) = \liminf_{l\to\infty} \inf_{\substack{\psi\in\bar C_{x_1}(0,T_{k_l}) \\ \tau_{\delta_{k_l}}(\psi)\le T_{k_l}}} S_{T_{k_l}}(\psi).\end{aligned}$$

We want to show that the right-hand side is less than or equal to $\hat S(\varphi^\star)$. Consider first the case when $T_{k_l} < T^\star$ for all l. Let $(\tilde T_r, \tilde\psi_r)_{r\in(0,\infty)}$ be the approximating sequence defined in the proof of Proposition 2.1(i) (only here with $r \in (0,\infty)$), i.e., such that $\forall r > 0 : \gamma(\tilde\psi_r) = \gamma(\varphi^\star)$, $\lim_{r\to\infty} S_{\tilde T_r}(\tilde\psi_r) = \hat S(\varphi^\star)$, and $\lim_{r\to\infty} \tilde T_r = T^\star$. Using the notation $\lambda = \lambda(\varphi^\star, \varphi^{\star\prime})$ and letting $\lambda_r = \lambda \vee 1/r$, we find that for $\forall r_1, r_2 > 0$:

$$\begin{aligned}|\tilde T_{r_1} - \tilde T_{r_2}| &\le \int_0^1 \left|\frac{1}{\lambda_{r_1}} - \frac{1}{\lambda_{r_2}}\right| d\alpha \le \left|\frac{1}{\lambda_{r_1}} - \frac{1}{\lambda_{r_2}}\right|_{[0,1]} \\ &= \left|\left(\frac{1}{\lambda} \wedge r_1\right) - \left(\frac{1}{\lambda} \wedge r_2\right)\right|_{[0,1]} \le |r_1 - r_2|.\end{aligned}$$

As a result, the function $r \mapsto \tilde T_r$ is continuous, and we can choose a sequence (r_l) such that $\tilde T_{r_l} = T_{k_l}$ for $\forall l \in \mathbb{N}$. Now since $\tilde\psi_{r_l}(\tilde T_{r_l}) = \varphi^\star(1) = x_2 \in B_{\delta_k}(x_2)$, we can complete estimate (D.5) as follows:

$$\begin{aligned}(\text{D.6})\quad \hat S(\tilde\varphi^\star) &\le \liminf_{l\to\infty} \inf_{\substack{\psi\in\bar C_{x_1}(0,T_{k_l}) \\ \tau_{\delta_{k_l}}(\psi)\le T_{k_l}}} S_{T_{k_l}}(\psi) \le \liminf_{l\to\infty} S_{T_{k_l}}(\tilde\psi_{r_l}) \\ &= \liminf_{l\to\infty} S_{\tilde T_{r_l}}(\tilde\psi_{r_l}) = \hat S(\varphi^\star) = \inf_{\varphi\in\bar C_{x_1}^{x_2}(0,1)} \hat S(\varphi).\end{aligned}$$

If $T_{k_l} \ge T^\star$ for some l, then we can define the path $\tilde\psi_{r_l}$ by first following the path $\psi^\star = \tilde\psi_{r=\infty}$ in time $T^\star$ (which in this case is well-defined since $T^\star < \infty$)

and then staying at x_2 for the remaining time $\triangle_l := T_{k_l} - T^\star$. As $l \to \infty$, we have $\triangle_l \to 0$, and thus the additional action on the second part of the path goes to 0 as well, so that $S_{\tilde{T}_{r_l}}(\tilde{\psi}_{r_l}) \to \hat{S}(\varphi^\star)$ still, and (D.6) also remains valid in this case.

Since by assumption of Proposition 2.3 we have

$$\tilde{\varphi}^\star(1) = \lim_{l\to\infty} \varphi_{k_l}(1) = \lim_{l\to\infty} \psi_{\delta_{k_l},T_{k_l}}(T_{k_l}) = x_2,$$

$\tilde{\varphi}^\star$ is in $\bar{C}^{x_2}_{x_1}(0,1)$, and so from (D.6) we can conclude that

$$\hat{S}(\tilde{\varphi}^\star) = \inf_{\varphi\in\bar{C}^{x_2}_{x_1}(0,1)} \hat{S}(\varphi) = \hat{S}(\varphi^\star).$$

The uniqueness of the minimizing curve $\varphi^\star$ now implies that $\gamma(\tilde{\varphi}^\star) = \gamma(\varphi^\star)$, terminating the proof. □

Step 3. For all $T, \delta > 0$ the set of paths $\{\psi \in \bar{C}_{x_1}(0,T) \mid \tau_\delta(\psi) \le T\}$ is regular with respect to S_T.

PROOF: First, note that the set $\{\tau_\delta \le T\} := \{\psi \in \bar{C}_{x_1}(0,T) \mid \tau_\delta(\psi) \le T\}$ is closed since its complement $\{\tau_\delta \le T\}^c = \{\tau_\delta > T\} = \{\psi \mid \gamma(\psi) \cap B_\delta(x_2) = \varnothing\}$ is open. Since closing the latter set amounts to replacing the closed ball $B_\delta(x_2)$ by the corresponding open ball, we find that the interior of the set $\{\tau_\delta \le T\}$ is $\{\tau_\delta \le T\}^0 = \{\tau^0_\delta \le T\}$, where τ^0_δ denotes the infimum of all times at which the path is inside the *open* ball with radius δ around x_2. Thus we must show

$$\inf_{\substack{\psi\in\bar{C}_{x_1}(0,T)\\ \tau_\delta(\psi)\le T}} S_T(\psi) \ge \inf_{\substack{\psi\in\bar{C}_{x_1}(0,T)\\ \tau^0_\delta(\psi)\le T}} S_T(\psi)$$

since the relation $\le$ is clear. We will show that for every $\psi \in \{\tau_\delta \le T\}$ we can construct functions $\tilde{\psi}_r \in \{\tau^0_\delta \le T\}$, $r > 0$, such that $|S_T(\tilde{\psi}_r) - S_T(\psi)|$ becomes arbitrarily small as $r \to 0^+$. The function $\tilde{\psi}_r$ will be constructed in such a way that it traverses $\gamma(\psi)$ at a slightly higher speed than ψ, and we will use the time we saved to make a small excursion from the point where ψ touches the outside of the ball $B_\delta(x_2)$ into its interior and back, so that in fact $\tau^0_\delta(\tilde{\psi}) \le T$.

In order to show that the action $S_T(\tilde{\psi}_r)$ differs only slightly from $S_T(\psi)$, it turns out that one can speed up the path ψ only at places where $|\dot{\psi}|$ is bounded away from ∞. To do so, we pick some $M > \operatorname{ess\,inf}_{0\le t\le T} |\dot{\psi}(t)|$, define for every $r \in (0, \frac{1}{2})$ the time rescaling G_r via its inverse by

$$G_r^{-1}(t) := \int_0^t (1 - r\mathbb{1}_{|\dot{\psi}|\le M})\,d\tau, \quad G_r^{-1} : [0,T] \to [0,T_r],$$
$$T_r := G_r^{-1}(T) < T,$$

where $\mathbb{1}_{|\dot\psi|\le M}$ denotes the indicator function on the set $\{t \in [0,T] : |\dot\psi(t)| \le M\}$, and set $\psi_r(s) := \psi(G_r(s))$. Using

$$G_r'(s) = \frac{1}{(G_r^{-1})'(G_r(s))} = \left[1 - r\,\mathbb{1}_{|\dot\psi|\le M}(G_r(s))\right]^{-1},$$

we find that

$$\begin{aligned} S_{T_r}(\psi_r) &= \int_0^{T_r} L(\psi_r(s), \dot\psi_r(s))ds \\ &= \int_0^{T_r} L\left(\psi(G_r(s)), \frac{\dot\psi(G_r(s))}{1 - r\,\mathbb{1}_{|\dot\psi|\le M}(G_r(s))}\right)ds \\ &= \int_0^{T} L\left(\psi(t), \frac{\dot\psi(t)}{1 - r\,\mathbb{1}_{|\dot\psi|\le M}(t)}\right)\left[1 - r\,\mathbb{1}_{|\dot\psi|\le M}(t)\right]dt. \end{aligned}$$

As $r \to 0^+$, the integrand in the last integral converges pointwise to $L(\psi(t), \dot\psi(t))$. To show that one can exchange limit and integral, observe that on $\{t \in [0,T] : |\dot\psi(t)| > M\}$ the integrand equals $L(\psi, \dot\psi)$ before taking the limit, and that on $\{t \in [0,T] : |\dot\psi(t)| \le M\}$ we can use the bounded convergence theorem since (i) $\frac{1}{2} \le 1 - r\,\mathbb{1}_{|\dot\psi|\le M} \le 1$, (ii) $\psi(t)$ traverses the compact set $\gamma(\psi)$, and (iii) $L(x,y)$ is continuous. Thus $\lim_{r\to 0^+} S_{T_r}(\psi_r) = S_T(\psi)$.

Now let $\nu_r := \frac{1}{2}(T - T_r) = \frac{r}{2}\int_0^T \mathbb{1}_{|\dot\psi|\le M}\,dt > 0$, and pick a point $x_\delta \in \gamma(\psi) \cap \partial B_\delta(x_2)$ at which ψ touches the boundary of $B_\delta(x_2)$. Consider

$$\chi^+_{\nu_r}(t) := x_\delta + t(x_2 - x_\delta) \quad \text{and} \quad \chi^-_{\nu_r}(t) := x_\delta + (\nu_r - t)(x_2 - x_\delta)$$

(for $0 \le t \le \nu_r$): $\chi^+_{\nu_r}$ starts at x_δ and enters the ball $B_\delta(x_2)$ in the direction of its center x_2; $\chi^-_{\nu_r}$ then goes back the opposite way. The corresponding actions

$$\begin{aligned} S_{\nu_r}(\chi^+_{\nu_r}) &= \int_0^{\nu_r} L(x_\delta + t(x_2 - x_\delta), x_2 - x_\delta)dt, \\ S_{\nu_r}(\chi^-_{\nu_r}) &= \int_0^{\nu_r} L(x_\delta + (\nu_r - t)(x_2 - x_\delta), x_\delta - x_2)dt \\ &= \int_0^{\nu_r} L(x_\delta + s(x_2 - x_\delta), x_\delta - x_2)ds \end{aligned}$$

converge to 0 as $r \to 0^+$ (and thus $\nu_r \to 0^+$). We can now define $\tilde\psi_r$ by piecing ψ_r, $\chi^+_{\nu_r}$, and $\chi^-_{\nu_r}$ together in such a way that $\tilde\psi_r$ moves from x_1 to x_δ along ψ_r, briefly enters and exits the interior of $B_\delta(x_2)$ via $\chi^+_{\nu_r}$ and $\chi^-_{\nu_r}$, and continues along the remaining part of ψ_r. The total time for this path is $T_r + 2\nu_r = T_r + (T - T_r) = T$, and the total action is

$$S_T(\tilde\psi_r) = S_{T_r}(\psi_r) + S_{\nu_r}(\chi^+_{\nu_r}) + S_{\nu_r}(\chi^-_{\nu_r}) \to S_T(\psi) + 0 + 0$$

as $r \to 0$. Since $\tau^0_\delta(\tilde\psi_r) \le T$ for every $r \in (0, \frac{1}{2})$, this completes the proof. □

Appendix E: Proof of Proposition 3.1

In the following lemma we will compute the derivatives of $\hat{\vartheta}(x, y)$ and $\lambda(x, y)$, which we will need later in the proof of Proposition 3.1 to compute the Euler-Lagrange equation for $\hat{S}$.

LEMMA E.1 (Derivatives of $\hat{\vartheta}$ and λ) *For all $x \in D$ and $y \in \mathbb{R}^n \setminus \{0\}$ we have*

$$\hat{\vartheta}_x(x, y) = -H_{\theta\theta}^{-1}\left(P_y H_{\theta x} + \lambda^{-1}\frac{y \otimes H_x}{\langle y, H_{\theta\theta}^{-1} y\rangle}\right), \tag{E.1}$$

$$\hat{\vartheta}_y(x, y) = \lambda H_{\theta\theta}^{-1} P_y, \tag{E.2}$$

$$\hat{\vartheta}_y(x, y)^T y = 0, \tag{E.3}$$

$$\lambda_x(x, y) = \frac{\lambda H_{x\theta} H_{\theta\theta}^{-1} y - H_x}{\lambda\langle y, H_{\theta\theta}^{-1} y\rangle}, \tag{E.4}$$

$$\lambda_y(x, y) = -\frac{\lambda H_{\theta\theta}^{-1} y}{\langle y, H_{\theta\theta}^{-1} y\rangle}, \tag{E.5}$$

where we abbreviate

$$P_y := I - \frac{y \otimes H_{\theta\theta}^{-1} y}{\langle y, H_{\theta\theta}^{-1} y\rangle}, \tag{E.6}$$

and where H_x, $H_{\theta x}$, $H_{x\theta}$, and $H_{\theta\theta}$ are evaluated at the point $(x, \hat{\vartheta}(x, y))$.

PROOF: All formulae can be obtained by implicit differentiation of equations (2.7), where $\lambda = \lambda(x, y)$ and $\hat{\vartheta} = \hat{\vartheta}(x, y)$.

First we differentiate $H(x, \hat{\vartheta}(x, y)) = 0$ both with respect to x and y to obtain

$$H_x^T + H_\theta^T \hat{\vartheta}_x = H_x^T + \lambda y^T \hat{\vartheta}_x = 0, \quad H_\theta^T \hat{\vartheta}_y = \lambda y^T \hat{\vartheta}_y = 0. \tag{E.7}$$

From the second equation we see that (E.3) holds since $\lambda = 0$ only if x is a critical point and since $\hat{\vartheta}_y$ is continuous.

Differentiating the second equation in (2.7), $H_\theta(x, \hat{\vartheta}(x, y)) = \lambda y$, with respect to x and y, we obtain

$$H_{\theta x} + H_{\theta\theta}\hat{\vartheta}_x = y\lambda_x^T, \quad H_{\theta\theta}\hat{\vartheta}_y = \lambda I + y\lambda_y^T. \tag{E.8}$$

Left-multiplying both equations by $\lambda y^T H_{\theta\theta}^{-1}$ and using equations (E.7), we conclude

$$\begin{aligned} \lambda y^T H_{\theta\theta}^{-1} H_{\theta x} - H_x^T &= \lambda\langle y, H_{\theta\theta}^{-1} y\rangle \lambda_x^T, \\ 0 &= \lambda^2 y^T H_{\theta\theta}^{-1} + \lambda\langle y, H_{\theta\theta}^{-1} y\rangle \lambda_y^T, \end{aligned}$$

which we can solve for λ_x^T and λ_y^T:

$$\lambda_x^T = \frac{\lambda y^T H_{\theta\theta}^{-1} H_{\theta x} - H_x^T}{\lambda \langle y, H_{\theta\theta}^{-1} y \rangle}, \quad \lambda_y^T = -\frac{\lambda y^T H_{\theta\theta}^{-1}}{\langle y, H_{\theta\theta}^{-1} y \rangle}, \tag{E.9}$$

proving (E.4) and (E.5). We can now solve equations (E.8) for $\hat{\vartheta}_x$ and $\hat{\vartheta}_y$ and plug in equations (E.9) to obtain

$$\begin{aligned}
\hat{\vartheta}_x &= H_{\theta\theta}^{-1}(y\lambda_x^T - H_{\theta x}) \\
&= H_{\theta\theta}^{-1}\left(\frac{\lambda y y^T H_{\theta\theta}^{-1} H_{\theta x} - y H_x^T}{\lambda \langle y, H_{\theta\theta}^{-1} y \rangle} - H_{\theta x}\right) \\
&= -H_{\theta\theta}^{-1}\left(P_y H_{\theta x} + \lambda^{-1} \frac{y H_x^T}{\langle y, H_{\theta\theta}^{-1} y \rangle}\right), \\
\hat{\vartheta}_y &= H_{\theta\theta}^{-1}(\lambda I + y\lambda_y^T) \\
&= H_{\theta\theta}^{-1}\lambda\left(I - \frac{y y^T H_{\theta\theta}^{-1}}{\langle y, H_{\theta\theta}^{-1} y \rangle}\right) = \lambda H_{\theta\theta}^{-1} P_y,
\end{aligned}$$

where

$$P_y = I - \frac{y y^T H_{\theta\theta}^{-1}}{\langle y, H_{\theta\theta}^{-1} y \rangle} = I - \frac{y \otimes H_{\theta\theta}^{-1} y}{\langle y, H_{\theta\theta}^{-1} y \rangle}.$$

This proves (E.1) and (E.2) and we are done. □

PROOF OF PROPOSITION 3.1: Starting from the representation (2.5) of the action $\hat{S}$, we obtain

$$\begin{aligned}
D\hat{S}(\varphi) &= \hat{\vartheta}_x^T \varphi' - \partial_\alpha(\hat{\vartheta} + \hat{\vartheta}_y^T \varphi') \\
&= \hat{\vartheta}_x^T \varphi' - \hat{\vartheta}_x \varphi' - \hat{\vartheta}_y \varphi'' - \partial_\alpha(\hat{\vartheta}_y^T \varphi') \\
&= (\hat{\vartheta}_x^T - \hat{\vartheta}_x)\varphi' - \hat{\vartheta}_y \varphi'' - \partial_\alpha(\hat{\vartheta}_y^T \varphi'). \qquad \text{(E.10)}
\end{aligned}$$

(E.3) in Lemma E.1 says that the last term in (E.10) vanishes. We can then apply formulae (E.1) and (E.2) for the derivatives of $\hat{\vartheta}$ to obtain

$$\begin{aligned}
\lambda H_{\theta\theta} D\hat{S}(\varphi) &= \lambda H_{\theta\theta}((\hat{\vartheta}_x^T - \hat{\vartheta}_x)\varphi' - \hat{\vartheta}_y \varphi'') \\
&= \left(P_{\varphi'} \lambda H_{\theta x} + \frac{\varphi' H_x^T}{\langle \varphi', H_{\theta\theta}^{-1} \varphi' \rangle}\right. \\
&\quad \left. - \lambda H_{\theta\theta} H_{\theta x}^T P_{\varphi'}^T H_{\theta\theta}^{-1} - \frac{H_{\theta\theta} H_x \varphi'^T H_{\theta\theta}^{-1}}{\langle \varphi', H_{\theta\theta}^{-1} \varphi' \rangle}\right)\varphi' - \lambda^2 P_{\varphi'} \varphi''
\end{aligned}$$

$$= \left(P_{\varphi'} \lambda H_{\theta x} + \frac{\varphi' H_x^T}{\langle \varphi', H_{\theta\theta}^{-1} \varphi' \rangle} \right) \varphi' - 0 - H_{\theta\theta} H_x - \lambda^2 P_{\varphi'} \varphi''$$

$$= P_{\varphi'} (-\lambda^2 \varphi'' + \lambda H_{\theta x} \varphi' - H_{\theta\theta} H_x).$$

The relation $\lambda = \langle H_\theta, \varphi' \rangle / |\varphi'|^2$ follows directly from (2.7).

To show the second representation of this term, we use (E.4) and (E.5) to compute

$$\begin{aligned}
\lambda \lambda' \varphi' &= \lambda (\partial_\alpha \lambda(\varphi, \varphi')) \varphi' \\
&= (\langle \lambda \lambda_x, \varphi' \rangle + \langle \lambda \lambda_y, \varphi'' \rangle) \varphi' \\
&= \frac{\langle \lambda H_{x\theta} H_{\theta\theta}^{-1} \varphi' - H_x, \varphi' \rangle - \langle \lambda^2 H_{\theta\theta}^{-1} \varphi', \varphi'' \rangle}{\langle \varphi', H_{\theta\theta}^{-1} \varphi' \rangle} \varphi' \\
&= \frac{\langle \lambda H_{\theta x} \varphi' - H_{\theta\theta} H_x - \lambda^2 \varphi'', H_{\theta\theta}^{-1} \varphi' \rangle}{\langle \varphi', H_{\theta\theta}^{-1} \varphi' \rangle} \varphi' \\
&= \frac{\varphi' \otimes H_{\theta\theta}^{-1} \varphi'}{\langle \varphi', H_{\theta\theta}^{-1} \varphi' \rangle} (-\lambda^2 \varphi'' + \lambda H_{\theta x} \varphi' - H_{\theta\theta} H_x) \\
&= (I - P_{\varphi'})(-\lambda^2 \varphi'' + \lambda H_{\theta x} \varphi' - H_{\theta\theta} H_x).
\end{aligned}$$

□

Appendix F: Update Formula for the Inner Loop

COMPUTING STEP 2: Given a vector $\hat{\vartheta}^p$ and

$$h = h(\hat{\vartheta}^p), \quad h_\theta = h_\theta(\hat{\vartheta}^p), \quad h_{\theta\theta} = h_{\theta\theta}(\hat{\vartheta}^p),$$

we must find θ_0, A, and c such that the quadratic function

$$f(\theta) := \frac{1}{2} \langle \theta - \theta_0, A(\theta - \theta_0) \rangle + c$$

fulfills

$$f(\hat{\vartheta}^p) = h, \quad f_\theta(\hat{\vartheta}^p) = h_\theta, \quad f_{\theta\theta}(\hat{\vartheta}^p) = h_{\theta\theta}. \tag{F.1}$$

Clearly, the last equation in (F.1) implies $A = h_{\theta\theta}$. From the second equation in (F.1) we obtain

$$A(\hat{\vartheta}^p - \theta_0) = h_\theta \quad \Leftrightarrow \quad \hat{\vartheta}^p - \theta_0 = A^{-1} h_\theta = h_{\theta\theta}^{-1} h_\theta.$$

Finally, the first equation in (F.1) tells us that

$$\begin{aligned} h &= \frac{1}{2}\langle \hat{\vartheta}^p - \theta_0, A(\hat{\vartheta}^p - \theta_0)\rangle + c \\ &= \frac{1}{2}\langle A^{-1}h_\theta, h_\theta\rangle + c \\ \Leftrightarrow \quad c &= h - \frac{1}{2}\langle h_\theta, A^{-1}h_\theta\rangle = h - \frac{1}{2}\langle h_\theta, h_{\theta\theta}^{-1}h_\theta\rangle. \end{aligned}$$

Summarizing, f is given by

$$f(\theta) = \frac{1}{2}\langle \theta - \theta_0, h_{\theta\theta}(\theta - \theta_0)\rangle + \left[h - \frac{1}{2}\langle h_\theta, h_{\theta\theta}^{-1}h_\theta\rangle\right],$$

where $\theta_0 = \hat{\vartheta}^p - h_{\theta\theta}^{-1}h_\theta$. Thus, if $f(\theta_0) = h - \frac{1}{2}\langle h_\theta, h_{\theta\theta}^{-1}h_\theta\rangle \geq 0$, then we return $\hat{\vartheta}^{p+1} = \theta_0$.

COMPUTING STEP 3: Suppose now that $f(\theta_0) < 0$ (i.e., the region $\{f < 0\}$ is nonempty), and let some direction φ' be given. We must find the point $\hat{\vartheta}^{p+1}$ such that

$$\text{(F.2)} \qquad f(\hat{\vartheta}^{p+1}) = 0 \quad \text{and} \quad f_\theta(\hat{\vartheta}^{p+1}) = \lambda\varphi' \quad \text{for some } \lambda \geq 0.$$

The second equation in (F.2) is equivalent to

$$h_{\theta\theta}(\hat{\vartheta}^{p+1} - \theta_0) = \lambda\varphi' \quad \Leftrightarrow \quad \hat{\vartheta}^{p+1} = \theta_0 + \lambda h_{\theta\theta}^{-1}\varphi'.$$

To obtain λ, we then use the first equation in (F.2):

$$\begin{aligned} 0 &= f(\hat{\vartheta}^{p+1}) \\ &= \frac{1}{2}\langle \hat{\vartheta}^{p+1} - \theta_0, h_{\theta\theta}(\hat{\vartheta}^{p+1} - \theta_0)\rangle + \left[h - \frac{1}{2}\langle h_\theta, h_{\theta\theta}^{-1}h_\theta\rangle\right] \\ &= \frac{1}{2}\lambda^2\langle h_{\theta\theta}^{-1}\varphi', h_{\theta\theta}h_{\theta\theta}^{-1}\varphi'\rangle + \left[h - \frac{1}{2}\langle h_\theta, h_{\theta\theta}^{-1}h_\theta\rangle\right] \\ \Rightarrow \quad \lambda &= +\left(\frac{\langle h_\theta, h_{\theta\theta}^{-1}h_\theta\rangle - 2h}{\langle \varphi', h_{\theta\theta}^{-1}\varphi'\rangle}\right)^{1/2} \end{aligned}$$

since we are interested in the nonnegative solution λ. The point we are looking for is thus

$$\begin{aligned} \hat{\vartheta}^{p+1} &= \theta_0 + \left(\frac{\langle h_\theta, h_{\theta\theta}^{-1}h_\theta\rangle - 2h}{\langle \varphi', h_{\theta\theta}^{-1}\varphi'\rangle}\right)_+^{1/2} h_{\theta\theta}^{-1}\varphi' \\ &= \hat{\vartheta}^p + h_{\theta\theta}^{-1}(\tilde{\lambda}(\hat{\vartheta}^p)\varphi' - h_\theta) \quad \text{with} \quad \tilde{\lambda}(\hat{\vartheta}^p) := \left(\frac{\langle h_\theta, h_{\theta\theta}^{-1}h_\theta\rangle - 2h}{\langle \varphi', h_{\theta\theta}^{-1}\varphi'\rangle}\right)_+^{1/2}. \end{aligned}$$

Note Added in Proof

In the proof stage, the authors noted that the following improvements could be made.

Relaxed Smoothness Assumptions

Assumption 2 requires that $H(x, \theta)$ be twice differentiable in both variables, but in fact it is enough to require that it be only once differentiable in x and twice in θ. This is significant since the smoothness of H in x is given by the smoothness of the drift vector field $b(x)$ and the diffusion matrix $a(x)$ (in the SDE case), or of the reaction rate functions $\nu_j(x)$ (in the Markov chain case). Thus, we modify Assumption 2 as follows:

ASSUMPTION 2 (MODIFIED) *The derivatives H_θ, H_x, $H_{\theta x} = (H_{x\theta})^T$, and $H_{\theta\theta}$ exist and are continuous.*

To achieve this improvement, all that has to be changed is the proof of Lemma 2.8, which is the only place that required the existence of H_{xx}. This is done below.

Passing Critical Points in Infinite Time

Interestingly, relaxing the smoothness assumptions sheds more light onto the question of what is necessary for a point to be passed in infinite time: If $H_{xx}(x_c, 0)$ does not exist at some critical point x_c, then this point may be passed in finite time. An example where this happens is given in Section 5, when $U(x) \approx cst \cdot |x - x_c|^\beta$ close to x_c for some $1 < \beta < 2$. We therefore introduce the following property that is sufficient to guarantee that a critical point is passed in infinite time, even under the reduced smoothness assumptions:

DEFINITION A critical point $x_c \in D$ is said to fulfill property (P) if $H(x, 0) = O(|x - x_c|^2)$ as $x \to x_c$.

Property (P) is a rather weak requirement: Looking at Assumption 1 and recalling that $H(x_c, 0) = 0$, we see that this property is automatically fulfilled if $H_{xx}(x_c, 0)$ exists (which explains why we did not need to require it previously). In particular, it is fulfilled if $H(x, 0) \equiv 0$ for all $x \in D$, as it is the case for the Hamiltonians of large deviations theory treated in this paper. Now while Lemma 2.2 remains unchanged (i.e., critical points are always passed at zero speed, even under the reduced smoothness assumptions), Lemma 2.8 is modified: To show that a critical point is passed in infinite time, we need to require property (P).

LEMMA 2.8 (MODIFIED)

(i) *Let x_c be a critical point with property* (P). *Then there exists a $C > 0$ such that for all x close enough to x_c and all $y \neq 0$, we have $\lambda(x, y) \leq C|x - x_c|/|y|$. In particular, for any $y \neq 0$ the function λ is Lipschitz-continuous at the point (x_c, y).*

(ii) *Suppose that φ is parametrized such that $|\varphi'| \equiv cst$ a.e., and let $\alpha_c \in [0,1]$ be such that $\varphi(\alpha_c)$ is a critical point with property* (P). *Then the function $\alpha \mapsto 1/\lambda(\varphi, \varphi')$ is not locally integrable at α_c. In particular, if the curve $\gamma(\varphi)$ contains a critical point with property* (P), *then $T^\star = \int_0^1 1/\lambda(\varphi, \varphi')\, d\alpha = \infty$.*

Let us summarize: For SDEs and continuous-time Markov chains, critical points are those points x with vanishing drift, $H_\theta(x,0) = 0$, and property (P) is always fulfilled; therefore points with vanishing drift are always passed at zero speed (Lemma 2.2(i)) and in infinite time (Lemma 2.8(ii)). This is case 3 below. For other Hamiltonians (see, e.g., Section 5), points with $H_\theta(x,0) = 0$ fall into one of the following three categories:

Case 1. The point fulfills $H(x,0) < 0$, and so x is not a critical point. By Lemma 2.2 we thus have $\lambda(x,y) > 0$ for any direction $y \neq 0$, and therefore the point x is passed at positive speed (and consequently in finite time).

Case 2. We have $H(x,0) = 0$, but property (P) is not fulfilled. In this case x is a critical point, so again by Lemma 2.2(i) we have $\lambda(x,y) = 0$ for any $y \neq 0$, and the point is passed at zero speed. But since property (P) is not fulfilled, it may or may not take infinite time to pass the point.

The latter may also depend on the direction from which the point is approached. To decide, one would have to check whether $1/\lambda(\varphi, \varphi')$ is locally integrable at that point; in the example in Section 5, this can be done by computing an explicit formula for $\lambda(x,y)$.

Case 3. We have $H(x,0) = 0$, and property (P) is fulfilled. Then the point is critical, $\lambda(x,y) = 0$ for all $y \neq 0$, and the point is passed at zero speed and (by Lemma 2.8(ii)) in infinite time.

PROOF OF LEMMA 2.8 (MODIFIED):

(i) Let $K \subset D$ be a compact ball around x_c and $C_1 > 0$ such that for all $x \in K$ we have $H(x,0) \geq -C_1|x - x_c|^2$. We abbreviate $\hat{\vartheta} = \hat{\vartheta}(x,y)$, do two Taylor expansions in x and θ, and use the defining property of $\hat{\vartheta}$, Assumptions 1 and 3, and Cauchy's inequality to find that for some constants $C_2, C_3 > 0$ and some vector $(\tilde{x}, \tilde{\theta})$ between $(x_c, 0)$ and $(x, \hat{\vartheta})$ we have

$$
\begin{aligned}
0 &= H(x, \hat{\vartheta}) \\
&= H(x,0) + \langle H_\theta(x,0), \hat{\vartheta}\rangle + \frac{1}{2}\langle \hat{\vartheta}, H_{\theta\theta}(x,\tilde{\theta})\hat{\vartheta}\rangle \\
&\geq -C_1|x - x_c|^2 + \langle \underbrace{H_\theta(x_c,0)}_{=0}, \hat{\vartheta}\rangle + \langle H_{\theta x}(\tilde{x},0)(x - x_c), \hat{\vartheta}\rangle + \frac{1}{2}\, m(x)|\hat{\vartheta}|^2
\end{aligned}
$$

$$\geq -C_2(|x-x_c|^2 + |x-x_c|\,|\hat{\vartheta}|) + \frac{1}{2}\,m_K|\hat{\vartheta}|^2$$

$$\geq -C_2\left(\left(1+\frac{C_2}{m_K}\right)|x-x_c|^2 + \frac{m_K}{4C_2}|\hat{\vartheta}|^2\right) + \frac{1}{2}\,m_K|\hat{\vartheta}|^2$$

$$= -C_2\left(1+\frac{C_2}{m_K}\right)|x-x_c|^2 + \frac{1}{4}\,m_K|\hat{\vartheta}|^2$$

$$\Rightarrow \qquad |\hat{\vartheta}|^2 \leq C_3|x-x_c|^2 \qquad \Rightarrow \qquad |\hat{\vartheta}| \leq \sqrt{C_3}|x-x_c|.$$

In particular, this shows that $|\hat{\vartheta}|$ stays bounded, so that the terms $H_{\theta x}$ and $H_{\theta\theta}$ below are bounded as well. We conclude that (for some new vector $(\tilde{x},\tilde{\theta})$ between $(x_c,0)$ and $(x,\hat{\vartheta})$) we have

$$\begin{aligned}\lambda(x,y)|y| &= |H_\theta(x,\hat{\vartheta})| \\ &= |\underbrace{H_\theta(x_c,0)}_{=0} + H_{\theta x}(\tilde{x},\tilde{\theta})(x-x_c) + H_{\theta\theta}(\tilde{x},\tilde{\theta})\hat{\vartheta}| \\ &\leq C_4(|x-x_c| + |\hat{\vartheta}|) \\ &\leq C_4(1+\sqrt{C_3})|x-x_c| =: C\,|x-x_c|.\end{aligned}$$

(ii) This is now a direct consequence of (i): Using that

$$|\varphi(\alpha)-\varphi(\alpha_c)| = \left|\int_{\alpha_c}^{\alpha}\varphi'(s)ds\right| \leq |\varphi'|\,|\alpha-\alpha_c|,$$

we conclude that for almost every α close to α_c, we have

$$\lambda(\varphi(\alpha),\varphi'(\alpha)) \leq C\,\frac{|\varphi(\alpha)-\varphi(\alpha_c)|}{|\varphi'(\alpha)|} \leq C\,|\alpha-\alpha_c|.$$

Thus we have for arbitrarily small $\varepsilon > 0$ that

$$\int\limits_{|\alpha-\alpha_c|<\varepsilon} \frac{d\alpha}{\lambda(\varphi,\varphi')} \geq \frac{1}{C}\int\limits_{|\alpha-\alpha_c|<\varepsilon} \frac{d\alpha}{|\alpha-\alpha_c|} = \infty.$$

□

Acknowledgment. The work of E. V.-E. is partially supported by the National Science Foundation via grants DMS02-09959 and DMS02-39625, and by the Office of Naval Research via grant N00014-04-1-0565. We thank Oliver Bühler, Weinan E, Bob Kohn, and Maria Reznikoff for useful suggestions and comments.

Bibliography

[1] Allen, R. J.; Warren, P. B.; ten Wolde, P. R. Sampling rare switching events in biochemical networks. *Phys. Rev. Lett*. **94** (2005), 018104.

[2] Da Prato, G.; Zabczyk, J. *Stochastic equations in infinite dimensions*. Encyclopedia of Mathematics and Its Applications, 44. Cambridge University Press, Cambridge, 1992.

[3] E, W.; Ren, W.; Vanden-Eijnden, E. String method for the study of rare events. *Phys. Rev. B* **66** (2002), 052301.

[4] E, W.; Ren, W.; Vanden-Eijnden, E. Minimum action method for the study of rare events. *Comm. Pure Appl. Math*. **57** (2004), no. 5, 637–656.

[5] Freidlin, M. I. Random perturbations of reaction-diffusion equations: the quasideterministic approximation. *Trans. Amer. Math. Soc*. **305** (1988), no. 2, 665–697.

[6] Freidlin, M. I.; Wentzell, A. D. *Random perturbations of dynamical systems*. 2nd ed. Grundlehren der Mathematischen Wissenschaften, 260. Springer, New York, 1998.

[7] Gardner, T. S.; Cantor, C. R.; Collins, J. J. Construction of a genetic toggle switch in Escherichia coli. *Nature* **403** (2000), 339–342.

[8] Heymann, M. The geometric minimum action method: a least action principle on the space of curves. Doctoral dissertation, Courant Institute of Mathematical Sciences, 2007.

[9] Jónsson, H.; Mills, G.; Jacobsen, K. W. Nudged elastic band method for finding minimum energy paths of transitions. *Classical and quantum dynamics in condensed phase simulations*, 385–404. Proceedings of the International School of Physics LERICI, Villa Marigola 7–18 July 1997. World Scientific, Singapore, 1998.

[10] Keller, H. B. *Numerical methods for two-point boundary value problems*. Dover, New York, 1992.

[11] Kleinert, H. *Path integrals in quantum mechanics, statistics, polymer physics, and financial markets*. 3rd ed. World Scientific, River Edge, N.J., 2004.

[12] Maier, R. S.; Stein, D. L. A scaling theory of bifurcations in the symmetric weak-noise escape problem. *J. Statist. Phys*. **83** (1996), no. 3-4, 291–357.

[13] Morton, K. W.; Mayers, D. F. *Numerical solution of partial differential equations. An introduction*. 2nd ed. Cambridge University Press, Cambridge, 2005.

[14] Nocedal, J.; Wright, S. J. *Numerical optimization*. Springer Series in Operations Research. Springer, New York, 1999.

[15] Olender, R.; Elber, R. Calculation of classical trajectories with a very large time step: Formalism and numerical examples. *J. Chem. Phys.* **105** (1996), no. 20, 9299–9315.

[16] Roma, D. M.; O'Flanagan, A.; Ruckenstein, A. E.; Sengupta, A. M.; Mukhopadhyay, R. Optimal path to epigenetic switching. *Phys. Rev. E* **71** (2005), 011902.

[17] Shwartz, A.; Weiss, A. *Large deviations for performance analysis*. Queues, communications, and computing. Stochastic Modeling Series. Chapman & Hall, London, 1995.

[18] Simon, B. Semiclassical analysis of low lying eigenvalues. II. Tunneling. *Ann. of Math. (2)* **120** (1984), no. 1, 89–118.

[19] Varadhan, S. R. S. *Large deviations and applications*. CBMS-NSF Regional Conference Series in Applied Mathematics, 46. Society for Industrial and Applied Mathematics (SIAM), Philadelphia, 1984.

[20] Warren, P. B., ten Wolde, P. R. Enhancement of the stability of genetic switches by overlapping upstream regulatory domains. *Phys. Rev. Lett*. **92** (2004), no. 12, 128101.

[21] Weiss, J. N. The Hill equation revisited: uses and misuses. *FASEB J*. **11** (1997), 835–841.

MATTHIAS HEYMANN
Courant Institute
251 Mercer Street
New York, NY 10012
E-mail: heymann@cims.nyu.edu

ERIC VANDEN-EIJNDEN
Courant Institute
251 Mercer Street
New York, NY 10012
E-mail: eve2@cims.nyu.edu

Received November 2006.